JYU DISSERTATIONS 469

Mikhail Blagov

# Exact Lock-In Range for Classical Phase-Locked Loops

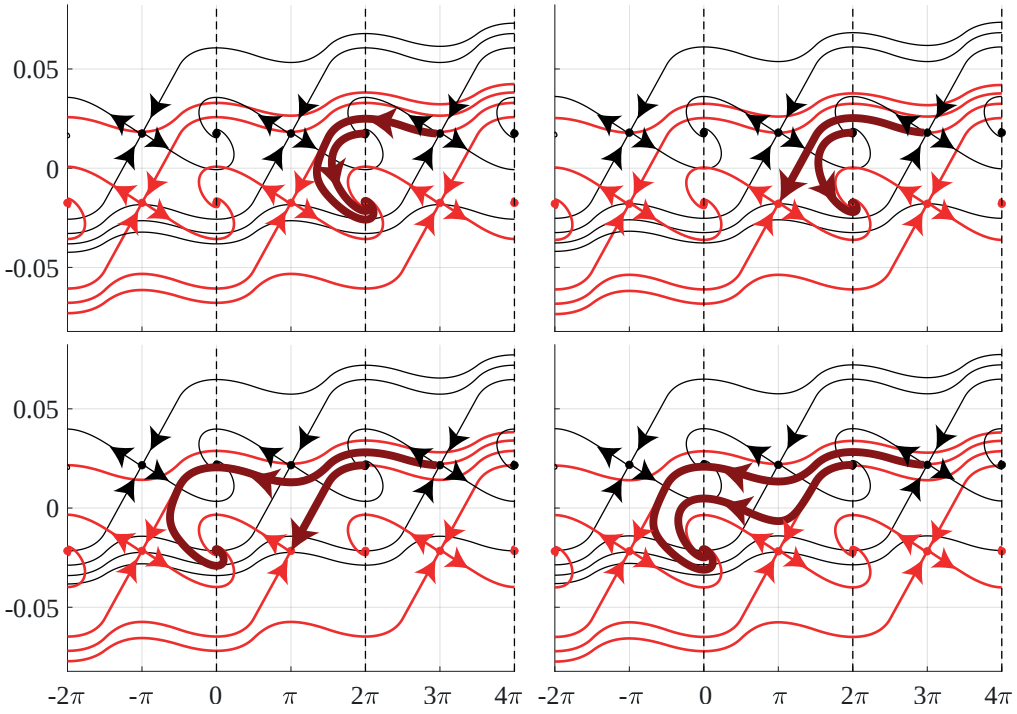


UNIVERSITY OF JYVÄSKYLÄ
FACULTY OF INFORMATION TECHNOLOGY

JYU DISSERTATIONS 469

Mikhail Blagov

# Exact Lock-In Range for Classical Phase-Locked Loops

Esitetään Jyväskylän yliopiston informaatioteknologian tiedekunnan suostumuksella
julkisesti tarkastettavaksi joulukuun 15. päivänä 2021 kello 10.

Academic dissertation to be publicly discussed, by permission of
the Faculty of Information Technology of the University of Jyväskylä,
on December 15, 2021 at 10 o'clock.

JYVÄSKYLÄN YLIOPISTO
UNIVERSITY OF JYVÄSKYLÄ

JYVÄSKYLÄ 2021

Editors
Timo Männikkö
Faculty of Information Technology, University of Jyväskylä
Ville Korkiakangas
Open Science Centre, University of Jyväskylä

Cover picture by Mikhail Blagov.



ISBN 978-951-39-8953-8 (PDF)
URN:ISBN:978-951-39-8953-8
ISSN 2489-9003

Permanent link to this publication: http://urn.fi/URN:ISBN:978-951-39-8953-8

# ABSTRACT

Blagov, Mikhail
Exact lock-in range for classical phase-locked loops
Jyväskylä: University of Jyväskylä, 2021, 36 p. (+included articles)
(JYU Dissertations
ISSN 2489-9003; 469)
ISBN 978-951-39-8953-8 (PDF)

Phase-locked loops (PLLs) are are widely used in various applications: Wireless communications, GPS navigation, gyroscope systems, computer architectures, electrical grids, and others. PLLs are inherently non-linear, but in engineering practice, they are actually designed and analyzed mostly using linear methods. Recent development in the manufacturing of electronics has led to ever higher operating frequencies and, hence, to more stringent requirements for the design of PLLs.

This dissertation is devoted to the study of phase-locked loops, in particular to their synchronization properties. The ability of the phase-locked loop to synchronize fast without cycle slipping is characterized by the loop's lock-in range.

The problem of determining the lock-in range is called the Gardner problem for lock-in range, named after IEEE Fellow F. M. Gardner, who formulated the problem in the 1960s. Mathematically rigorous formulation of the lock-in range by N. Kuznetsov, however, is only a few years old, and the first approaches to improve the estimates of the lock-in range using non-linear methods were proposed by K.D. Aleksandrov in his doctoral dissertation.

This work furthers the mathematically rigorous study of the lock-in range and is devoted to the exact calculation of the lock-in in range for a classical phase-locked loop with active proportionally integrating and lead-lag filters. For phase space, phase-locked loop models with piecewise-linear phase detectors characteristized by an exact lock-in range is obtained for both the considered filter types. For the phase-space phase-locked loop model with an active proportionally integrating filter and tangential that is characteristic of a phase detector, the lock-in range is proven to be infinite. All theorems have strict mathematical proof and have been confirmed by numeric simulation.

Keywords: PLL, phase-locked loops, lock-in range, Gardner problem, exact lock-in range

# TIIVISTELMÄ (ABSTRACT IN FINNISH)

Blagov, Mikhail
Tarkka lukitusalue klassisille vaihelukituille silmukoille
Jyväskylä: University of Jyväskylä, 2021, 36 s. (+artikkelit)
(JYU Dissertations
ISSN 2489-9003; 469)
ISBN 978-951-39-8953-8 (PDF)

Vaihelukittuja silmukoita (PLL, phase locked loop) käytetään laajasti erilaisissa sovelluksissa: langattomassa viestinnässä, GPS-navigaatiossa, gyroskooppijärjestelmissä, tietokonearkkitehtuureissa, sähköverkoissa ja muissa. PLL:t ovat toimintaperiaatteeltaan epälineaarisia, mutta teollisuudessa niitä suunnitellaan ja analysoidaan yhä enimmäkseen lineaarisilla menetelmillä. Jatkuvasti kehittyvä elektroniikan valmistusteknologia mahdollistaa yhä korkeammat toimintataajuudet, mikä puolestaan asettaa yhä tiukempia vaatimuksia PLL-piirien suunnittelulle.

Tässä työssä tutkitaan vaihelukittuja silmukoita ja erityisesti niiden synkronointiominaisuuksia. Vaihelukitun silmukan keskeisin ominaisuus on kyky synkronoitua nopeasti ohjaavaan signaaliin, hukkaamatta yhtään sykliä ohjaussignaalin taajuuden muuttuessa. Taajuusikkunaa, jossa tämä onnistuu, kutsutaan silmukan lukitusalueeksi.

IEEE-Fellow F. M. Gardner muotoili lukitusalueen määrittämisen ongelman ongelman 1960-luvulla.

Lukitusalueen matemaattisesti eksakti määritelmä on kuitenkin vain muutaman vuoden vanha ja ensimmäiset arviot, jotka hyödyntävät silmukan epälineaarisia piirteitä esitti K.D. Aleksandrov väitöskirjassaan 2016.

Tämä työ jatkaa matemaattisesti tarkkaa lukitusalueen analyysiä. Työssä johdetaan uusia tuloksia yleisesti käytettyjen vaihelukittujen silmukoiden lukitusalueista. Ns. kanttiaaltoa käyttäville silmukoille lukkiutumisalue voidaan määrittää tarkasti tapauksessa, jossa käytetään tavanomaisia aktiivisia suhteellisesti integroivia PI-suotimia tai ns. lead-lag -suotimia. Silmukoille, joissa käytetään aktiivista PI-suodatinta ja vaiheilmaisin kykenee antamaan rajattoman vasteen (ns. tangentiaalinen vaiheilmaisin), lukitusalue on itseasiassa ääretön. Toisin sanoen lukitus pystyy seuraamaan kaikkia taajuusmuutoksia. Silmukoiden ominaisuudet todistetaan matemaattisesti ja ominaisuuksia havainnollistetaan kattavin numeerisin simuloinnein.

Avainsanat: PLL, vaihelukitut silmukat, lukitusalue, Gardner-ongelma, tarkka lukitusalue

**Author**

Mikhail Blagov
Faculty of Information Technology,
University of Jyväskylä, Finland,
Faculty of Mathematics and Mechanics,
St. Petersburg State University, Russia

**Supervisors**

Professor Nikolay V. Kuznetsov
Faculty of Information Technology,
University of Jyväskylä, Finland,
Faculty of Mathematics and Mechanics,
St. Petersburg State University, Russia

Professor Pekka Neittaanmäki
Faculty of Information Technology,
University of Jyväskylä, Finland

Professor Timo Tiihonen
Faculty of Information Technology,
University of Jyväskylä, Finland

Professor Renat V. Yuldashev
Faculty of Mathematics and Mechanics,
St. Petersburg State University, Russia

**Reviewers**

Professor Vladimir Rasvan
Department of Automation,
Electronics and Mechatronics,
University of Craiova, Romania

Professor Vanya R. Barseghyan
Chair of Mechanics,
Faculty of Mathematics and Mechanics,
Yerevan State University, Republic of Armenia

**Opponent**

Professor Leonid S. Chechurin
Industrial Management Department,
Lappeenranta-Lahti University of Technology, Finland

## ACKNOWLEDGEMENTS

This thesis was completed in the Doctoral School of the Faculty of Information Technology, University of Jyväskylä.

I would like to express my sincere gratitude to my supervisors Prof. Nikolay V. Kuznetsov, Prof. Pekka Neittaanmäki, Prof. Timo Tiihonen, and Prof. Renat V. Yuldashev for their guidance, productive discussions, additional comments, and continuous support.

I also would like to thank Mikhail Y. Lobachev for the productive collaboration during last two years.

I greatly appreciate the opportunity to participate in the Educational and Research Double Degree Program organized by University of Jyväskylä (Faculty of Information Technology) and Saint Petersburg State University (Department of Applied Cybernetics).

This work is funded by the Leading Scientific schools of the Russian Federation grant NSh-2624.2020.1.

I'm very grateful to my wife Svetlana A. Lyubchich for granting me inspiration to complete this dissertation.

Finally, I would like to express my deepest thanks to my mother, Elena N. Blagova, for her endless support.

## LIST OF FIGURES

# CONTENTS

## LIST OF INCLUDED ARTICLES

PI N.V. Kuznetsov, D.G. Arseniev, M.V. Blagov, Z. Wei, M.Y. Lobachev, M.V. Yuldashev, R.V. Yuldashev. The Gardner problem and cycle slipping bifurcation for type 2 phase-locked loops. *Int. J. Bifurcation and Chaos*, 2022 (accepted), JuFo 1.

PII M.V. Blagov, N.V. Kuznetsov, M.Y. Lobachev, M.V. Yuldashev, R.V. Yuldashev. The conservative lock-in range for PLL with lead-lag filter and triangular phase detector characteristic. *arXiv:2112.01602*, 2021.

PIII M.V. Blagov, O.A. Kuznetsova, E.V. Kudryashova, N.V. Kuznetsov, T.N. Mokaev, R.N. Mokaev, M.V. Yuldashev, R.V. Yuldashev. Hold-in, Pull-in and Lock-in Ranges for Phase-locked Loop with Tangential Characteristic of the Phase Detector. *Procedia Computer Science, Vol. 150, pp. 558–566, https://doi.org/10.1016/j.procs.2019.02.093*, 2019, JuFo 1.

PIV M.V. Blagov, E.V. Kudryashova, N.V. Kuznetsov, G.A. Leonov, M.V. Yuldashev, R.V. Yuldashev. Computation of lock-in range for classic PLL with lead-lag filter and impulse signals. *IFAC-PapersOnLine, Vol. 49, I. 14, pp. 42–44 https://doi.org/10.1016/j.ifacol.2016.07.972*, 2016, JuFo 1.

PV M.V. Blagov, N.V. Kuznetsov, G.A. Leonov, M.V. Yuldashev, R.V. Yuldashev. Simulation of PLL with impulse signals in MATLAB: Limitations, hidden oscillations, and pull-in range. *2015 7th International Congress on Ultra Modern Telecommunications and Control Systems and Workshops (ICUMT), pp. 85–90. https://doi.org/10.1109/ICUMT.2015.7382410*, 2015, JuFo 1.

# 1 INTRODUCTION

The interest to study phase-locked loops (PLL) comes from their wide applications. Initially described by A. Appleton in 1923 (Appleton (1923)) and H. Bellescize (Bellescize (1932)), PLL circuits have gained an important application in radio and telecommunication systems since the 1940s (Wendt and Fredentall (1943); George (1951); Gruen (1953); Richman (1953, 1954)).

These circuits became widely used in wireless communications (Du and Swamy (2010); Rouphael (2014); Best et al. (2016); Cho (2006); Ho (2005); Helaluddin (2008); Rosenkranz and Schaefer (2016), GPS navigation systems (Kaplan and Hegarty (2017)), gyroscope systems (Aaltonen and Halonen (2010); Senkal and Shkel (2020); Kuznetsov et al. (2022)), computer architectures (Kolumbán (2005); Best (2007, 2018)), electrical grids (Karimi-Ghartemani (2014); Kuznetsov et al. (2020, 2021b,a)), and others.

The first ideas of the mathematical analysis of such systems belong to Italian academician F. Tricomi (Tricomi (1933)) and are based on the analysis of system phase portraits. These ideas were further developed in the works of A.A. Andronov (Andronov and Khaikin (1937)). Fundamental monographs devoted to the problems of numerical simulation and analysis of PLL were published in 1966 by F. Gardner (Gardner (1966)), A. Viterbi (Viterbi (1966)), V.V. Shakhgildyan, and A.A. Lyakhovkin (Shakhgil'dyan and Lyakhovkin (1966)). These books are devoted primarily to engineering approaches to analyse two-dimensional PLL models.

PLL systems are substantially nonlinear, hence the full analysis must be nonlinear. However, linear methods are still widely used in engineering practice, and some problems of PLL analysis have not yet been solved using nonlinear methods. This was stated by Daniel Abramovitch (Abramovitch (2002)): *"In fact, the control theory used in most PLL texts is straight linear system design with a small amount of non- linear heuristics <...>. The stability analysis and design of the loops tends to be done by a combination of linear analysis, rule of thumb, and simulation."* One of the possible reasons for this is stated in Tranter et al. (2010): *Nonlinear analysis techniques are well beyond the scope of most undergraduate courses in communication theory*.

The lack of adequate nonlinear analysis has resulted in the wide use of various conjectures and heuristics about the behaviour of PLLs that are based on linear analysis and linear estimates of key engineering characteristics of PLL's pull-in range (corresponding to global stability of the dynamical system). As examples of such conjectures, one can consider Egan's conjecture about the pull-in range (Egan (2007, 2011)) and Kapranov's conjecture that pull-in ranges of the second-order type 1 PLLs are defined by self-exciting oscillations (Kapranov (1956)). Corresponding counterexamples can be found in (Gubar' (1961); Kuznetsov et al. (2021c)).

Along with this, by virtue of the development of electronics manufacturing technologies, operational frequencies increased, which required further refinement of the operation range estimates. On the other side, mathematical models can now be accurately implemented in practice, including software realizations of phase-locked loops. This unlocks the use of models with marginally stable filters (with pole at the origin) along with the classically stable ones. Marginally stable filters allow the extention of the stability area of the closed system and increase the speed of the frequency lock (Egan (2007, 2011)). These facts require further development of nonlinear PLL analysis to increase the accuracy of the system properties estimates.

Nonlinear approaches for PLL study have been actively developed as part of the scope of the Educational and Research Double Degree Program organized by University of Jyväskylä (Faculty of Information Technology) and Saint Petersburg State University (Department of Applied Cybernetics). Several doctoral dissertations have been devoted to the topic (Kuznetsov (2008); Kudryashova (2009); Yuldashev (2013a,b); Aleksandrov (2016)). One of the actively studied problems within the program is the Gardner problem of the lock-in range estimation (Gardner (2005)), which is further refinement of the PLL behavior inside the pull-in range. It considers the ability of the PLL to synchronize in a short time. *"If, for some reason, the frequency difference between input and VCO is less than the loop bandwidth, the loop will lock up almost instantaneously without slipping cycles. The maximum frequency difference for which this fast acquisition is possible is called the lock-in frequency"*. A rigorous approach to the Gardner problem was suggested by N.V. Kuznetsov (Leonov and Kuznetsov (2014); Leonov et al. (2015b); Kuznetsov et al. (2019, 2021c)). The first analytical estimate of the lock-in range was obtained in the doctoral dissertation of K.D. Aleksandrov (Aleksandrov (2016)) and made engineering estimates more accurate.

Research questions of this dissertation are related to the Gardner problem:

**RQ1** Is the approximate estimate of the lock-in range by R.E. Best (Best (2007, 2018)) valid in general? Can it be refined using the rigorous analytical methods for phase-locked loops with an active proportionally-integrating filter and piecewise-linear phase detector characteristic?

**RQ2** Is the approximate estimate of the lock-in range by R.E. Best (Best (2007, 2018)) valid in general? Can it be refined using the rigorous analytical methods for phase-locked loops with a lead-lag filter and piecewise-linear phase detector characteristic?

**RQ3** Can the lock-in range of a phase-locked loop be infinite (this question is inspired by Egan's conjecture about the infinite pull-in range of phase-locked loops (Egan (2011)))?

These questions are inspired by modern engineering applications of phase-locked loops in satellite communication systems (Best (2007, 2018)), electrical grids (Karimi-Ghartemani (2014); Kuznetsov et al. (2021b,a)), and gyroscopy (Senkal and Shkel (2020); Kuznetsov et al. (2022)). These questions are also topics of interest for Finnish researchers and engineers (see e.g. Kihara et al. (2002); Aaltonen and Halonen (2010)).

In this dissertation, the definition of a lock-in range is modified according to engineering requirements and an analytic exact lock-in range is obtained. Results, related to **RQ1**, are considered in included articles (**PI**), to **RQ2** in included articles (**PII; PIV; PV**), to **RQ2** and in included article (**PIII**). See FIGURE 1 for the detailed mapping to chapters.

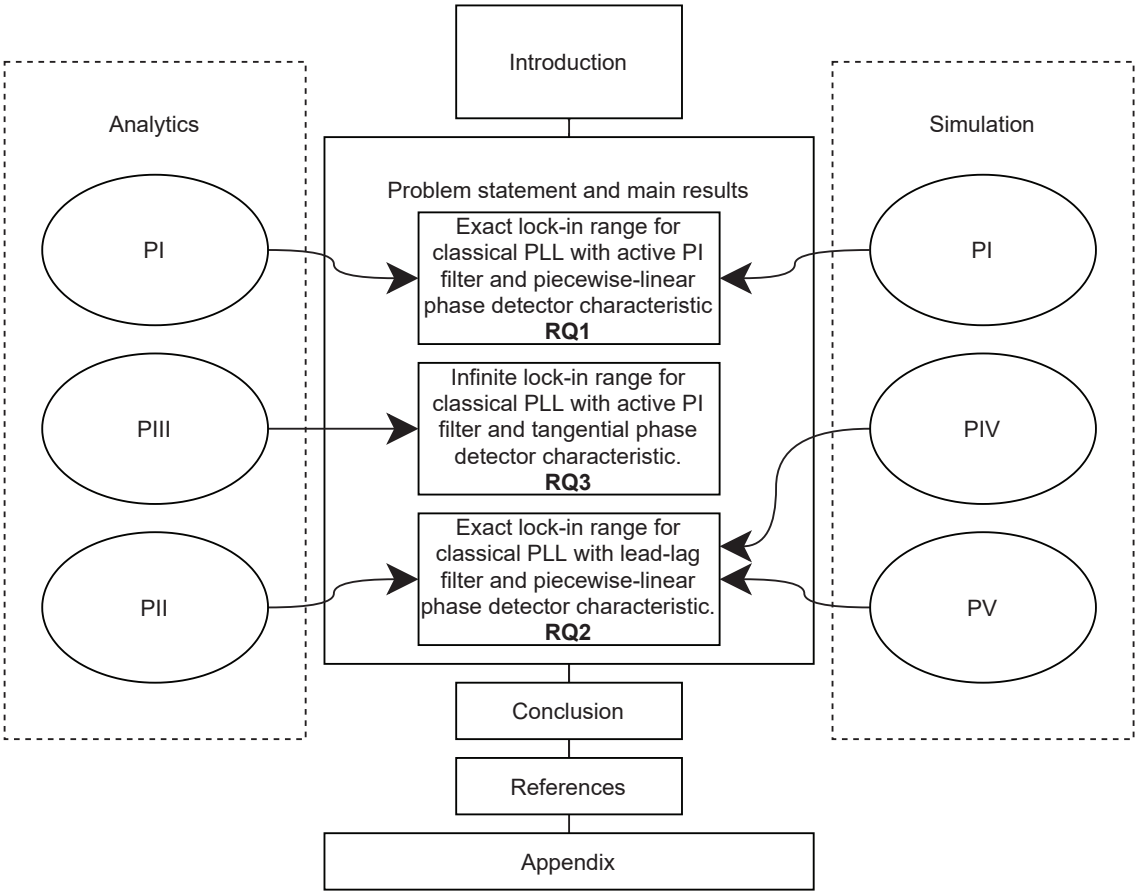


FIGURE 1 Structure of the chapters and their connection with included articles.

# 2 PROBLEM STATEMENT AND MAIN RESULTS ON RESEARCH QUESTIONS

## 2.1 Mathematical model of PLL and lock-in range definition

*Mathematical model of PLL in the signal's phase space* (Gardner (2005); Egan (2007); Leonov et al. (2015b); Best (2018)) is shown in Fig.2. Here, the outputs of the

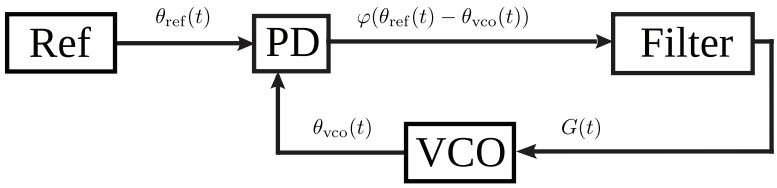


FIGURE 2 PLL model in the signal's phase space.

reference oscillator and VCO are phases $\theta_{\mathrm{ref}}(t)$ and $\theta_{\mathrm{vco}}(t)$ correspondingly. They are supplied to the input of a nonlinear block called a phase detector. The output of the phase detector — $K_{\mathrm{vco}}\varphi(\theta_{\mathrm{ref}}(t)-\theta_{\mathrm{vco}}(t))$. Here $\varphi(\theta_e)$ — and functions of phase difference $\theta_e=\theta_{\mathrm{ref}}(t)-\theta_{\mathrm{vco}}(t)$ is called a phase detector characteristic. The magnitude $K_{\mathrm{vco}}$ is called a VCO gain. The form of phase detector characteristic $\varphi(\theta_e)$ depends on the form of reference and VCO signal's waveforms. Various signals' waveforms lead to different characteristic functions in the model (Leonov et al. (2015a)).

The frequency of the input signal (reference frequency $\omega_{\mathrm{ref}}$) is usually assumed to be constant:

$$\dot{\theta}_{\mathrm{ref}}(t)=\omega_{\mathrm{ref}}(t)\equiv\omega_{\mathrm{ref}}. \tag{1}$$

Consider the system of differential equations describing the loop filter:

$$\begin{aligned}\dot{x}&=Ax+b\varphi(\theta_e(t)),\\ G(t)&=c^*x+h\varphi(\theta_e(t)).\end{aligned} \tag{2}$$

Tuning of the VCO is considered to be linear

$$\dot{\theta}_{\text{vco}}(t) = \omega_{\text{vco}}^{\text{free}} + K_{\text{vco}} G(t). \tag{3}$$

Combine equations (1), (2) and (3) to get an autonomous system of differential equations describing the model in FIGURE. 2:

$$\begin{cases} \dot{x} = Ax + b\varphi(\theta_e), \\ \dot{\theta}_e = \omega_e^{\text{free}} - K_{\text{vco}} \left( c^* x + h\varphi(\theta_e) \right). \end{cases} \tag{4}$$

Here $A$ – constant $n \times n$ matrix, $x(t) \in \mathbb{R}^n$ – vector describing filter state, $b$, $c$ and $h$ – constant vectors, $\dot{\theta}_{\text{ref}}(t) \equiv \omega_{\text{ref}}$ – constant frequency of the reference oscillator, $\omega_{\text{vco}}^{\text{free}}$ – free-running VCO frequency, $K_{\text{vco}} > 0$ – VCO gain. $\omega_e^{\text{free}} = \omega_{\text{ref}} - \omega_{\text{vco}}^{\text{free}}$ is called a frequency detuning between the reference oscillator and VCO, and its absolute value $|\omega_e^{\text{free}}|$ is called a frequency deviation.

Consider the mathematical definitions of PLL operation ranges according to (Kuznetsov et al. (2015); Leonov et al. (2015b); Best et al. (2016)).

**Definition 1.** *Maximal interval of frequency deviation $|\omega_e^{\text{free}}| \in [0, \omega_h)$ such that an asymptotically stable equilibrium exists and varies continuously while $\omega_e^{\text{free}}$ varies continuously within the interval is called a hold-in range.*

The hold-in range corresponds to the local stability of the dynamical system (4). It allows the system to return to a synchronized state (equilibrium) after a small change in input frequency. The hold-in range is widely used in engineering practice, see, e.g. (Viterbi (1966); Gardner (1966); Blanchard (1976); Best (2007); Pederson and Mayaram (2008); Bakshi and Godse (2009); Best (2018)).

From a practical point of view, it is important to guarantee tending the system towards a stationary set for any initial state of the model, see e.g. (Viterbi (1966); Gardner (1966); Blanchard (1976); Best (2007); Talbot (2012); Best (2018)).

**Definition 2.** *Maximal interval of frequency deviation $|\omega_e^{\text{free}}| \in [0, \omega_p)$ from the hold-in range such that mathematical model of PLL in signal's phase space* (4) *is globally asymptotically stable (i.e. every solution of the system* (4) *tends to some equilibrium as $t \to +\infty$) is called a pull-in range.*

Often, besides the tendence to the stationary set, the characteristics of the transient process are important.

**Definition 3.** *A cycle slipping occurs in PLL if*

$$\sup_{t>0} |\theta_e(0) - \theta_e(t)| \geqslant 2\pi.$$

The definition of cycle slipping in the present work is considered in accordance to (Stensby (1997)). It is more practical oriented than that was previously-studied in (Aleksandrov (2016)) definition, where the condition
$\limsup_{t\to\infty} |\theta_e(0) - \theta_e(t)| \geqslant 2\pi$. was considered. Detailed discussion of the definitions can be found in (Kuznetsov et al. (2015); **PII**).

**Definition 4.** *A* lock-in range *is the largest interval of frequency errors* $|\omega_e^{\text{free}}|$ *from the pull-in range such that the PLL model being in an equilibrium*[1]*, after any abrupt change of* $\omega_e^{\text{free}}$ *within the interval acquires an equilibrium without cycle slipping (*$\sup\limits_{t>0} |\theta_e(0) - \theta_e(t)| < 2\pi$*).*

The boundary of the lock-in range $\omega_l$ is called the lock-in frequency. The notion of the lock-in range defined above has appeared in many engineering monographs, (see, e.g. Best (1984); Wolaver (1991); Hsieh and Hung (1996); Irwin (1997); Craninckx and Steyaert (1998); Kihara et al. (2002); Abramovitch (2002); De Muer and Steyaert (2003); Dyer (2004); Shu and Sanchez-Sinencio (2005); Goldman (2007); Best (2007); Egan (2007); Baker (2011); Kroupa (2012); Middlestead (2017); Best (2018) and other).

## 2.2 Exact lock-in range for classical PLL with active PI filter and piecewise-linear phase detector characteristic

Consider the main results related to the research question **RQ1**. Following the classical monographs (Kolumbán (2005); Best (2007); Baker (2011); Best (2018)) and modern applications (Kuznetsov et al. (2021b)), consider the PLL with the active proportionally integrating filter $F(s) = \frac{1+\tau_2 s}{\tau_1 s}$, where $\tau_1 > 0$, $\tau_2 > 0$ are filter parameters (see e.g. (Best (2007, 2018)) for their physical meaning). Then system (4) takes the form of:

$$\begin{cases} \dot{x} = \frac{1}{\tau_1}\varphi(\theta_e), \\ \dot{\theta}_e = \omega_e^{\text{free}} - K_{\text{vco}}\left(x + \frac{\tau_2}{\tau_1}\varphi(\theta_e)\right). \end{cases} \tag{5}$$

Consider the phase detector characteristic in the form

$$\varphi(\theta_e) = \begin{cases} k\theta_e - 2\pi k n, & \text{if } -\frac{1}{k} + 2\pi n \le \theta_e(t) \le \frac{1}{k} + 2\pi n, \\ -\frac{1}{\pi - \frac{1}{k}}\theta_e + \frac{1}{\pi - \frac{1}{k}}(\pi + 2\pi n), & \text{if } \frac{1}{k} + 2\pi n \le \theta_e(t) \le -\frac{1}{k} + 2\pi(n+1), \end{cases} \tag{6}$$

where $n \in \mathbb{Z}$, $k \in \left(\frac{1}{\pi}, +\infty\right)$ [2]. This form of phase detector characteristic allows one to not only obtain analytical estimates of operational ranges but also effectively simulate PLL.

The hold-in and pull-in ranges of the classical second-order PLL with PI filters are infinite, see e.g. (Kuznetsov et al. (2021c)). To prove that this a generalization of classical stability theory, methods for systems with cylindrical phase

[1] Note that the method of the lock-in range calculation suggested in (Aleksandrov (2016)) considers only stable equilibria, which allowed to obtain an estimate of the lock-in range only. In this dissertation all equilibria are considered and analytical exact lock-in range is obtained.

[2] The classical triangular characteristic corresponds to the case $k = \frac{2}{\pi}$, see FIGURE. 3.

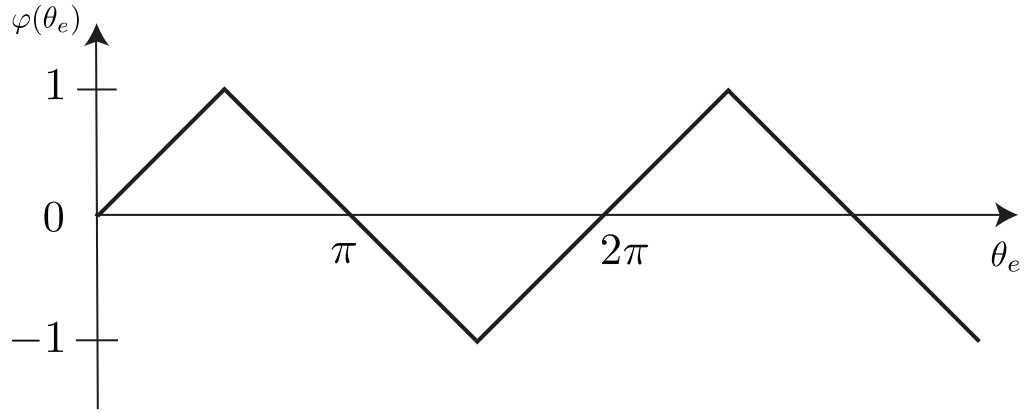


FIGURE 3 Piecewise-linear phase detector characteristic (6), $k = \frac{2}{\pi}$.

spaces and discontinuous nonlinearities can be used. An extension of the Lyapunov method for systems with non-unique equilibria was developed for this purpose by Y.N. Bakaev (Bakaev (1959, 1960)) and G.A. Leonov (Leonov (1971, 1976); Gelig et al. (1978); Leonov and Kuznetsov (2014)).

Further refinement of the pull-in range in connection with the Gardner problem and cycle slipping estimation is provided by the following theorem:

**Theorem 1.** *Exact lock-in frequency of model* (5) *with piecewise-linear PD characteristic* (6) *is*

$$\omega_l = \frac{1}{2}\sqrt{\frac{K_{\text{vco}}(d+\frac{c-a}{2})^{\frac{c-a}{c}}(d-\frac{c+a}{2})^{\frac{c+a}{c}}}{\tau_1}}, \tag{7}$$

*where $a$, $b$ and $c$ are evaluated as*

$$a = \sqrt{\frac{K_{\text{vco}}}{\tau_1}}\tau_2, \quad b = \sqrt{|a^2 - \frac{4}{k}|}, \quad c = \sqrt{a^2 + 4(\pi - \frac{1}{k})}, \tag{8}$$

*and $d$ is the unique solution of one of the equations:*

$$\begin{cases} (d-\frac{a-b}{2})^{\frac{b-a}{b}}(d-\frac{a+b}{2})^{\frac{b+a}{b}} = \pi(\frac{c+b}{c-b})^{\frac{a}{b}},\ d > \frac{a+b}{2}, \quad a^2k > 4, \\ d = \frac{a}{2}\Big(1 + \dfrac{1}{W(\frac{a}{2\sqrt{\pi}}\exp(-\frac{a}{2\sqrt{\pi}}))}\Big), \quad a^2k = 4, \\ \Big(d^2 - ad + \frac{1}{k}\Big)\exp\Big(\frac{2a}{b}\arctan\frac{b}{a-2d}\Big) = \pi\exp\Big(\frac{2a}{b}\arctan\frac{b}{c}\Big),\ d > \frac{a}{2}, \quad a^2k < 4. \end{cases} \tag{9}$$

*Here $W(x)$ is the Lambert W function.*

Notice that $\omega_l$ and $\omega_l$ are continuous functions of variable $k$ (as $a$ is fixed): The cases $a^2k > 4$ and $a^2k < 4$ in formula (7) approach the case $a^2k = 4$ as $k \to \frac{4}{a^2}$ (as $b \to 0$).

*Proof.* The proof of Theorem 1 is given in **PI** and is based on the following idea. Hold-in and pull-in ranges are known to be infinite for the second-order PLL

with an active PI filter. This is an interesting case when the Egan conjecture is fulfilled (Kuznetsov et al. (2021c)). The phase detector characteristic of the system is piecewise-linear, which allows it to analytically integrate in the intervals of linearity. In order to do this, the system is converted into a single differential equation using the approach suggested in (Belyustina (1959); Huque and Stensby (2013)). Then, the lock-in range definition is interpreted in terms of phase plane trajectories. The combination of the above steps allows to formulate two subsequent Cauchy problems, which gives an exact formula for the lock-in range calculation. □

Based on Theorem 1, an analytical-numerical method of the lock-in range calculation is implemented and diagrams of the lock-in range dependent on the system parameters useful for engineering practice (see e.g. (Belyustina et al. (1972))) are composed (see. FIGURE 4). In FIGURE 5 the lock-in range estimates

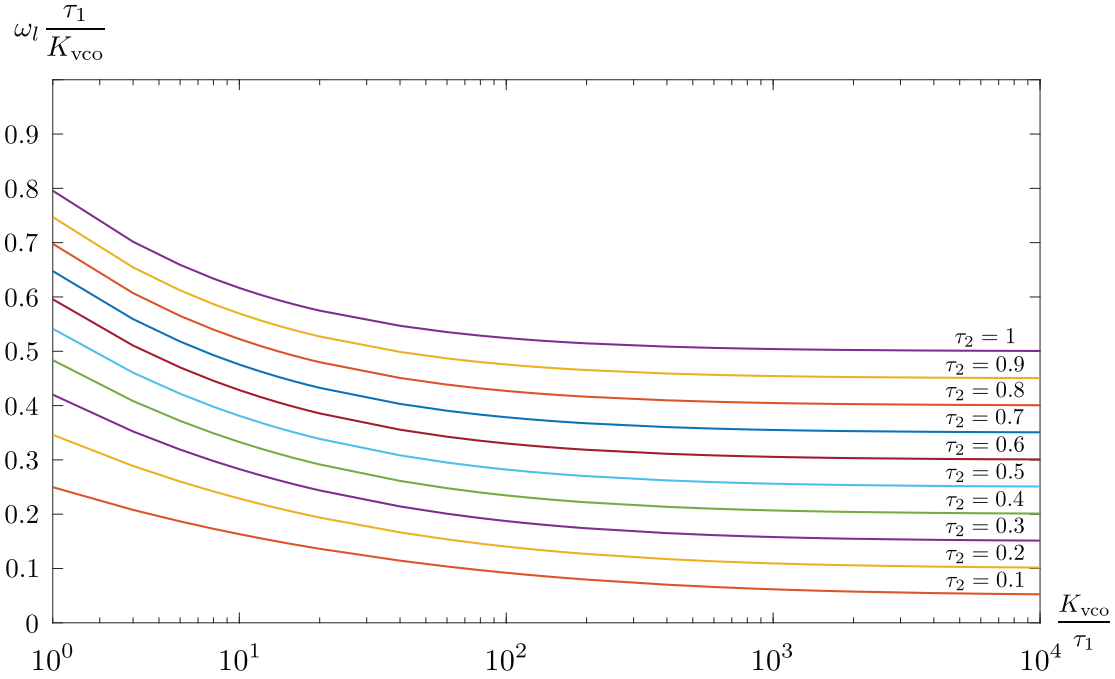


FIGURE 4 The lock-in range of PLL with PI filter (5) and triangular characteristic of phase detector (6).

obtained in this dissertation are compared with the results of K.D. Aleksandrov (Aleksandrov (2016)) and linear estimate by R.E. Best (Best (2007, 2018)).

## 2.3 Infinite lock-in range for classical PLL with an active PI filter and tangential phase detector characteristic

This chapter contains main results related to the research question **RQ3**. Consider analog PLL model (5) with a tangential characteristic of phase detector. It was

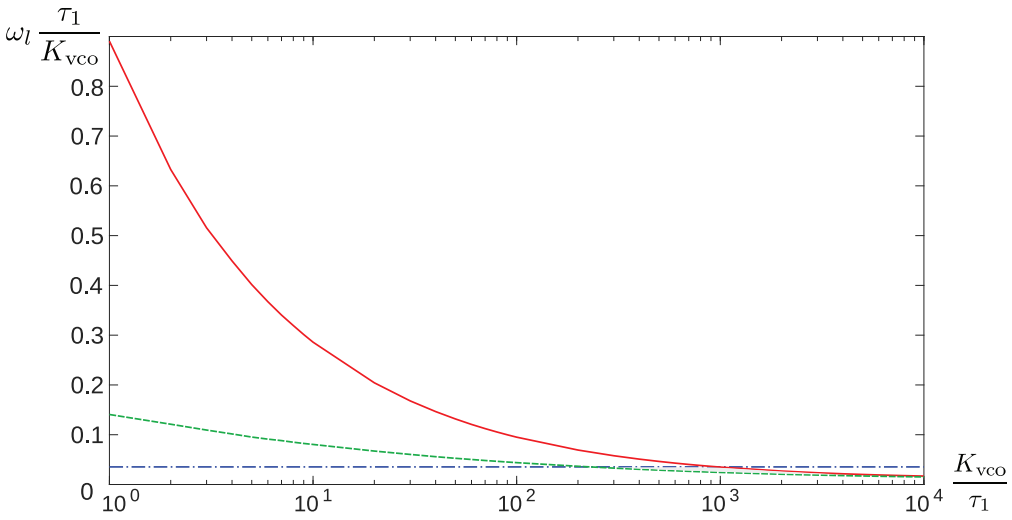


FIGURE 5 Comparison of the obtained lock-in range with earlier known results Aleksandrov (2016) and Best (2007, 2018). The diagram is given for $\tau_2 = 0.0225$. Here the blue dot-dash line is linear estimate by R.E. Best, the red solid line is an estimate of K.D. Aleksandrov, and the green dashed line is the exact lock-in range obtained in this dissertation. Note that the linear estimate is more conservative for small $\frac{K_{\text{vco}}}{\tau_1}$ and is not valid for large $\frac{K_{\text{vco}}}{\tau_1}$.

introduced by American engineer L. Robinson[3] (Robinson (1965)), and allows increasing the lock-in range in practice.

$$\varphi(\theta_e) = \tan(\theta_e). \tag{10}$$

**Theorem 2.** *For a classical PLL with a PI filter and tangential phase detector characteristic $\varphi(\theta_e) = \tan(\theta_e)$, the pull-in and lock-in ranges are infinite.*

*Proof.* The proof of Theorem 2 is given in **PIII** and is based on phase portrait analysis of the system with discontinuous phase detector characteristics.

First, the hold-in and the pull-in ranges are considered. The first is infinite as equilibria of the system exist for any phase errors. To prove the pull-in range is infinite, a generalization of classic LaSalle's invariance principle for periodic functions with infinite number of equilibria is used (see Leonov and Kuznetsov (2014)). The principle requires one to construct a Lyapunov function (11).

$$V(\theta_e, y) = y^2 + \frac{2}{\tau_1}\int_0^{\theta_e} \tan\theta_e d\theta_e. \tag{11}$$

To study the lock-in range, phase plane trajectories are considered. Rigorous consideration of their behavior proves the fact that all of them tend to the equilibrium in the same band $-\frac{\pi}{2} + \pi n \leqslant \theta_e < \frac{\pi}{2} + \pi n$, $n \in \mathbb{Z}$ and cycle slipping is impossible. □

Complex implementation of the circuit allows one to construct a phase-locked loop with an infinite lock-in range.

[3] North American Aviation, Inc.

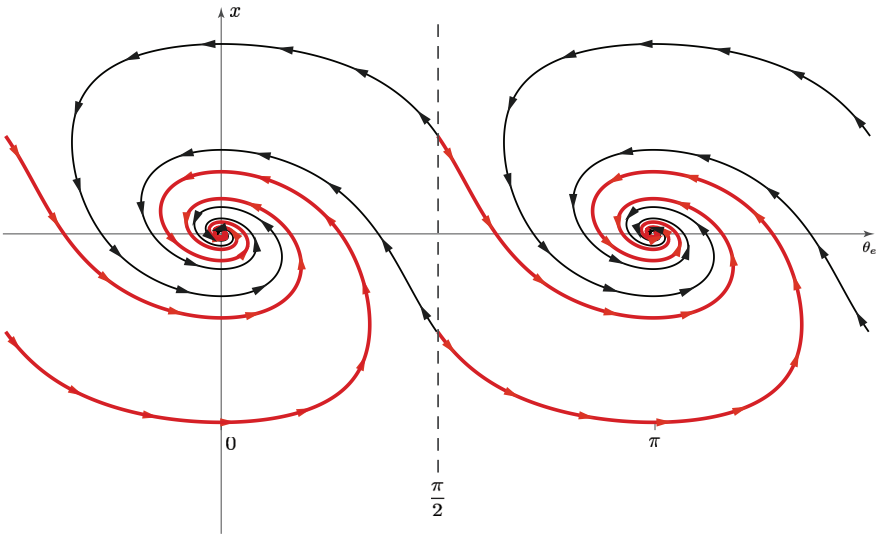


FIGURE 6 Phase portrait of PLL model with tangential phase detector characteristic.

## 2.4 Exact lock-in range for classical PLL with lead-lag filter and piecewise-linear phase detector characteristic

This chapter contains the main results related to the research question **RQ2**. For some analog applications, it is necessary to use stable filters (without poles at the origin) (Shakhgil'dyan and Lyakhovkin (1972); Best (2007, 2018)). In such cases, a stable filter is used. Consider such a filter with a transfer function $F(s) = \frac{1+\tau_2 s}{1+(\tau_1+\tau_2)s}$, where $\tau_1 > \tau_2 > 0$ are filter parameters (see e.g. (Best (2007, 2018)) for the physical meaning of them), which is called a lead-lag filter. In this case, system (4) takes form

$$\begin{cases} \dot{x} = -\dfrac{1}{\tau_1+\tau_2}x + \dfrac{\tau_1}{\tau_1+\tau_2}\varphi(\theta_e), \\ \dot{\theta}_e = \omega_e^{\text{free}} - K_{\text{vco}}\left(\dfrac{1}{\tau_1+\tau_2}x + \dfrac{\tau_2}{\tau_1+\tau_2}\varphi(\theta_e)\right). \end{cases} \tag{12}$$

Consider the piecewise-linear phase detector characteristic (6).

**Theorem 3.** *The lock-in frequency of model* (12) *with triangular PD characteristic* (6) *is*

*$\omega_l$, which is the unique solution of the system of two variables $(\omega_l,\ y_{\mathrm{AB}})$:*

$$
\begin{cases}
(2\omega_l)^2\left(\sqrt{\frac{\tau_1+\tau_2}{kK_{\mathrm{vco}}}}-\frac{\eta-\kappa}{kK_{\mathrm{vco}}}\right)^{\frac{\kappa-\eta}{\kappa}}\left(\sqrt{\frac{\tau_1+\tau_2}{kK_{\mathrm{vco}}}}-\frac{\eta+\kappa}{kK_{\mathrm{vco}}}\right)^{\frac{\kappa+\eta}{\kappa}}= \\
=\left(y_{\mathrm{AB}}-(\eta-\kappa)\frac{\omega_l+K_{\mathrm{vco}}}{kK_{\mathrm{vco}}}\right)^{\frac{\kappa-\eta}{\kappa}}\left(y_{\mathrm{AB}}-(\eta+\kappa)\frac{\omega_l+K_{\mathrm{vco}}}{kK_{\mathrm{vco}}}\right)^{\frac{\kappa+\eta}{\kappa}}, \\
\begin{cases}
\left(y_{\mathrm{AB}}-(\xi-\rho)\frac{\omega_l+K_{\mathrm{vco}}}{kK_{\mathrm{vco}}}\right)^{\frac{\rho-\xi}{\rho}}\left(y_{\mathrm{AB}}-(\xi+\rho)\frac{\omega_l+K_{\mathrm{vco}}}{kK_{\mathrm{vco}}}\right)^{\frac{\rho+\xi}{\rho}}= \\
=(\kappa-\eta+\xi-\rho)^{\frac{\rho-\xi}{\rho}}(\kappa-\eta+\xi+\rho)^{\frac{\rho+\xi}{\rho}}\left(\frac{K_{\mathrm{vco}}-\omega_l}{kK_{\mathrm{vco}}}\right)^2, \quad \textit{if} \quad \xi>1, \\
\frac{-\frac{K_{\mathrm{vco}}+\omega_l}{kK_{\mathrm{vco}}}}{y_{\mathrm{AB}}-\frac{K_{\mathrm{vco}}+\omega_l}{kK_{\mathrm{vco}}}}+\ln(2|y_{\mathrm{AB}}-\frac{K_{\mathrm{vco}}+\omega_l}{kK_{\mathrm{vco}}}|)= \\
=\frac{1}{\kappa-\eta+1}+\ln\left(2(\kappa-\eta+1)\frac{K_{\mathrm{vco}}-\omega_l}{kK_{\mathrm{vco}}}\right), \quad \textit{if} \quad \xi=1, \\
\frac{1}{2}\ln(y_{\mathrm{AB}}^2-2\xi y_{\mathrm{AB}}\frac{K_{\mathrm{vco}}+\omega_l}{kK_{\mathrm{vco}}}+(\frac{K_{\mathrm{vco}}+\omega_l}{kK_{\mathrm{vco}}})^2)-\frac{\xi}{\rho}\arctan\left(\frac{y_{\mathrm{AB}}-\xi\frac{K_{\mathrm{vco}}+\omega_l}{kK_{\mathrm{vco}}}}{-(\frac{K_{\mathrm{vco}}+\omega_l}{kK_{\mathrm{vco}}})\rho}\right)= \\
=\frac{1}{2}\ln\left(\left((\kappa-\eta)^2+2\xi(\kappa-\eta)+1\right)\left(\frac{K_{\mathrm{vco}}-\omega_l}{kK_{\mathrm{vco}}}\right)^2\right)- \\
-\frac{\xi}{\rho}\arctan\left(\frac{\kappa-\eta+\xi}{\rho}\right)+\frac{\pi\xi}{\rho}, \quad \textit{if} \quad \xi<1
\end{cases}
\end{cases}
\tag{13}
$$

*where*

$$
\begin{aligned}
\xi &= \frac{k\tau_2K_{\mathrm{vco}}+1}{2\sqrt{kK_{\mathrm{vco}}(\tau_1+\tau_2)}}, \\
\eta &= \frac{k\tau_2K_{\mathrm{vco}}-\mu}{2\sqrt{kK_{\mathrm{vco}}(\tau_1+\tau_2)}}, \\
\mu &= \pi k-1, \\
\rho &= \sqrt{|\xi^2-1|}, \\
\kappa &= \sqrt{\eta^2+\mu}.
\end{aligned}
$$

*Proof.* The proof of Theorem 3 is given in **PII** and is based on the same ideas as proof of Theorem 1. □

Based on Theorem 3, an analytical-numerical method of the lock-in range calculation is implemented, and diagrams of the lock-in range useful for engineering practice (see e.g. (Belyustina et al. (1972))) are composed (see. FIGURE 7).

The comparison of the obtained estimates is given in FIGURE 8. Here, the lock-in range estimates obtained in this dissertation are compared with the linear estimate by R.E. Best (Best (2007, 2018)).

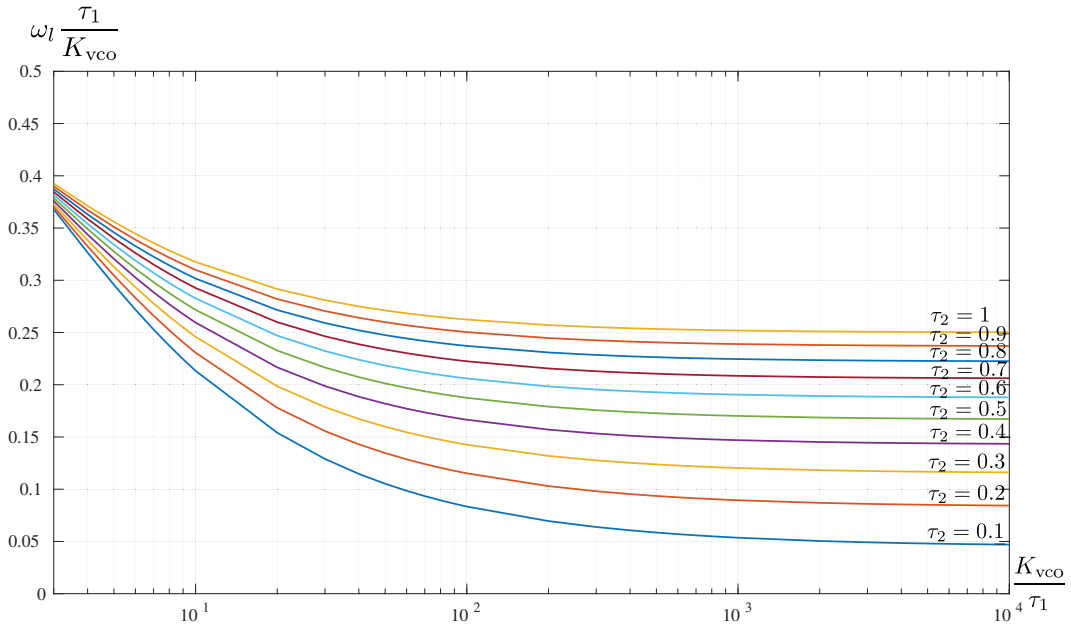


FIGURE 7 The lock-in range of PLL with a lead-lag filter (12) and triangular characteristic of phase detector (6) for fixed $\tau_1$.

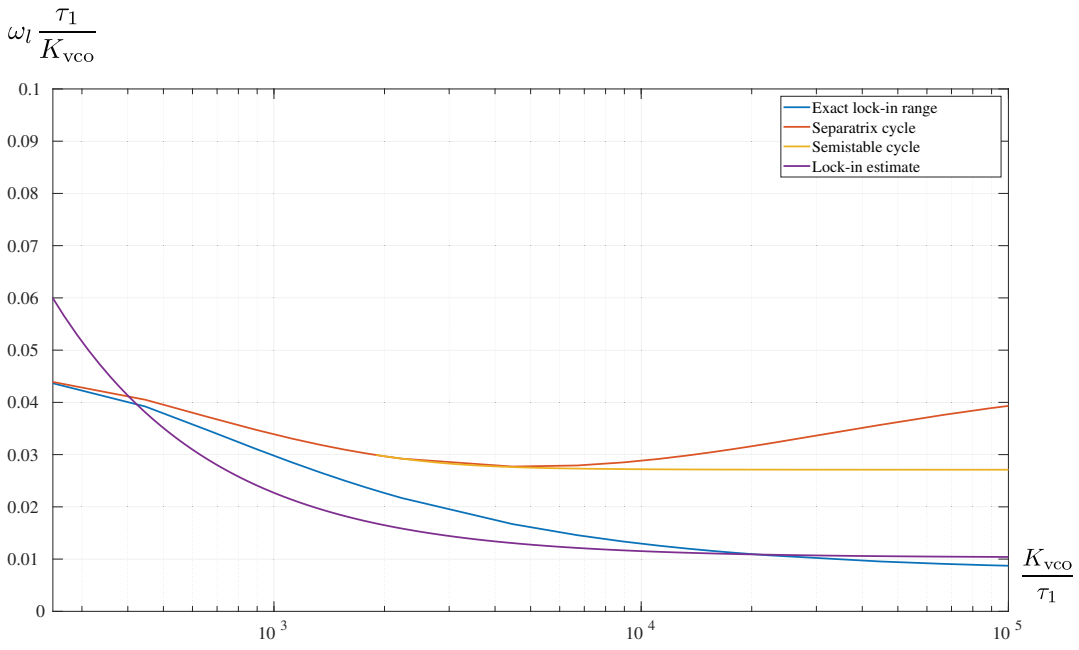


FIGURE 8 Comparison of the obtained lock-in range with earlier known results (Best (2007, 2018)) and the pull-in range (**PV**,Gubar' (1961); Shakhtarin (1969); Belyustina et al. (1972)). The diagram is given for $\tau_2 = 0.0185$. Parameters below the red and yellow lines correspond to global stability, pull-in range. The blue line is the estimate of an exact lock-in range obtained in this dissertation, and the purple line is the linear estimate of the lock-in range by R.E. Best. Note that the linear estimate is more conservative for some cases and is not valid for others.

# 3 INCLUDED ARTICLES AND AUTHOR'S CONTRIBUTION

The main results were published in the five included articles.

In **PI** (N.V. Kuznetsov, D.G. Arseniev, M.V. Blagov, Z. Wei, M.Y. Lobachev, M.V. Yuldashev, R.V. Yuldashev. The Gardner problem and cycle slipping bifurcation for type 2 phase-locked loops. Int. J. Bifurcation and Chaos, 2022 (accepted)), the author obtained an exact analytic formula for the lock-in range of PLL with an active PI filter and piecewise-linear characteristic of the phase detector and provided numerical calculations of the lock-in range.

In **PIII** (M.V. Blagov, N.V. Kuznetsov, M.Y. Lobachev, M.V. Yuldashev, R.V. Yuldashev. The conservative lock-in range for PLL with lead-lag filterand triangular phase detector characteristic. arXiv:2112.01602, 2021), the author proved that the lock-in range of PLL with an active PI filter and tangential phase detector characteristic is infinite.

In **PII** (M.V. Blagov, O.A. Kuznetsova, E.V. Kudryashova, N.V. Kuznetsov, T.N. Mokaev, R.N. Mokaev, M.V. Yuldashev, R.V. Yuldashev. Hold-in, Pull- in and Lock-in Ranges for Phase-locked Loop with Tangential Characteristic of the Phase Detector. Procedia Computer Science, Vol. 150, pp. 558–566, 2019), the author obtained an exact analytic formula for the lock-in range of PLL with lead-lag filter and a triangular characteristic of the phase detector.

In **PIV** (M.V. Blagov, E.V. Kudryashova, N.V. Kuznetsov, G.A. Leonov, M.V. Yuldashev, R.V. Yuldashev. Computation of lock-in range for classic PLL with lead-lag filter and impulse signals. IFAC-PapersOnLine, Vol. 49, I. 14, pp. 42–44, 2016) and **PV** (M.V. Blagov, N.V. Kuznetsov, G.A. Leonov, M.V. Yuldashev, R.V. Yuldashev. Simulation of PLL with impulse signals in MATLAB: Limitations, hidden oscillations, and pull-in range. 2015 7th International Congress on Ultra Modern Telecommunications and Control Systems and Workshops (ICUMT), pp. 85–90, 2015) initial numerical estimates of the lock-in range and pull-in range for classical phase-locked loop with lead-lag filter were obtained by the author.

In all the above publications, the author's contribution is proving analytical theorems (obtaining exact analytic formulas for the lock-in range) and numerical modeling.

The results of the study were also reported at the 7th International Congress on Ultra Modern Telecommunications and Control Systems and Workshops (Brno, Czech Republic, 2015), 13th International Symposium «Intelligent Systems 2018» (Saint-Petersburg, Russia, 2018), 11th Russian multiconference on control (Saint-Petersburg, Russia, 2018), 11th IFAC Symposium on Nonlinear Control Systems (Vienna, Austria, 2019), 13th Russian conference on control (Moscow, Russia, 2019), at the seminars of the Department of Applied Cybernetics (St. Petersburg State University, Russia), and at the seminars of the Faculty of Information Technology (University of Jyväskylä, Finland).

# 4 CONCLUSION AND DISCUSSION

This dissertation is devoted to the study of classical PLL systems with PI and lead-lag filters, which are widely used in modern engineering applications in electrical grids (Karimi-Ghartemani (2014); Kuznetsov et al. (2021b,a)), satellite communications systems (Best (2007, 2018)), and gyroscopy (Senkal and Shkel (2020); Kuznetsov et al. (2022)).

Answers to all the research questions were given:

**RQ1** Well-known approximate estimates of the lock-in range by R.E. Best (Best (2007, 2018)) and K.D. Aleksandrov (Aleksandrov (2016)) were refined using the rigorous analytical methods for phase-locked loops with active proportionally-integrating filter and the piecewise-linear phase detector characteristic. The estimate of the lock-in range by R.E. Best is not valid in general and may cause incorrect conclusions about phase-locked loop behavior.

**RQ2** Similar approximate estimates of the lock-in range by R.E. Best (Best (2007, 2018)) were refined for phase-locked loops with the lead-lag filter and piecewise-linear phase detector characteristic. The estimate of the lock-in range by R.E. Best is not valid in general and may cause incorrect conclusions about phase-locked loop behavior.

**RQ3** The lock-in range of a classical phase-locked loop with a proportionally-integrating filter and tangential phase detector characteristic was proven to be infinite.

The obtained diagrams of the lock-in range can be used for the synthesis and design of phase-lock loops in various applications. Despite this, there is room for further development of the theory and algorithms. As the next step of the research, the lock-in range for a phase-locked loop with discontinuous sawtooth phase detector characteristics can be calculated for given filters. Furthermore, the same approach to study the lock-in range can be applied to phase-locked loops with higher-order filters and piecewise-linear phase detector characteristics.

# YHTEENVETO (SUMMARY IN FINNISH)

Tässä väitöskirjassa tutkittiin monissa sovelluksissa, kuten sähköverkoissa, satelliittiviestinnässä tai gyroskoopeissa, käytettäviä vaihelukittuja silmukoita ((phase-locked loop, PLL))ja niiden synkronotumista, kun silmukoissa käytetään yleisiä suhteellisesti integroivia (PI) ja johdinviive suodattimia.

Keskeiset tutkimuskysymykset liittyvät silmukoiden kykyyn synkronoitua ohjaavan signaalin taajuusmuutoksiin. Tähän liittyviä käsitteitä ovat 'pull in' -alue, (taajuusväli, jonka sisällä pysyvistä häiriöistä silmukka ylipäätään toipuu synkrooniin), sekä lukitusalue ('lock-in', jonka sisällä yhtään tahtia ei jää väliin synkronoitumisen aikana. Näihin liittyviä konkreettisia tutkimuskysymyksiä ovat:

**RQ1** Onko vaihelukitun silmukan lukitusalueen koolle aiemmin esitetty arvio (Best (2007, 2018)) yleisesti voimassa. Voidaanko sitä tarkentaa epälineaarisen analyysin keinoin tyypillisessä sovellustilanteessa, jossa käsitellään suorakaidepulsseja ja paloittain lineaarisia vaihetunnistimia sekä PI-suodattimia.

**RQ2** Onko vastaava lukitussalueelle esitetty arvio (Best (2007, 2018)) yleisesti voimassa silmukoille, joita suodatetaan stabiileilla johdinviivesuodattimilla.

**RQ3** Voiko vaihelukitun silmukan lukitusalue olla ääretön. Egan (2011) on esittänyt konjektuurin, jonka mukaan tietyissä tilanteissa faasilukitut silmukat pystyvät toipumaan mielivaltaisen suurista häiriöistä eli niiden 'pull-in' alue on äärettömän suuri. Päteekö tämä myös lukitusalueille.

Työssä annetaan vastaukset kaikkiin tutkimuskysymyksiin:

**RQ1** R.E. Bestin ja K.D. Aleksandrovin aiemmin esittämiä arvioita tarkennettiin johtamalla analyyttisesti tarkat lausekkeet lukitusalueen koolle vaihelukittuille silmukoille, joissa on aktiivinen suhteellisesti integroiva suodatin ja paloittain lineaarinen vaiheilmaisin. R.E. Bestin esittämä arvio lukitusalueesta ei ole yleisesti ottaen pätevä ja voi aiheuttaa vääriä johtopäätöksiä vaihelukitun silmukan käyttäytymisestä.

**RQ2** R.E. Bestin aiemmat likimääräiset arviot lukitusalueesta tarkennettiin vaihelukittuille silmukoille, joissa on johdinviivesuodatin ja paloittain lineaarinen vaiheilmaisin. R.E. Bestin arvio lukitusalueesta ei ole yleisesti ottaen pätevä ja voi aiheuttaa vääriä johtopäätöksiä vaihelukitun silmukan käyttäytymisestä.

**RQ3** Klassisen vaihelukitun silmukan, jossa on suhteellisesti integroiva suodatin ja tangentiaalinen vaiheilmaisin, lukitusalue osoitettiin äärettömäksi.

Työssä johdettuja tarkkoja kaavioita lukitusalueesta voidaan käyttää vaihelukitussilmukoiden synteesiin ja suunnitteluun eri sovelluksissa.

Tästä huolimatta teorian ja algoritmien kehittämisen varaa on edelleen.

Tutkimuksen seuraavana vaiheena voidaan laskea annetuille suodattimille lukitusalue vaihelukitulle silmukalle, jossa on epäjatkuva paloittain lineaarinen

vaiheilmaisin. Lisäksi samaa lähestymistapaa lukitusalueen tutkimiseen voidaan soveltaa vaihelukittuihin silmukoihin, joissa on korkeamman asteen suodattimet ja paloittain lineaarinen vaiheilmaisin.

## REFERENCES


Aaltonen, L. & Halonen, K. A. I. 2010. An analog drive loop for a capacitive MEMS gyroscope. Analog Integrated Circuits and Signal Processing 63 (3), 465 – 476. doi:10.1007/s10470-009-9395-6. ⟨URL:https://doi.org/10.1007/s10470-009-9395-6⟩.

Abramovitch, D. 2002. Phase-locked loops: A control centric tutorial. In American Control Conf. Proc., Vol. 1. IEEE, 1–15.

Aleksandrov, K. (Ed.) 2016. Phase-Locked Loops withActive PI Filter: the Lock-InRange Computation. Jyväskylä University Printing House. Jyväskylä studies in computing 239.

Andronov, A. & Khaikin, S. 1937. Theory of oscillations. M.-L.: ONTI. ([English transl.: Andronov A.A., Chaikin S.E. Theory of Oscillations. Princeton University Press. 1949]).

Appleton, E. 1923. Automatic synchronization of triode oscillators. Proc. Cambridge Phil. Soc. 21 (3), 231.

Bakaev, Y. 1959. Some questions of nonlinear theory of phase systems. Works of VVIA N.E. Zhukovsky 800.

Bakaev, Y. 1960. Construction of working zones and phase control systems. Izv. Akad. Nauk SSSR (in Russian) 2, 132–136.

Baker, R. 2011. CMOS: Circuit Design, Layout, and Simulation, Vol. 18. John Wiley & Sons. IEEE Press Series on Microelectronic Systems.

Bakshi, U. & Godse, A. 2009. Linear ICs and applications. Technical Publications.

Bellescize, H. 1932. La réception synchrone. L'onde Électrique 11, 230-340.

Belyustina, L., Kiveleva, G. & Shalfeev, V. 1972. Application of a computer to calculation if the pull-in range of nonlinear pll systems. Radiofizika (in Russian) 27 (7), 36-39.

Belyustina, L. 1959. The study of a nonlinear pll system. Izv. vuzov. Radiofizika (in Russian) 2 (2), 277–291.

Best, R., Kuznetsov, N., Leonov, G., Yuldashev, M. & Yuldashev, R. 2016. Tutorial on dynamic analysis of the Costas loop. IFAC Annual Reviews in Control 42, 27–49. doi:10.1016/j.arcontrol.2016.08.003.

Best, R. 1984. Phase-locked Loops: Design, Simulation, and Applications. McGraw Hill.

Best, R. 2007. Phase locked loops: design, simulation, and applications. McGraw-Hill Professional.

Best, R. 2018. Costas Loops: Theory, Design, and Simulation. Springer International Publishing.

Blanchard, A. 1976. Phase-Locked Loops. Wiley.

Cho, P. 2006. Optical phase-locked loop performance in homodyne detection using pulsed and CW LO. In Optical Amplifiers and Their Applications/Coherent Optical Technologies and Applications. Optical Society of America, JWB24.

Craninckx, J. & Steyaert, M. 1998. Wireless CMOS Frequency Synthesizer Design. Springer.

De Muer, B. & Steyaert, M. 2003. CMOS Fractional-N Synthesizers: Design for High Spectral Purity and Monolithic Integration. Springer.

Du, K. & Swamy, M. 2010. Wireless Communication Systems: from RF subsystems to 4G enabling technologies. Cambridge University Press.

Dyer, S. 2004. Wiley Survey of Instrumentation and Measurement. Wiley.

Egan, W. 2007. Phase-Lock Basics (2nd edition). New York: John Wiley & Sons.

Egan, W. 2011. Advanced frequency synthesis by phase lock. John Wiley & Sons.

Gardner, F. 1966. Phaselock Techniques. New York: John Wiley & Sons, 182.

Gardner, F. 2005. Phaselock Techniques (3rd edition). New York: John Wiley & Sons, 550.

Gelig, A., Leonov, G. & Yakubovich, V. 1978. Stability of Nonlinear Systems with Nonunique Equilibrium (in Russian). Nauka. ((English transl: Stability of Stationary Sets in Control Systems with Discontinuous Nonlinearities, 2004, World Scientific)).

George, T. 1951. Analysis of synchronizing systems for dot-interlaced color television. Proceedings of the IRE 39 (2), 124–131.

Goldman, S. 2007. Phase-Locked Loops Engineering Handbook for Integrated Circuits. Artech House.

Gruen, W. 1953. Theory of afc synchronization. Proceedings of the IRE 8 (41), 1043–1048.

Gubar', N. 1961. Investigation of a piecewise linear dynamical system with three parameters. Journal of Applied Mathematics and Mechanics 25 (6), 1011-1023.

Helaluddin, G. M. 2008. An improved optical Costas loop PSK receiver: simulation analysis. Journal of Scientific & Industrial Research 67, 203-208.

Ho, K. 2005. Phase-Modulated Optical Communication Systems. Springer.

Hsieh, G. & Hung, J. 1996. Phase-locked loop techniques. A survey. Industrial Electronics, IEEE Transactions on 43 (6), 609-615.

Huque, A. & Stensby, J. 2013. An analytical approximation for the pull-out frequency of a PLL employing a sinusoidal phase detector. ETRI Journal 35 (2), 218–225.

Irwin, J. 1997. The Industrial Electronics Handbook. Taylor & Francis.

Kaplan, E. & Hegarty, C. 2017. Understanding GPS/GNSS: Principles and Applications (3rd edition). Artech House.

Kapranov, M. 1956. The lock-in band of a phase locked loop. Radiotekhnika (in Russian) 11 (12), 37–52.

Karimi-Ghartemani, M. 2014. Enhanced phase-locked loop structures for power and energy applications. John Wiley & Sons.

Kihara, M., Ono, S. & Eskelinen, P. 2002. Digital Clocks for Synchronization and Communications. Artech House, 269.

Kolumbán, G. 2005. The Encyclopedia of RF and Microwave Engineering, Vol. 4. New-York: John Wiley & Sons, 3735–3767.

Kroupa, V. 2012. Frequency Stability: Introduction and Applications. Wiley-IEEE Press. IEEE Series on Digital & Mobile Communication, 328.

Kudryashova, E. (Ed.) 2009. Cycles in Continuousand Discrete Dynamical SystemsComputations, Computer-assisted Proofs,and Computer Experiments. Jyvaskyla University Printing House. Jyväskylä studies in computing 107.

Kuznetsov, N., Belyaev, Y., Styagkina, A., Tulaev, A., Yuldashev, M. & Yuldashev, R. 2022. Estimation of PLL impact on MEMS-gyroscopes parameters. Gyroscopy and Navigation. ((in print)).

Kuznetsov, N., Leonov, G., Yuldashev, M. & Yuldashev, R. 2015. Rigorous mathematical definitions of the hold-in and pull-in ranges for phase-locked loops. IFAC-PapersOnLine. 48 (11), 710-713.

Kuznetsov, N., Lobachev, M., Yuldashev, M., Yuldashev, R., Volskiy, S. & Sorokin, D. 2021a. Automatic control of inverters in electrical networks: Capture range and cycle slipping. Journal of Physics: Conference Series 1864. doi:10.1088/1742-6596/1864/1/012063. (art. num. 012063).

Kuznetsov, N., Lobachev, M., Yuldashev, M., Yuldashev, R., Volskiy, S. & Sorokin, D. 2021b. On the generalized Gardner problem for phase-locked loops in electrical grids. Doklady Mathematics 103 (3), 157–161.

Kuznetsov, N., Lobachev, M., Yuldashev, M. & Yuldashev, R. 2021c. The Egan problem on the pull-in range of type 2 PLLs. Transactions on Circuits and Systems II: Express Briefs 68 (4), 1467–1471. doi:10.1109/TCSII.2020.3038075.

Kuznetsov, N., Mokaev, T., Kudryashova, E., Kuznetsova, O. & Danca, M.-F. 2019. On lower-bound estimates of the Lyapunov dimension and topological entropy for the Rossler systems. IFAC-PapersOnLine 52 (18), 97-102.

Kuznetsov, N., Volskiy, S., Sorokin, D., Yuldashev, M. & Yuldashev, R. 2020. Power supply system for aircraft with electric traction. In 2020 21st International Scientific Conference on Electric Power Engineering (EPE), 1-5. doi: 10.1109/EPE51172.2020.9269181.

Kuznetsov, N. 2008. Stability and Oscillations of Dynamical Systems: Theory and Applications. Jyvaskyla University Printing House. Jyväskylä studies in computing 96.

Leonov, G., Kuznetsov, N., Yuldashev, M. & Yuldashev, R. 2015a. Computation of the phase detector characteristic of classical pll. Doklady Mathematics 91 (2), 246-249.

Leonov, G., Kuznetsov, N., Yuldashev, M. & Yuldashev, R. 2015b. Hold-in, pull-in, and lock-in ranges of pll circuits: rigorous mathematical definitions and limitations of classical theory. IEEE Transactions on Circuits and Systems I: Regular Papers. 62, 2454-2464.

Leonov, G. & Kuznetsov, N. 2014. Nonlinear mathematical models of phase-locked loops. Stability and oscillations. Cambridge Scientific Publishers.

Leonov, G. A. 1976. A certain class of dynamical systems with cylindrical phase space. Siberian Math. J. 17, 72-90.

Leonov, G. A. 1971. Concerning stability of nonlinear controlled systems with non-single equilibrium state. Automation and Remote Control 32 (10), 1547–1552.

Middlestead, R. 2017. Digital Communications with Emphasis on Data Modems: Theory, Analysis, Design, Simulation, Testing, and Applications. Wiley.

Pederson, D. & Mayaram, K. 2008. Analog Integrated Circuits for Communication: Principles, Simulation and Design. Springer.

Richman, D. 1953. Theory of synchronization, applied to ntsc color television. In Proceedings of the IRE, Vol. 41, 403–403.

Richman, D. 1954. Color-carrier reference phase synchronization accuracy in ntsc color television. Proceedings of the IRE 42 (1), 106–133.

Robinson, L. 1965. Phase-lock receivers. (US Patent 3,204,185).

Rosenkranz, W. & Schaefer, S. 2016. Receiver design for optical inter-satellite links based on digital signal processing. In 18th International Conference on Transparent Optical Networks (ICTON). IEEE, 1–4.

Rouphael, T. 2014. Wireless Receiver Architectures and Design: Antennas, RF, Synthesizers, Mixed Signal, and Digital Signal Processing. Elsevier Science.

Senkal, D. & Shkel, A. 2020. Whole-Angle MEMS Gyroscopes: Challenges and Opportunities. Wiley. IEEE Press Series on Sensors. ⟨URL:https://books.google.fi/books?id=WpreDwAAQBAJ⟩.

Shakhgil'dyan, V. & Lyakhovkin, A. 1966. Fazovaya avtopodstroika chastoty (in Russian) (1st edition). Moscow: Svyaz'.

Shakhgil'dyan, V. & Lyakhovkin, A. 1972. Sistemy fazovoi avtopodstroiki chastoty (in Russian) (2nd edition). Moscow: Svyaz'.

Shakhtarin, B. 1969. Study of a piecewise-linear system of phase-locked frequency control. Radiotechnica and electronika (in Russian) 8, 1415-1424.

Shu, K. & Sanchez-Sinencio, E. 2005. CMOS PLL synthesizers: analysis and design. Springer.

Stensby, J. 1997. Phase-Locked Loops: Theory and Applications. Taylor & Francis, 382.

Talbot, D. 2012. Frequency Acquisition Techniques for Phase Locked Loops. Wiley-IEEE Press.

Tranter, W., Bose, T. & Thamvichai, R. 2010. Basic Simulation Models of Phase Tracking Devices Using MATLAB. Morgan & Claypool. Synthesis lectures on communications.

Tricomi, F. 1933. Integrazione di unequazione differenziale presentatasi in elettrotechnica. Annali della R. Shcuola Normale Superiore di Pisa 2 (2), 1-20.

Viterbi, A. 1966. Principles of coherent communications. New York: McGraw-Hill, 321.

Wendt, K. & Fredentall, G. 1943. Automatic frequency and phase control of synchronization in TV receivers. Proc. IRE 31 (1), 1-15.

Wolaver, D. 1991. Phase-locked Loop Circuit Design. Prentice Hall.

Yuldashev, M. (Ed.) 2013a. Mathematical Models and Simulation of Costas Loops. Jyväskylä University Printing House. Jyväskylä studies in computing 174.

Yuldashev, R. (Ed.) 2013b. Synthesis of Phase-Locked Loop. Analytical Methods and Simulation. Jyväskylä University Printing House. Jyväskylä studies in computing 175.

## APPENDIX 1 COMPUTATION OF THE EXACT LOCK-IN RANGE FOR PLL WITH PI FILTER

Calculation of the lock-in frequency for PLL with PI filter (5) and triangular phase-detector characteristic (6) ($k = \frac{2}{\pi}$).

```
function omega_l = omega_l_formula_pi(tau_1, tau_2, k, K_vco)
%omega_l_formula_pi Calculates the lock-in
%frequency for classical PLL with PI
%filter

a = sqrt(K_vco/tau_1)*tau_2;
b = sqrt(abs(a.^2-4/k));
c = sqrt(a.^2-4/k + 4*pi);

syms y;

if (a^2*k < 4)
    fcn = (y^2 - a*y + 1/k) * ...
        exp( 2*a/b*atan(b/(a - 2*y))) -...
        pi*exp(2*a/b*atan(b/c));
    d = vpasolve(fcn, y, [a/2 Inf]);
else
    if abs(a^2*k - 4) < 0.001
        d = a/2*(1 + 1/(lambertw(a/(2*sqrt(pi)))*...
        exp(-a/(2*sqrt(pi)))));
    else
        fcn = (y - (a-b)/2)^((b-a)/(b))*...
            (y - (a+b)/2)^((b+a)/(b)) ...
            - pi*((c+b)/(c-b))^(a/b);
        d= vpasolve(fcn, y, [(a+b)/2 Inf]);
    end
end

omega_l = 1/2*sqrt((K_vco*(d + (c-a)/2)^((c-a)/c)*...
    (d - (c+a)/2)^((c+a)/c))/tau_1);

end
```

## APPENDIX 2 COMPUTATION OF THE EXACT LOCK-IN RANGE FOR PLL WITH LEAD-LAG FILTER

Calculation of the lock-in frequency for PLL with lead-lag filter (12) and triangular phase-detector characteristic (6) ($k = \frac{2}{\pi}$).

```
function out = omega_l_conservative(tau_1, tau_2, k, K_vco)

    out = 0;
    mu = pi*k - 1;
    xi = (k*tau_2*K_vco + 1)/(2*sqrt(k*K_vco*(tau_1 + tau_2)));
    eta = (k*tau_2*K_vco - mu)/(2*sqrt(k*K_vco*(tau_1 + tau_2)));
    rho = sqrt(abs(xi^2 - 1));
    kappa = sqrt(eta^2 + mu);

    syms y_ab zomega_lc;

    curve1 = (2*zomega_lc)^2*...
        (sqrt((tau_1 + tau_2)/(k*K_vco)) - ...
        (eta - kappa)/(k*K_vco))^((kappa - eta)/kappa)*...
        (sqrt((tau_1 + tau_2)/(k*K_vco)) - ...
        (eta + kappa)/(k*K_vco))^((kappa + eta)/kappa)  == ...
        (y_ab - (eta - kappa)*((zomega_lc + K_vco)/...
        (k*K_vco)))^((kappa - eta)/kappa)*...
        (y_ab - (eta + kappa)*((zomega_lc + K_vco)/...
        (k*K_vco)))^((kappa + eta)/kappa);

    if xi > 1
        curve2 = (y_ab - (xi - rho)*...
            ((zomega_lc + K_vco)/...
            (k*K_vco)))^((rho - xi)/(rho))*...
            (y_ab - (xi + rho)*...
            ((zomega_lc + K_vco)/(k*K_vco)))^...
                ((rho + xi)/(rho)) == ...
            (kappa - eta + xi - rho)^((rho - xi)/...
            (rho))*(kappa - eta + xi + rho)^...
                ((rho + xi)/(rho))*...
            ((K_vco - zomega_lc)/(k*K_vco))^2;
    else
        if (abs(xi - 1) < 0.001)
            curve2 = (-(K_vco + zomega_lc)/...
            (k*K_vco))/...
            (y_ab -(K_vco + zomega_lc)/(k*K_vco)) + ...
                log(2*abs(y_ab -(K_vco + zomega_lc)/...
                    (k*K_vco))) == ...
                1/(kappa - eta + 1) + ...
```

```
                ln(2*(kappa - eta + 1)*...
                    (K_vco - zomega_lc)/(k*K_vco));
        else
            curve2 = 1/2*log(y_ab^2 - ...
                2*xi*y_ab*(K_vco + zomega_lc)/...
            (k*K_vco) + ((K_vco + zomega_lc)/(k*K_vco))^2) -...
                xi/rho*atan((y_ab - xi*...
                    (K_vco + zomega_lc)/(k*K_vco))/...
                (-(K_vco + zomega_lc)/(k*K_vco)*rho)) == ...
            1/2*log(...
            ((kappa - eta)^2 + 2*xi*(kappa-eta) + 1)*...
            ((K_vco - zomega_lc)/(k*K_vco))^2 ...
            ) - xi/rho*atan((kappa - eta + xi)/rho) + pi*xi/rho;
        end
    end

    res = vpasolve([curve1, curve2], [0 Inf; 0 K_vco]);
    if ~isempty(eval(res.zomega_lc))
        out = eval(res.zomega_lc);
    end
end
```

# ORIGINAL PAPERS

# PI

## THE GARDNER PROBLEM AND CYCLE SLIPPING BIFURCATION FOR TYPE 2 PHASE-LOCKED LOOPS

by

N.V. Kuznetsov, D.G. Arseniev, M.V. Blagov, Z. Wei, M.Y. Lobachev, M.V. Yuldashev, R.V. Yuldashev 2022 (accepted), JuFo 1

Int. J. Bifurcation and Chaos

International Journal of Bifurcation and Chaos




# The Gardner problem and cycle slipping bifurcation for type 2 phase-locked loops

Nikolay V. Kuznetsov
*Faculty of Mathematics and Mechanics, Saint Petersburg State University, Russia*
*Faculty of Information Technology, University of Jyväskylä, Finland*
*Institute for Problems in Mechanical Engineering of the Russian Academy of Sciences, Russia*
*nkuznetsov239@gmail.com*

Dmitry G. Arseniev
*Peter the Great Saint Petersburg Polytechnic University, Russia*
*Saint Petersburg State University, Russia*

Mikhail V. Blagov
*Faculty of Mathematics and Mechanics, Saint Petersburg State University, Russia*
*Faculty of Information Technology, University of Jyväskylä, Finland*

Mikhail Y. Lobachev
*Faculty of Mathematics and Mechanics, Saint Petersburg State University, Russia*
*Industrial Management Department, LUT University, Finland*

Zhouchao Wei
*School of Mathematics and Physics, China University of Geosciences, China,*

Marat V. Yuldashev, Renat V. Yuldashev
*Faculty of Mathematics and Mechanics, Saint Petersburg State University, Russia*

Received (to be inserted by publisher)

In the present work, a second-order type 2 PLL with a piecewise-linear phase detector characteristic is analysed. An exact solution to the Gardner problem on the lock-in range is obtained for the considered model. The solution is based on a study of cycle slipping bifurcation and improves well-known engineering estimates.

*Keywords*: Phase-locked loop, PLL, type II PLL, type 2 PLL, Gardner problem, lock-in range, cycle slipping, Lyapunov functions, nonlinear analysis, global stability.

## 1. Introduction

Phase-locked loops (PLLs) are nonlinear control systems which are designed to synchronize a voltage-controlled oscillator (VCO) signal with a reference one. PLLs have many applications in energy and robotic systems, satellite navigation, wireless and optical communications, cyber-physical systems [Du & Swamy, 2010; Karimi-Ghartemani, 2014; Rosenkranz & Schaefer, 2016; Best *et al.*, 2016; Kaplan & Hegarty, 2017; Kuznetsov *et al.*, 2020c; Zelenskii *et al.*, 2021; Zelensky *et al.*, 2021; Kuznetsov *et al.*, 2022]. Analog PLLs can be described by systems of nonlinear differential equations with periodic right-hand sides, which are

also known as pendulum-like systems. In 1933, F. Tricomi was the first, who conducted nonlinear analysis [Tricomi, 1933] of the systems which are equivalent to the second-order PLLs with lag filters (see, e.g., [Gardner, 2005]). It was proven that the global stability of those systems is determined by separatrices of a saddle, which correspond to a heteroclinic bifurcation in the system. Further, bifurcations of the second-order PLLs with lead-lag filters and different nonlinear characteristics of phase detectors were studied in [Andronov *et al.*, 1937; Kapranov, 1956; Belyustina, 1959; Gubar', 1961; Shakhtarin, 1969].

PLL systems with lag and lead-lag loop filters can be classified as type 1 PLLs, because transfer functions of such filters do not have poles at the origin. In engineering practice, so-called type 2 PLLs, that have loop filters with exactly one pole at the origin, are most often used nowadays [Gardner, 2005]. The second-order type 2 analog PLLs are always globally stable (see, e.g., [Kuznetsov *et al.*, 2021a]), i.e., these PLLs acquire lock for any reference frequency. However, synchronization in the systems may take long time. In order to reduce the long acquisition time, the lock-in concept has been introduced. According to the concept, the locked PLL re-acquires a locked state without cycle slipping after an abrupt change of the reference frequency. The problem of estimation of the reference frequencies where the concept is held was posed by F. Gardner in his monograph [Gardner, 2005]. A rigorous approach to the Gardner problem and analytical estimates of the lock-in range were suggested in [Kuznetsov *et al.*, 2015, 2019b, 2021a,c,b].

The system where such abrupt reference frequency change occurs can be considered as a switching system. The Gardner problem requires to study cycle slipping bifurcation of the system when a trajectory, starting from an equilibrium of the system before the switch tends to an equilibrium of the system after the switch. This task is similar to the problem of the heteroclinic bifurcation estimation in type 1 PLL systems.

## 2. Mathematical Model and Stability Analysis

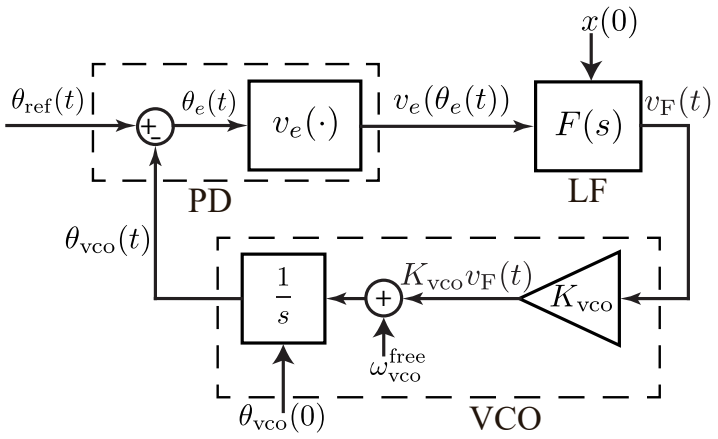


Fig. 1. Baseband model of analog PLLs.

Consider analog PLL baseband model in Fig. 1 [Gardner, 2005; Viterbi, 1966; Best, 2007; Leonov *et al.*, 2012, 2015b]. Here $\theta_{\rm ref}(t) = \omega_{\rm ref}t + \theta_{\rm ref}(0)$ is a phase of the reference signal, a phase of the VCO is $\theta_{\rm vco}(t)$, $\theta_e(t) = \theta_{\rm ref}(t) - \theta_{\rm vco}(t)$ is a phase error. A phase detector (PD) generates a signal $v_e(\theta_e(t))$ where $v_e(\cdot)$ is a characteristic of the phase detector. In the present paper, a piecewise-linear PD characteristic, which is continuous and corresponds to square waveforms of the reference and the VCO signals, is considered:

$$v_e(\theta_e) = \begin{cases} k\theta_e - 2\pi km, & -\frac{1}{k} + 2\pi m \le \theta_e(t) < \frac{1}{k} + 2\pi m, \\ -\frac{1}{\pi - \frac{1}{k}}\theta_e + \frac{1}{\pi - \frac{1}{k}}(\pi + 2\pi m), & \frac{1}{k} + 2\pi m \le \theta_e(t) < -\frac{1}{k} + 2\pi(m+1), \end{cases} \tag{1}$$

here $k > \frac{1}{\pi}$, $m \in \mathbb{Z}$ (see Fig. 2).

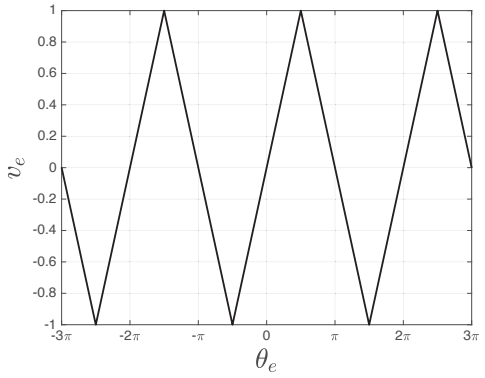


Fig. 2. Triangular PD characteristic (piecewise-linear PD characteristic (1) with $k = \frac{2}{\pi}$).

The state of the loop filter is represented by $x(t) \in \mathbb{R}$ and the transfer function is

$$F(s) = \frac{1 + s\tau_2}{s\tau_1}, \quad \tau_1 > 0,\ \tau_2 > 0.$$

The output of the loop filter $v_{\mathrm{F}}(t) = \frac{1}{\tau_1}(x(t) + \tau_2 v_e(\theta_e(t))$ is used to control the VCO frequency $\omega_{\mathrm{vco}}(t)$, which is proportional to the control voltage:

$$\omega_{\mathrm{vco}}(t) = \dot{\theta}_{\mathrm{vco}}(t) = \omega_{\mathrm{vco}}^{\mathrm{free}} + K_{\mathrm{vco}} v_{\mathrm{F}}(t)$$

where $K_{\mathrm{vco}} > 0$ is a gain and $\omega_{\mathrm{vco}}^{\mathrm{free}}$ is a free-running frequency of the VCO.

The behavior of PLL baseband model in the state space is described by a second-order nonlinear ODE:

$$\begin{aligned} \dot{x} &= v_e(\theta_e), \\ \dot{\theta}_e &= \omega_e^{\mathrm{free}} - \frac{K_{\mathrm{vco}}}{\tau_1}\Big(x + \tau_2 v_e(\theta_e)\Big) \end{aligned} \tag{2}$$

where $\omega_e^{\mathrm{free}} = \omega_{\mathrm{ref}} - \omega_{\mathrm{vco}}^{\mathrm{free}}$ is a frequency error and $v_e(\theta_e)$ is defined in (1). It is usually supposed that the reference frequency (hence, $\omega_e^{\mathrm{free}}$ too) can be abruptly changed and that the synchronization occurs between those changes. Thus, existence of locked states, acquisition and transient processes after the reference frequency change are of interest.

## 2.1. *Local stability analysis*

The PLL baseband model in Fig. 1 is locked if the phase error $\theta_e(t)$ is constant. For the locked states of practically used PLLs, the loop filter state is constant too and, thus, the locked states of model in Fig. 1 correspond to the equilibria of model (2) [Kuznetsov *et al.*, 2015].

**Definition 2.1.** [Kuznetsov *et al.*, 2015; Leonov *et al.*, 2015a; Best *et al.*, 2016] A *hold-in range* is the largest symmetric interval of frequency errors $|\omega_e^{\mathrm{free}}|$ such that an asymptotically stable equilibrium exists and varies continuously while $\omega_e^{\mathrm{free}}$ varies continuously within the interval.

Observe that system (2) is $2\pi$-periodic in $\theta_e$ and has an infinite number of equilibria $\Big(\frac{\tau_1\omega_e^{\mathrm{free}}}{K_{\mathrm{vco}}},\ \pi m\Big)$, $m \in \mathbb{Z}$. The characteristic polynomial of system (2) linearized at stationary states $\Big(\frac{\tau_1\omega_e^{\mathrm{free}}}{K_{\mathrm{vco}}}, \pi m\Big)$ is

$$\chi(s) = s^2 + \frac{K_{\mathrm{vco}}\tau_2}{\tau_1} v_e'(\pi m)s + \frac{K_{\mathrm{vco}}}{\tau_1} v_e'(\pi m).$$

The nonlinearity $v_e(\theta_e)$ decreases $\Big(v_e'(\pi + 2\pi m) = -\frac{1}{\pi - \frac{1}{k}} < 0\Big)$ for $\frac{1}{k} + 2\pi m < \theta_e(t) < -\frac{1}{k} + 2\pi(m+1)$, and equilibria $\Big(\frac{\tau_1\omega_e^{\mathrm{free}}}{K_{\mathrm{vco}}}, \pi + 2\pi m\Big)$ are saddles. The nonlinearity $v_e(\theta_e)$ increases $(v_e'(2\pi m) = k > 0)$ for

$-\frac{1}{k}+2\pi m<\theta_e(t)<\frac{1}{k}+2\pi m$, and the equilibria $\left(\frac{\tau_1\omega_e^{\text{free}}}{K_{\text{vco}}},2\pi m\right)$ are asymptotically stable:

- if $\frac{K_{\text{vco}}\tau_2^2 k}{\tau_1}>4$ then the equilibria $\left(\frac{\tau_1\omega_e^{\text{free}}}{K_{\text{vco}}},2\pi m\right)$ are asymptotically stable nodes,
- if $\frac{K_{\text{vco}}\tau_2^2 k}{\tau_1}=4$ then the equilibria $\left(\frac{\tau_1\omega_e^{\text{free}}}{K_{\text{vco}}},2\pi m\right)$ are asymptotically stable degenerate nodes,
- if $\frac{K_{\text{vco}}\tau_2^2 k}{\tau_1}<4$ then the equilibria $\left(\frac{\tau_1\omega_e^{\text{free}}}{K_{\text{vco}}},2\pi m\right)$ are asymptotically stable focuses.

Since an asymptotically stable equilibrium exists for any frequency error $\omega_e^{\text{free}}$, the hold-in range of model (2) is infinite for any loop parameters $K_{\text{vco}}>0,\ \tau_1>0,\ \tau_2>0$.

## 2.2. *Global stability analysis*

**Definition 2.2.** [Kuznetsov *et al.*, 2015; Leonov *et al.*, 2015a; Best *et al.*, 2016] A *pull-in range* is the largest symmetric interval of frequency errors $|\omega_e^{\text{free}}|$ from the hold-in range such that an equilibrium is acquired for an arbitrary initial state.

In 1959, Andrew J. Viterbi applied the phase-plane analysis and stated that the second-order type 2 PLL models with sinusoidal PD characteristic have infinite (theoretically) hold-in and pull-in ranges for any loop parameters [Viterbi, 1959, p.12], [Viterbi, 1966]. However, his proof was incomplete (see, e.g. discussion in [Alexandrov *et al.*, 2015]). Later, Viterbi's statement was rigorously proved using the direct Lyapunov method ideas [Bakaev, 1963; Aleksandrov *et al.*, 2016; Kuznetsov *et al.*, 2021a].

To analyse the pull-in range of system (2) with piecewise-linear PD characteristic, we apply the direct Lyapunov method and the corresponding theorem on global stability for the cylindrical phase space (see, e.g. [Leonov & Kuznetsov, 2014; Kuznetsov *et al.*, 2020b]). If there is a continuous function $V(x,\theta_e):\mathbb{R}^n\to\mathbb{R}$ such that

(i) $V(x,\theta_e+2\pi)=V(x,\theta_e)\quad\forall x\in\mathbb{R}^{n-1},\forall\theta_e\in\mathbb{R}$;

(ii) for any solution $(x(t),\theta_e(t))$ of system (2) the function $V(x(t),\theta_e(t))$ is nonincreasing;

(iii) if $V(x(t),\theta_e(t))\equiv V(x(0),\theta_e(0))$, then $(x(t),\theta_e(t))\equiv\ (x(0),\theta_e(0))$;

(iv) $V(x,\theta_e)+\theta_e^2\to+\infty$ as $||x||+|\theta_e|\to+\infty$

then any trajectory of system (2) tends to an equilibrium (for brevity, we shall call such systems *globally stable*).

Consider the following Lyapunov function:

$$V(x,\theta_e)=\frac{K_{\text{vco}}}{2\tau_1}\left(x-\frac{\tau_1\omega_e^{\text{free}}}{K_{\text{vco}}}\right)^2+\int_0^{\theta_e}v_e(\sigma)d\sigma. \tag{3}$$

Its derivative along the trajectories of system (2) is

$$\dot V(x,\theta_e)=-\frac{K_{\text{vco}}\tau_2}{\tau_1}v_e^2(\theta_e)<0\quad\forall\theta_e\neq\pi m,\ m\in\mathbb{Z}.$$

Since the derivative along any solution other than stationary states is not identically zero, system (2) is globally stable for any $\omega_e^{\text{free}}$ and, hence, the pull-in range is infinite.

In 1981, William F. Egan conjectured [Egan, 1981, p.176] that a higher-order *type 2 PLL with an infinite hold-in range also has an infinite pull-in range*, and supported it with some third-order PLL implementations (see also [Egan, 2007, p.161]). However, this conjecture is not valid in general and corresponding counterexamples were recently provided in [Kuznetsov *et al.*, 2021a].

Notice that a similar conjecture on the pull-in range for the second-order type 1 PLLs is known as *the Kapranov conjecture* [Kapranov, 1956], where it is supposed that the global stability of the corresponding model is determined by the birth of self-excited oscillations only, not hidden ones [Leonov & Kuznetsov, 2013; Chen *et al.*, 2017]. Discussions of counterexamples to the Kapranov conjecture can be found in [Kuznetsov *et al.*, 2017; Kuznetsov, 2020].

## 3. The lock-in range of second-order type 2 analog PLL with piecewise-linear PD characteristic

Although a PLL model can be globally stable with infinite pull-in range, the acquisition process can take long time. To decrease the synchronization time, a lock-in range concept is frequently exploited [Gardner, 2005; Kolumbán, 2005; Best, 2007].

**Definition 3.1.** [Kuznetsov *et al.*, 2015; Leonov *et al.*, 2015a; Best *et al.*, 2016] A *lock-in range* is the largest interval of frequency errors $|\omega_e^{\text{free}}|$ from the pull-in range such that the PLL model being in an equilibrium, after any abrupt change of $\omega_e^{\text{free}}$ within the interval acquires an equilibrium without cycle slipping ($\sup\limits_{t>0}|\theta_e(0)-\theta_e(t)|<2\pi$).

*Remark 3.1.* Sometimes the upper limit is considered in the cycle slipping definition instead of the supremum: $\limsup\limits_{t\to+\infty}|\theta_e(0)-\theta_e(t)| \geq 2\pi$. For any $\omega_e^{\text{free}}$ the following inequality is valid: $\sup\limits_{t>0}|\theta_e(0)-\theta_e(t)| \geq \limsup\limits_{t\to+\infty}|\theta_e(0)-\theta_e(t)|$. However, bifurcation values determining the lock-in range $[0,\omega_l)$ are the same for both definitions of cycle slipping (see Fig. 3).

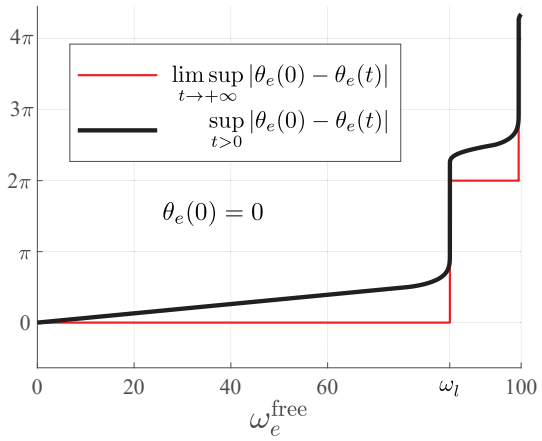


Fig. 3. Comparison of cycle slipping definitions (see Remark 3.1) for model (2) with parameters $\tau_1 = 0.0633$, $\tau_2 = 0.0225$, $K_{\text{vco}} = 250$.

From a mathematical point of view, system (2) can initially be in an unstable equilibrium (at one of the saddles) or can acquire it by a separatrix after a change of $\omega_e^{\text{free}}$ (see [Kuznetsov *et al.*, 2019a, 2020a]). Corresponding behavior is not observed in practice: system state is disturbed by noise and can't remain in unstable equilibrium. In this paper, two cycle-slipping-related characteristics of the system are considered: *the lock-in range* $|\omega_e^{\text{free}}| \in [0,\omega_l)$ where the equilibria are considered to be stable and *the conservative lock-in range* $|\omega_e^{\text{free}}| \in [0,\omega_l^c) \subset [0,\omega_l)$ which takes into account the unstable behavior described above.

For the considered model boundary values $\omega_l$ and $\omega_l^c$ are determined by *cycle slipping bifurcation*. It happens when the system being in an equilibrium state is exposed to an abrupt change of $\omega_e^{\text{free}}$, and the corresponding trajectory of the system after the switch tends to the nearest unstable equilibrium by the corresponding saddle separatrix. In other words, $\sup\limits_{t>0}|\theta_e(0)-\theta_e(t)| = \limsup\limits_{t\to+\infty}|\theta_e(0)-\theta_e(t)| = \pi$ for $\theta_e(0)=2\pi$ (see Fig. 4, lower left picture) and $\sup\limits_{t>0}|\theta_e(0)-\theta_e(t)| = \limsup\limits_{t\to+\infty}|\theta_e(0)-\theta_e(t)| = 2\pi$ for $\theta_e(0)=3\pi$ (see Fig. 4, upper right picture). For a larger $\omega_e^{\text{free}}$ supremum $\sup\limits_{t>0}|\theta_e(0)-\theta_e(t)| > 2\pi$ and cycle slipping occurs. Since the lock-in range is defined as a half-open interval, boundary values $\omega_e^{\text{free}} = \omega_l$ and $\omega_e^{\text{free}} = \omega_l^c$ are not included in it.

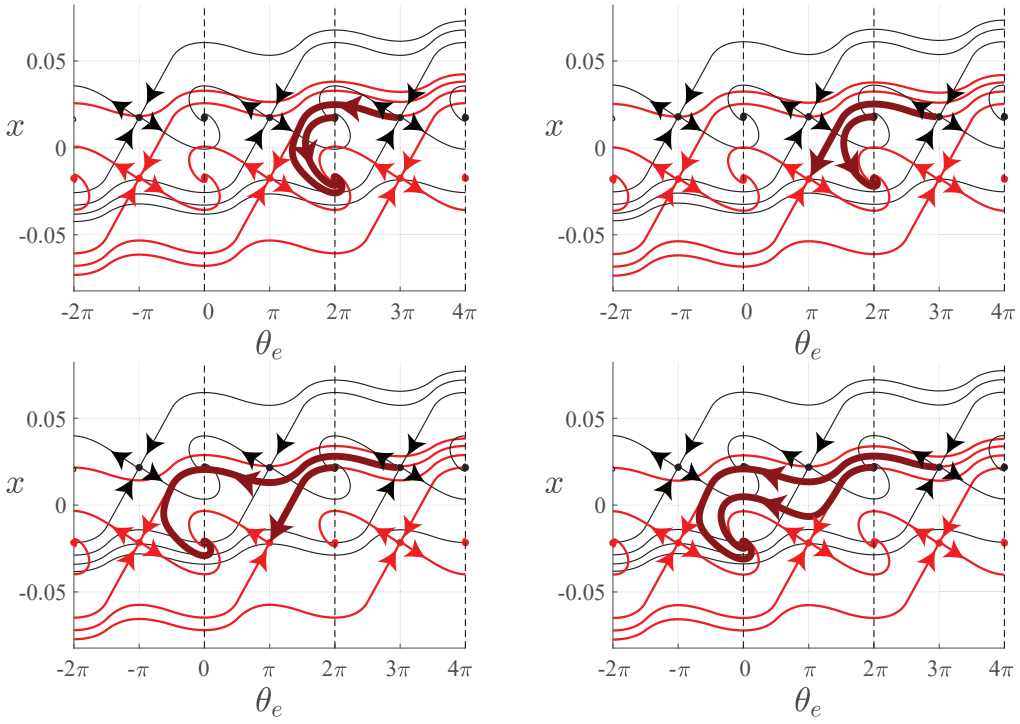


Fig. 4. Phase portraits for model (2) with the following parameters: $F(s) = \frac{1+s\tau_2}{s\tau_1}$, $\tau_1 = 0.0633$, $\tau_2 = 0.0225$, $K_{\rm vco} = 250$. Black dots are equilibria of the model with positive $\omega_e^{\rm free} = |\omega|$. Red color is for the model with negative $\omega_e^{\rm free} = -|\omega|$. Separatrices pass in and out of the saddles equilibria. Upper left subfigure: $\omega = 69 < \omega_l^c$, upper right subfigure: $\omega = \omega_l^c \approx 70.79$ (evaluated by Theorem 2), lower left subfigure: $\omega = \omega_l \approx 85.27$ (evaluated by Theorem 1), lower right subfigure: $\omega = 86 > \omega_l$.

In practice, the lock-in range can be estimated in the following way. Without loss of generality we can fix $\omega_{\rm vco}^{\rm free}$ and vary $\omega_{\rm ref}$ only. Let initially $\omega_e^{\rm free} = \omega_{\rm ref} - \omega_{\rm vco}^{\rm free} = 0$ and the system is in a stable equilibrium. Then we abruptly increase the reference frequency by sufficiently small frequency step $\Delta\omega > 0$ (i.e., the reference frequency becomes $\omega_{\rm ref} = \omega_{\rm vco}^{\rm free} + \Delta\omega$) and observe whether corresponding transient process converges to a locked state without cycle slipping (see Fig. **??**). After that we abruptly decrease the reference frequency by $2\Delta\omega$ (i.e., the reference frequency becomes $\omega_{\rm ref} = \omega_{\rm vco}^{\rm free} - \Delta\omega$). If the transient process converges to the locked state without cycle slipping, then $[0, \Delta\omega) \subset [0, \omega_l)$. Frequency step $\Delta\omega > 0$ should be increased until cycle slipping occurs.

Using changes of variables we represent system (2) as the first-order differential equation [Belyustina, 1959; Huque & Stensby, 2011] and following [Aleksandrov *et al.*, 2016; Kuznetsov *et al.*, 2019a] we formulate and prove theorems providing exact values for the lock-in range and for the conservative lock-in range.

**Theorem 1.** *The lock-in frequency of model* (2) *with the piecewise-linear PD characteristic* (1) *is*

$$\omega_l = \begin{cases} \frac{a\sqrt{\pi}}{2\tau_2}\left(\frac{c+b}{c-b}\right)^{\frac{a}{2b}}, & a^2k > 4, \\ \frac{a\sqrt{\pi}}{2\tau_2}\exp(\frac{a}{2\sqrt{\pi}}), & a^2k = 4, \\ \frac{a\sqrt{\pi}}{2\tau_2}\exp\left(\frac{a}{b}\arctan\frac{b}{c}\right), & a^2k < 4 \end{cases} \tag{4}$$

*where*

$$a = \sqrt{\frac{K_{\rm vco}}{\tau_1}}\tau_2, \quad b = \sqrt{|a^2 - \frac{4}{k}|}, \quad c = \sqrt{a^2 + 4(\pi - \frac{1}{k})}. \tag{5}$$

**Theorem 2.** *The conservative lock-in frequency of model* (2) *with piecewise-linear PD characteristic* (1)

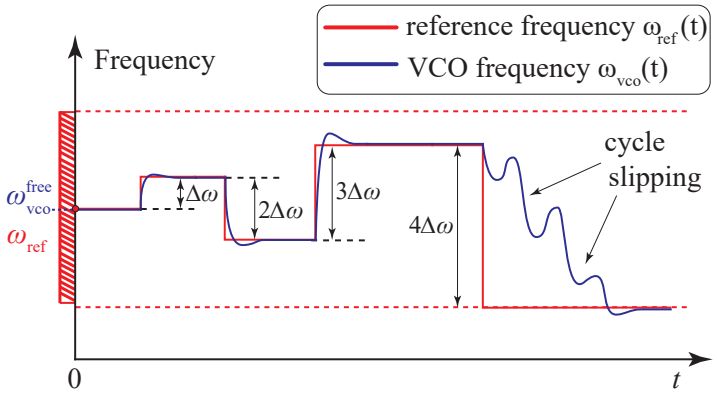


Fig. 5. The lock-in range calculation.

*is*

$$\omega_l^c = \frac{1}{2}\sqrt{\frac{K_{\rm vco}(d+\frac{c-a}{2})^{\frac{c-a}{c}}(d-\frac{c+a}{2})^{\frac{c+a}{c}}}{\tau_1}}, \tag{6}$$

*where* $a$, $b$ *and* $c$ *are evaluated by* (5), *and* $d$ *is the unique solution of one of the equations:*

$$\begin{cases} (d-\frac{a-b}{2})^{\frac{b-a}{b}}(d-\frac{a+b}{2})^{\frac{b+a}{b}} = \pi(\frac{c+b}{c-b})^{\frac{a}{b}}, \ d > \frac{a+b}{2}, \quad a^2k > 4, \\ d = \frac{a}{2}\Big(1+\dfrac{1}{W(\frac{a}{2\sqrt{\pi}}\exp(-\frac{a}{2\sqrt{\pi}}))}\Big), \quad a^2k = 4, \\ \Big(d^2-ad+\frac{1}{k}\Big)\exp\Big(\frac{2a}{b}\arctan\frac{b}{a-2d}\Big) = \pi\exp\Big(\frac{2a}{b}\arctan\frac{b}{c}\Big), \ d > \frac{a}{2}, \quad a^2k < 4. \end{cases} \tag{7}$$

*Here* $W(x)$ *is the Lambert* $W$ *function.*

*Proof.* [Proof of Theorem 1 and Theorem 2] The proof given in Appendix A is based on the fact that system (2) is piecewise-linear and can be integrated analytically on the linear segments. ■

Notice that $\omega_l$ and $\omega_l^c$ are continuous functions of variable $k$ (as $a$ is fixed): the cases $a^2k > 4$ and $a^2k < 4$ in formulae (4), (6) approach the case $a^2k = 4$ as $k \to \frac{4}{a^2}$ (as $b \to 0$).

## 4. Conclusions

In this work, the exact formulae for the lock-in range and the conservative lock-in range for the second-order type 2 PLL with a piecewise-linear phase detector characteristic were derived. In engineering literature, the following approximate estimate for the lock-in range can be found:

$$\omega_l \approx \frac{K_{\rm vco}\tau_2}{\tau_1} \tag{8}$$

(see [Best, 2007, p.69] where $\omega_l \approx \pi\zeta\omega_n$, $\omega_n = \sqrt{K_dK_{\rm vco}/\tau_1}$, $\zeta = \omega_n\tau_2/2$, $K_d = \frac{2}{\pi}$, and [Gardner, 2005, p.187] where $K_d = 1, K_o = K_{\rm vco}$). However, estimate (8) intersects the exact lock-in frequency value (4) for some values of parameters. Taking into account that for type 2 PLLs a pull-out frequency[1] $\omega_{\rm po}$ is twice

[1] In 1966, such concept as pull-out frequency was introduced by F. Gardner [Gardner, 1966, p.37]. In the literature, the following explanations of the pull-out frequency $\omega_{\rm po}$ can be found: "some frequency-step limit below which the loop does not slip cycles but remains in lock" [Gardner, 1966, p.37], [Gardner, 2005, p.116], "the maximum value of the input reference frequency step that can be applied to a phase-locked PLL, yet the loop is able to relock without slipping a cycle" [Stensby, 1997; Huque & Stensby, 2011, 2013] (see also [Best, 2007, p.59]). Since using a linear change of variables the value $\omega_e^{\rm free}$ can be excluded

the value of the lock-in frequency, one more approximate estimate for the lock-in range is exploited:

$$\omega_l \approx 0.7995\sqrt{\frac{2K_{\rm vco}}{\pi\tau_1}} + 1.23\frac{\tau_2 K_{\rm vco}}{\pi\tau_1}$$

(see [Best, 2007, p.84] where $2\omega_l = \omega_{\rm po} \approx 2.46\omega_n(\zeta + 0.65)$, $\omega_n = \sqrt{K_d K_{\rm vco}/\tau_1}$, $\zeta = \omega_n\tau_2/2$, $K_d = \frac{2}{\pi}$).

A.S. Huque and J. Stensby analysed system (2) with a triangular PD characteristic [the piecewise-linear PD characteristic (1) with $k = \frac{2}{\pi}$] in [Huque & Stensby, 2011; Huque, 2011]. However, in those works the global stability of system (2) was not analysed. In these works, the following formula for a pull-out frequency was derived:

$$\omega_{\rm po} = \frac{a^2}{\tau_2}\exp\left(\frac{1}{2}\ln|m_-^2 - m_- + a'| - \frac{1}{\sqrt{4a'-1}}\arctan\left(\frac{1-2m_-}{\sqrt{4a'-1}}\right) + \frac{\pi}{2\sqrt{4a'-1}}\right) \tag{9}$$

where $a' = \frac{\pi}{2a^2}$, $m_- = \frac{1}{2}(1 - \sqrt{4a'+1})$. For $a^2 < 2\pi$ the lock-in frequency $\omega_l = \frac{1}{2}\omega_{\rm po}$ with $\omega_{\rm po}$ from (9) coincides with the corresponding case in (4), however for $a^2 \geq 2\pi$ formula (9) is formally not applicable and equations (4) should be used.

It's important to note that obtained lock-in range formula (4) is also a lower analytical estimate for the lock-in range of the second-order type 2 PLL with a sinusoidal PD characteristic. For these systems several engineering estimates are known (see, e.g., [Gardner, 2005, p.117] and [Huque & Stensby, 2013] for the pull-out range estimates, and [Gardner, 2005, p.187], [Kolumbán, 2005, p.3748], [Best, 2007, p.67], [Best *et al.*, 2016], [Best, 2018, p.18] for the lock-in range estimates).

The further development of such systems analysis is connected with consideration of higher-order loop filters and discontinuous phase detector characteristics for revealing hidden oscillations and providing the global stability [Zhu *et al.*, 2020; Kuznetsov *et al.*, 2021c].

## Acknowledgments

The work is funded by Team Finland Knowledge programme (163/83/2021) and by the Ministry of Science and Higher Education of the Russian Federation as part of World-class Research Center program: Advanced Digital Technologies (contract No. 075-15-2020-934 dated 17.11.2020). Z. Wei acknowledges support from the National Natural Science Foundation of China (Nos. 12172340 and 11772306).

## Appendix A Proof of Theorem 1 and Theorem 2

*Proof.* [Proof of Theorem 1 and Theorem 2] Let's find the lock-in range of model (2) with piecewise-linear PD characteristic (1). As it was noted in section 3, the lock-in frequency can be determined by such an abrupt change of $\omega_e^{\rm free}$ that the corresponding trajectory tends to the nearest unstable equilibrium (by the corresponding separatrix). Suppose that initially the frequency error was equal to $\omega_e^{\rm free} = -\omega < 0$, but then changed to $\omega_e^{\rm free} = \omega > 0$. Hence, initially the system is in equilibrium $x^{\rm eq} = -\frac{\tau_1\omega}{K_{\rm vco}}$, $\theta_e^{\rm eq} = 0$, but after the switch the corresponding trajectory tends to $x^{\rm eq} = \frac{\tau_1\omega}{K_{\rm vco}}$, $\theta_e^{\rm eq} = 0$ without cycle slipping if $\omega < \omega_l$.

Such $\omega_l$ is determined by such frequency error $\omega_e^{\rm free}$ that a trajectory being in stable equilibrium (before the switch) $x^{\rm eq} = -\frac{\tau_1\omega_l}{K_{\rm vco}}$, $\theta_e^{\rm eq} = 0$ tends to saddle equilibrium (after the switch) $x^{\rm eq} = \frac{\tau_1\omega_l}{K_{\rm vco}}$, $\theta_e^{\rm eq} = \pi$ by the corresponding separatrix. Thus, the lock-in frequency $\omega_l$ corresponds to the case

$$-\frac{\tau_1\omega_l}{K_{\rm vco}} = Q(0, \omega_l) \tag{A.1}$$

from the type 2 PLL systems [Kuznetsov *et al.*, 2021a], such concept is consistent for them and corresponds to the lock-in frequency in the following way: $\omega_{\rm po} = 2\omega_l$. However, equilibria of type 1 PLLs depend on the frequency error $\omega_e^{\rm free}$ and, hence, the correct pull-out frequency definition should take into account the initial value of the frequency error corresponding to the locked state.

where $\frac{\tau_1\omega_e^{\text{free}}}{K_{\text{vco}}}$ is $x$-coordinate of equilibrium of model (2) and $x = Q(\theta_e, \omega_e^{\text{free}})$ is the lower separatrix of saddle equilibrium $(\frac{\tau_1\omega_e^{\text{free}}}{K_{\text{vco}}}, \pi)$ (see Fig. 4).

After the change of variables $\tau = \sqrt{\frac{K_{\text{vco}}}{\tau_1}}t$, $y = \sqrt{\frac{\tau_1}{K_{\text{vco}}}}\omega_e^{\text{free}} - \sqrt{\frac{K_{\text{vco}}}{\tau_1}}(x + \tau_2 v_e(\theta_e))$, for $\theta_e(t) \in (-\frac{1}{k} + 2\pi n,\ \frac{1}{k} + 2\pi n)$ and $\theta_e(t) \in (\frac{1}{k} + 2\pi n,\ -\frac{1}{k} + 2\pi(n+1))$ system (2) is represented as follows:

$$\begin{aligned} \dot{y} &= -a v_e'(\theta_e) y - v_e(\theta_e), \\ \dot{\theta}_e &= y, \end{aligned} \tag{A.2}$$

where $a = \tau_2\sqrt{\frac{K_{\text{vco}}}{\tau_1}}$.

Upper separatrix $y = S(\theta_e)$ of the phase plane of (A.2) corresponds to separatrix $x = Q(\theta_e, \omega_e^{\text{free}})$ from (2) (see Fig. A.1) and has the form

$$S(\theta_e) = \sqrt{\frac{\tau_1}{K_{\text{vco}}}}\omega_e^{\text{free}} - \sqrt{\frac{K_{\text{vco}}}{\tau_1}}(Q(\theta_e, \omega_e^{\text{free}}) + \tau_2 v_e(\theta_e)).$$

Thus, relation (A.1) takes the form

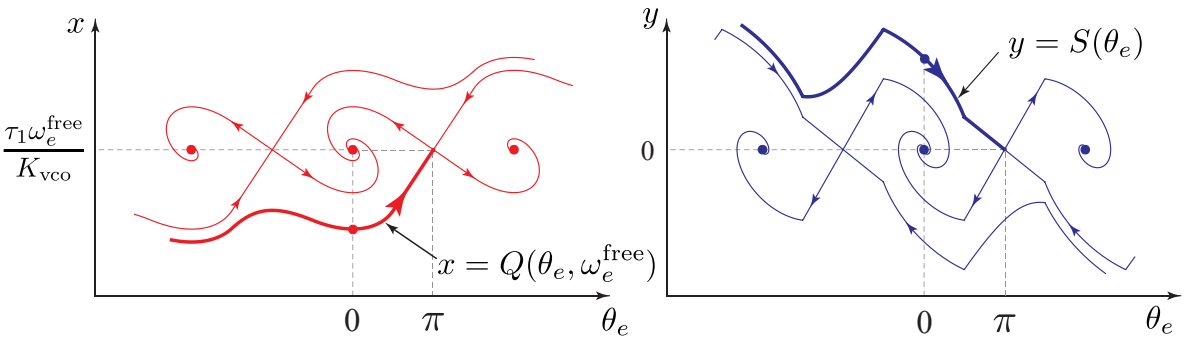


Fig. A.1. Phase plane portraits of (2) and (A.2).

$$-\frac{\tau_1\omega_l}{K_{\text{vco}}} = \frac{\tau_1\omega_l}{K_{\text{vco}}} - \sqrt{\frac{\tau_1}{K_{\text{vco}}}}S(0).$$

Hence, $\omega_l = \frac{a}{2\tau_2}S(0)$. Analogously to the phase plane analysis for $\omega_l$, we get the following formula for the conservative lock-in frequency[2]: $\omega_l^c = \frac{a}{2\tau_2}S(-\pi)$. Denote

$$y_l = S(0), \qquad y_l^c = S(-\pi)$$

and get the formulae for $\omega_l$ and $\omega_l^c$:

$$\omega_l = \frac{a}{2\tau_2}y_l, \tag{A.3}$$

$$\omega_l^c = \frac{a}{2\tau_2}y_l^c. \tag{A.4}$$

The computation of $y_l$ and $y_l^c$ from formulae (A.3), (A.4) consists of the following stages. Let's divide the phase plane to the following domains:

[2]To be more precise, for the conservative lock-in frequency it should be formally written $\omega_l^c = \min(\omega_l,\ \frac{a}{2\tau_2}S(-\pi))$, however, $S(0) - S(-\pi) = -\sqrt{\frac{K_{\text{vco}}}{\tau_1}}(Q(0, \omega_e^{\text{free}}) - Q(-\pi, \omega_e^{\text{free}})) > 0$ because $\dot{x} = v_e(\theta_e) < 0$ as $\theta_e \in [-\pi, 0]$.

- I: $\{(y,\ \theta_e) \mid \frac{1}{k} \le \theta_e \le \pi;\ \theta_e, y \in \mathbb{R}\}$,
- II: $\{(y,\ \theta_e) \mid -\frac{1}{k} \le \theta_e \le \frac{1}{k};\ \theta_e, y \in \mathbb{R}\}$,
- III: $\{(y,\ \theta_e) \mid -\pi \le \theta_e \le -\frac{1}{k};\ \theta_e, y \in \mathbb{R}\}$.

In the open domains, system (A.2) is a linear one and can be integrated analytically. Firstly, we compute $S(\frac{1}{k})$, which is possible due to the continuity of (2). Using the obtained value as the initial data of the Cauchy problem and finding its solution in the domain II, we can compute $y_l = S(0)$ and $S(-\frac{1}{k})$. Here exist three cases depending on the stable equilibrium type: an asymptotically stable focus, an asymptotically stable node, and an asymptotically stable degenerated node. For every case described above we perform separate computations. Using the obtained value as the initial data of the Cauchy problem and finding its solution in the domain III, we can compute $y_l^c = S(-\pi)$ (see Fig. A.2).

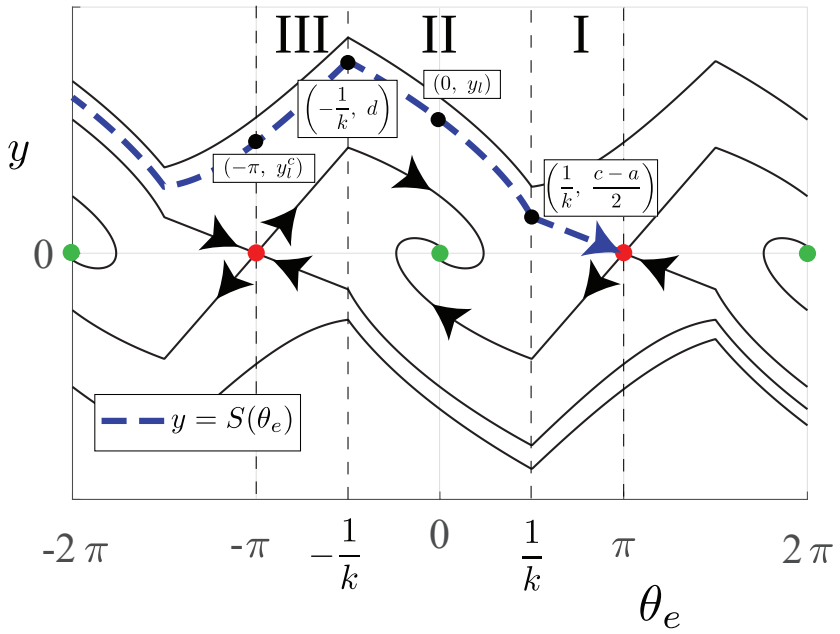


Fig. A.2. The separatrix integration. Firstly, we compute $S(\frac{1}{k})$ and use it as the initial data of the Cauchy problem. Secondly, finding its solution in the domain II, we compute $y_l = S(0)$, which is used for the lock-in frequency $\omega_l$ computation (see (A.3)), and $S(-\frac{1}{k})$. Finally, we use $S(-\frac{1}{k})$ as the initial data of the Cauchy problem and find its solution in the domain III, determining $y_l^c = S(-\pi)$, which is used for the conservative lock-in frequency $\omega_l^c$ computation (see (A.4)). Parameters: $\tau_1 = 0.0633$, $\tau_2 = 0.0225$, $K_{\text{vco}} = 250$, $k = \frac{2}{\pi}$.

**Domain I**.
The saddle separatrix is locally described by the saddle's eigenvectors

$$V_+^s = \begin{pmatrix} 1 \\ \frac{c-a}{2} \end{pmatrix}, \quad V_-^s = \begin{pmatrix} 1 \\ \frac{-c-a}{2}. \end{pmatrix}$$

Eigenvector $V_-^s$ points to a saddle and $V_+^s$ has the opposite direction. Since in the considered domain the system is a linear one, then the separatrix coincides with the line corresponding to $V_-^s$:

$$S(\theta_e) = \frac{c-a}{2\left(\pi - \frac{1}{k}\right)}(\pi - \theta_e), \quad \frac{1}{k} < \theta_e < \pi.$$

Let's obtain the limit value in $\theta_e = \frac{1}{k}$:

$$S(\frac{1}{k}) = \frac{c-a}{2} > 0.$$

**Domain II**. If $-\frac{1}{k} < \theta_e(t) < \frac{1}{k}$ then system (A.2) is

$$\begin{aligned} \dot{y} &= -aky - k\theta_e, \\ \dot{\theta}_e &= y. \end{aligned} \tag{A.5}$$

In the domains $\{y > 0\}$ and $\{y < 0\}$, variable $\theta_e(t)$ changes monotonically and the behaviour of system (A.5) can be described by the first-order differential equation[3]:

$$\frac{dy}{d\theta_e} = -ak - \frac{k\theta_e}{y}. \tag{A.6}$$

The obtained equation is Chini's equation [Chini, 1924; Cheb-Terrab & Kolokolnikov, 2003], which is a generalization of Abel and Riccati equations. The change of variables $z = \frac{y}{\theta_e}$ maps equation (A.6) into a separable one[4]:

$$\frac{zdz}{z^2 + akz + k} = -\frac{d\theta_e}{\theta_e}. \tag{A.7}$$

If $z^2 + akz + k \neq 0$ then solutions of system (A.6) and system (A.7) coincide in domains $0 < \theta_e < \frac{1}{k}$ and $-\frac{1}{k} < \theta_e < 0$. Depending on the type of an asymptotically stable equilibrium, the following cases appear (see section 2.1):

- $a^2k > 4$ (the equation $z^2 + akz + k = 0$ describes the eigenvectors of the stable node),
- $a^2k = 4$ (the equation $z^2 + akz + k = 0$ describes the eigenvector of the stable degenerate node),
- $a^2k < 4$ (here the case $z^2 + akz + k = 0$ is not possible).

**Case** $a^2k > 4$. Let's take into account the location of separatrix $y = S(\theta_e)$, satisfying (A.6), during its integration on intervals. The eigenvectors of the stable node

$$V_+^n = \begin{pmatrix} 1 \\ -\frac{a-b}{2} \end{pmatrix}, \quad V_-^n = \begin{pmatrix} 1 \\ -\frac{a+b}{2} \end{pmatrix}$$

are described by lines $y = -\frac{a+b}{2}k\theta_e$ and $y = -\frac{a-b}{2}k\theta_e$, respectively, and intersect the boundary $\theta_e = \frac{1}{k}$ of domains I and II in points $-\frac{a-b}{2} < 0$ and $-\frac{a+b}{2} < 0$. Hence, the separatrix, intersecting the boundary $\theta_e = \frac{1}{k}$ of domains I and II in point $\frac{c-a}{2} > 0$, remains over the eigenvectors within the domain II and satisfies the following inequality: $(S(\theta_e) + \frac{a+b}{2}k\theta_e)(S(\theta_e) + \frac{a-b}{2}k\theta_e) > 0$ as $\theta_e \in [-\frac{1}{k}, \frac{1}{k}]$.

Assuming $(z + \frac{a+b}{2}k)(z + \frac{a-b}{2}k) > 0$, the general solution of equation (A.7) is as follows [5]:

$$N_1(z) = -\ln|\theta_e| + C$$

where

$$N_1(z) = \frac{1}{2}\ln\Big(\big(z + \frac{a-b}{2}k\big)^{\frac{b-a}{b}}\big(z + \frac{a+b}{2}k\big)^{\frac{b+a}{b}}\Big), \quad C = \text{const}.$$

[3]The similar transition to the first-order differential equation was used in [Belyustina, 1959; Huque & Stensby, 2011, 2013].
[4]The same change of variables was used in [Huque & Stensby, 2011, 2013].
[5]Taking derivative of $N_1(z)$, we have

$$\begin{aligned} N_1'(z) = \frac{1}{2}\frac{1}{\big(z + \frac{a-b}{2}k\big)^{\frac{b-a}{b}}\big(z + \frac{a+b}{2}k\big)^{\frac{b+a}{b}}}\Big(\frac{b-a}{b}\big(z + \frac{a-b}{2}k\big)^{\frac{-a}{b}}\big(z + \frac{a+b}{2}k\big)^{\frac{b+a}{b}} + \\ + \frac{b+a}{b}\big(z + \frac{a-b}{2}k\big)^{\frac{b-a}{b}}\big(z + \frac{a+b}{2}k\big)^{\frac{a}{b}}\Big) = \frac{1}{2}\Big(\frac{b-a}{b}\big(z + \frac{a-b}{2}k\big)^{-1} + \frac{b+a}{b}\big(z + \frac{a+b}{2}k\big)^{-1}\Big) = \\ = \frac{1}{2(z + \frac{a-b}{2}k)(z + \frac{a+b}{2}k)}\Big(\frac{b-a}{b}\big(z + \frac{a+b}{2}k\big) + \frac{b+a}{b}\big(z + \frac{a-b}{2}k\big)\Big) = \frac{z}{(z + \frac{a-b}{2}k)(z + \frac{a+b}{2}k)} = \\ = \frac{z}{z^2 + akz + k}. \end{aligned}$$

Since for separatrix $y = S(\theta_e)$ inequality $(y + \frac{a+b}{2}k\theta_e)(y + \frac{a-b}{2}k\theta_e) > 0$ is valid, we get that the separatrix on interval $0 < \theta_e(t) \le \frac{1}{k}$ satisfies $N(y, \theta_e) = C_{(0,\frac{1}{k})}$ where

$$N(y,\theta_e) = \frac{1}{2}\ln\Big(\big(y + \frac{a-b}{2}k\theta_e\big)^{\frac{b-a}{b}}\big(y + \frac{a+b}{2}k\theta_e\big)^{\frac{b+a}{b}}\Big),$$
$$C_{(0,\frac{1}{k})} = \lim_{\theta_e\to\frac{1}{k}-0} N(\frac{c-a}{2},\theta_e) = \frac{1}{2}\ln\Big((\frac{c-b}{2})^{\frac{b-a}{b}}(\frac{c+b}{2})^{\frac{b+a}{b}}\Big) = \frac{1}{2}\ln\Big(\pi(\frac{c+b}{c-b})^{\frac{a}{b}}\Big).$$

Thus, if $a^2k > 4$, then separatrix $y = S(\theta_e)$ in domain $0 < \theta_e(t) \le \frac{1}{k}$ is described by equation

$$\big(y + \frac{a-b}{2}k\theta_e\big)^{\frac{b-a}{b}}\big(y + \frac{a+b}{2}k\theta_e\big)^{\frac{b+a}{b}} = \pi(\frac{c+b}{c-b})^{\frac{a}{b}}. \tag{A.8}$$

Substituting $\theta_e \to +0$ into (A.8), we get

$$y_l = \sqrt{\pi}(\frac{c+b}{c-b})^{\frac{a}{2b}}. \tag{A.9}$$

Then, substituting (A.9) into (A.3), we get the first case of formula (4).

To determine the conservative lock-in frequency, we firstly need to get $d = S(-\frac{1}{k})$, then to obtain the equation for the separatrix in domain III, and, finally, to determine $y_l^c = S(-\pi)$. Since the separatrix on interval $-\frac{1}{k} < \theta_e(t) < 0$ satisfies $N(y, \theta_e) = C_{(-\frac{1}{k},0)}$ and $\lim\limits_{\theta_e\to+0} N(y,\theta_e) = \lim\limits_{\theta_e\to-0} N(y,\theta_e) = \ln y$ as $y > 0$, then $C_{(-\frac{1}{k},0)} = C_{(0,\frac{1}{k})} = \frac{1}{2}\ln\Big(\pi(\frac{c+b}{c-b})^{\frac{a}{b}}\Big)$.

Thus, if $a^2k > 4$, then separatrix $y = S(\theta_e)$ in domain II is described by equation (A.8). Substituting $\theta_e = -\frac{1}{k}$ into (A.8), we get

$$(d - \frac{a-b}{2})^{\frac{b-a}{b}}(d - \frac{a+b}{2})^{\frac{b+a}{b}} = \pi(\frac{c+b}{c-b})^{\frac{a}{b}}. \tag{A.10}$$

Since the separatrix is over the eigenvectors ($y > -\frac{a\pm b}{2}k\theta_e$), then

$$d > \frac{a+b}{2}.$$

Notice that if $d = \frac{a+b}{2}$, then the left-hand side of equation (A.10) equals to zero, but the right-hand side is positive. Then the left-hand side increases monotonically as value $d$ increases and tends to infinity as $d \to +\infty$. Thus, equation (A.10) has unique solution $d$ greater than $\frac{a+b}{2}$.

**Case** $a^2k = 4$.

In domain II, separatrix $y = S(\theta_e)$ is over eigenvector

$$V^{dn} = \begin{pmatrix} 1 \\ -\frac{a}{2} \end{pmatrix},$$

which is described by line $y = -\frac{2}{a}\theta_e$ and intersects the boundary $\theta_e = \frac{1}{k}$ of domains I and II in point $-\frac{a}{2} < 0$. Hence, the separatrix, intersecting the boundary $\theta_e = \frac{1}{k}$ of domains I and II in point $\frac{c-a}{2} > 0$, remains over the eigenvector within the domain II and satisfies the following inequality: $S(\theta_e) > -\frac{2}{a}\theta_e$.

The general solution of (A.7) is as follows[6]:

$$N_1(z) = -\ln|\theta_e| + C$$

where

$$N_1(z) = \frac{2}{2+az} + \ln|2+az|, \quad C = \text{const}.$$

[6]Taking derivative of $N_1(z)$, we have

$$N_1'(z) = -\frac{2a}{(2+az)^2} + \frac{a}{2+az} = \frac{a^2z}{(2+az)^2} = \frac{z}{(\frac{2}{a}+z)^2} = \frac{z}{z^2+akz+k}.$$

Since for separatrix $y = S(\theta_e)$ inequality $S(\theta_e) > -\frac{2}{a}\theta_e.$ is valid, we get that the separatrix on interval $0 < \theta_e(t) \le \frac{1}{k}$ satisfies $N(y, \theta_e) = C_{(0,\frac{1}{k})}$ where

$$N(y,\theta_e) = \frac{2\theta_e}{2\theta_e + ay} + \ln(2\theta_e + ay),$$
$$C_{(0,\frac{1}{k})} = \lim_{\theta_e \to \frac{1}{k}-0} N(\frac{c-a}{2}, \theta_e) = \frac{2}{k}\frac{1}{\frac{2}{k} + a\sqrt{\pi} - \frac{a^2}{2}} + \ln(\frac{2}{k} + a\sqrt{\pi} - \frac{a^2}{2}) = \frac{a}{2\sqrt{\pi}} + \ln(a\sqrt{\pi}).$$

Thus, if $a^2k = 4$, then separatrix $y = S(\theta_e)$ in domain $0 < \theta_e(t) \le \frac{1}{k}$ is described by equation

$$\frac{2\theta_e}{2\theta_e + ay} + \ln(2\theta_e + ay) = \frac{a}{2\sqrt{\pi}} + \ln(a\sqrt{\pi}). \tag{A.11}$$

Substituting $\theta_e \to +0$ into (A.11), we get

$$y_l = \sqrt{\pi}\exp(\frac{a}{2\sqrt{\pi}}). \tag{A.12}$$

Then, substituting (A.12) into (A.3), we get the second case of formula (4).

To determine the conservative lock-in frequency, we firstly need to determine $d = S(-\frac{1}{k})$. Since the separatrix on interval $-\frac{1}{k} < \theta_e(t) < 0$ satisfies $N(y, \theta_e) = C_{(-\frac{1}{k},0)}$ and $\lim\limits_{\theta_e \to +0} N(y, \theta_e) = \lim\limits_{\theta_e \to -0} N(y, \theta_e) = \ln(ay)$ as $y > 0$, then $C_{(-\frac{1}{k},0)} = C_{(0,\frac{1}{k})} = \frac{a}{2\sqrt{\pi}} + \ln(a\sqrt{\pi})$.

Thus, if $a^2k = 4$, then separatrix $y = S(\theta_e)$ in domain II is described by equation (A.11). Substituting $\theta_e = -\frac{1}{k}$ into (A.11), we get

$$(d - \frac{a}{2})\exp\Big(\frac{\frac{a}{2}}{\frac{a}{2} - d}\Big) = \sqrt{\pi}e^{\frac{a}{2\sqrt{\pi}}}.$$

Notice that in the considered case it is possible to obtain an explicit formula for $d$:

$$d = \frac{a}{2}\Big(1 + \frac{1}{W(\frac{a}{2\sqrt{\pi}}\exp(-\frac{a}{2\sqrt{\pi}})}\Big) \tag{A.13}$$

where $W(x)$ is the Lambert W function[7].

**Case** $a^2k < 4$.

The general solution of (A.6) is as follows[8]:

$$N_1(z) = -\ln|\theta_e| + C$$

where

$$N_1(z) = \frac{1}{2}\ln(z^2 + akz + k) - \frac{a}{b}\arctan(\frac{a + \frac{2}{k}z}{b}), \quad C = \text{const}.$$

Then separatrix $y = S(\theta_e)$ in domain $0 < \theta_e \le \frac{1}{k}$ satisfies $N(y, \theta_e) = C_{(0,\ \frac{1}{k})}$ where

$$N(y,\theta_e) = \frac{1}{2}\ln(y^2 + aky\theta_e + k\theta_e^2) - \frac{a}{b}\arctan\Big(\frac{a\theta_e + \frac{2}{k}y}{b\theta_e}\Big),$$
$$C_{(0,\ \frac{1}{k})} = \lim_{\theta_e \to \frac{1}{k}-0} N(\frac{c-a}{2}, \theta_e) = \frac{1}{2}\ln\pi - \frac{a}{b}\arctan\frac{c}{b}.$$

[7]For $x > 0$ function $W(x)$ is a single-valued one and can be evaluated in standard numeric computing platforms.

[8]Taking derivative of $N_1(z)$, we have

$$N_1'(z) = \frac{2z + ak}{2(z^2 + akz + k)} - \frac{2a}{b^2k}\frac{1}{1 + (\frac{a + \frac{2}{k}z}{b})^2} = \frac{2z + ak}{2(z^2 + akz + k)} - \frac{2ak}{b^2k^2 + (ak + 2z)^2} =$$
$$= \frac{2z + ak}{2(z^2 + akz + k)} - \frac{2ak}{4z^2 + 4akz + (a^2 + b^2)k^2} = \frac{2z + ak}{2(z^2 + akz + k)} - \frac{ak}{2(z^2 + akz + k)} = \frac{z}{z^2 + akz + k}.$$

Thus, if $a^2k < 4$, then separatrix $y = S(\theta_e)$ in domain $0 < \theta_e \le \frac{1}{k}$ is described by equation

$$\frac{1}{2}\ln(y^2 + aky\theta_e + k\theta_e^2) - \frac{a}{b}\arctan\Big(\frac{a\theta_e + \frac{2}{k}y}{b\theta_e}\Big) = \frac{1}{2}\ln\pi - \frac{a}{b}\arctan\frac{c}{b}. \tag{A.14}$$

Substituting $\theta_e \to +0$ into (A.14), we get

$$y_l = \sqrt{\pi}\exp\Big(\frac{a}{b}\arctan\frac{b}{c}\Big). \tag{A.15}$$

Then, substituting (A.15) into (A.3), we get the third case of formula (4). Thus, Theorem 1 is proved.

To determine the conservative lock-in frequency, we firstly need to determine $d = S(-\frac{1}{k})$. Since the separatrix on interval $-\frac{1}{k} < \theta_e(t) < 0$ satisfies $N(y, \theta_e) = C_{(-\frac{1}{k},0)}$ and $\lim\limits_{\theta_e \to +0} N(y, \theta_e) = \ln y - \frac{\pi a}{2b}$, $\lim\limits_{\theta_e \to -0} N(y, \theta_e) = \ln y + \frac{\pi a}{2b}$, then $C_{(-\frac{1}{k},0)} - \frac{\pi a}{2b} = C_{(0,\frac{1}{k})} + \frac{\pi a}{2b}$.

Thus, if $a^2k < 4$, then separatrix $y = S(\theta_e)$ in domain II is described by

$$\begin{aligned}
&\frac{1}{2}\ln(y^2 + aky\theta_e + k\theta_e^2) - \frac{a}{b}\arctan\Big(\frac{a\theta_e + \frac{2}{k}y}{b\theta_e}\Big) = \frac{1}{2}\ln\pi - \frac{a}{b}\arctan\frac{c}{b}, \quad \text{if } 0 < \theta_e(t) \le \frac{1}{k}\\
&y = y_l, \quad \text{if } \theta_e(t) = 0\\
&\frac{1}{2}\ln(y^2 + aky\theta_e + k\theta_e^2) - \frac{a}{b}\arctan\Big(\frac{a\theta_e + \frac{2}{k}y}{b\theta_e}\Big) = \frac{1}{2}\ln\pi + \frac{a}{b}\Big(\pi - \arctan\frac{c}{b}\Big), \quad \text{if } -\frac{1}{k} \le \theta_e(t) < 0.
\end{aligned} \tag{A.16}$$

Substituting $\theta_e = -\frac{1}{k}$ into (A.16), we get

$$\Big(d^2 - ad + \frac{1}{k}\Big)\exp\Big(\frac{2a}{b}\arctan\frac{2d-a}{b} - \frac{\pi a}{b}\Big) = \pi\exp\Big(\frac{2a}{b}\arctan\frac{b}{c}\Big). \tag{A.17}$$

Notice that if $d = 0$, then the left-hand side of equation (A.10) is less than the right-hand side:

$$\frac{1}{k}\exp\Big(\frac{2a}{b}\arctan\frac{-a}{b} - \frac{\pi a}{b}\Big) < \frac{1}{k} < \pi < \pi\exp\Big(\frac{2a}{b}\arctan\frac{b}{c}\Big).$$

Then the left-hand side increases monotonically as value $d$ increases and tends to infinity as $d \to +\infty$. Thus, equation (A.17) has unique positive solution $d$.

Notice also that if $d = \frac{a}{2}$, then the left-hand side of equation (A.10) is less than the right-hand side too:

$$b^2\exp(-\frac{\pi a}{b}) < a^2\exp(-\frac{\pi a}{b}) < 4\pi\exp(-\frac{\pi a}{b}) < 4\pi\frac{b^2}{\pi^2a^2} < \frac{4}{\pi} < \pi < \pi\exp\Big(\frac{2a}{b}\arctan\frac{b}{c}\Big).$$

Thus, $d > \frac{a}{2}$ and equation (A.17) can be reduced to the following:

$$\Big(d^2 - ad + \frac{1}{k}\Big)\exp\Big(\frac{2a}{b}\arctan\frac{b}{a-2d}\Big) = \pi\exp\Big(\frac{2a}{b}\arctan\frac{b}{c}\Big). \tag{A.18}$$

**Domain III**

If $-\pi \le \theta_e(t) < -\frac{1}{k}$ then system (A.2) is

$$\begin{aligned}
\dot{y} &= \frac{a}{\pi - \frac{1}{k}}y + \frac{1}{\pi - \frac{1}{k}}(\theta_e + \pi),\\
\dot{\theta_e} &= y.
\end{aligned} \tag{A.19}$$

Analogously to the analysis in domain II, let's study for $y > 0$ the first-order differential equation

$$\frac{dy}{d\theta_e} = \frac{1}{\pi - \frac{1}{k}}(a + \frac{\theta_e + \pi}{y}) \tag{A.20}$$

and make the change of variables $z = \frac{y}{\theta_e + \pi}$ mapping equation (A.20) into a separable one:

$$(\pi - \frac{1}{k})\frac{zdz}{\left(\pi - \frac{1}{k}\right)z^2 - az - 1} = -\frac{d\theta_e}{\theta_e + \pi}. \tag{A.21}$$

If $-\pi < \theta_e(t) < -\frac{1}{k}$ then the solutions of system (A.20) and system (A.21) coincide.

Separatrix $y = S(\theta_e)$ is over the separatrices of saddle $(0,\ -\pi)$, which are described by the equations

$$y = \frac{\pm c - a}{2(\pi - \frac{1}{k})}(-\pi - \theta_e), \quad -\pi < \theta_e < -\frac{1}{k}.$$

Thus, the following inequality is valid for the separatrix: $(S(\theta_e)+\frac{c-a}{2(\pi-\frac{1}{k})}(\pi+\theta_e))(S(\theta_e)-\frac{c+a}{2(\pi-\frac{1}{k})}(\pi+\theta_e)) > 0$.

Assuming $(z + \frac{c-a}{2(\pi-\frac{1}{k})})(z - \frac{c+a}{2(\pi-\frac{1}{k})}) > 0$, the general solution of equation (A.21) is as follows[9]:

$$M_1(z) = -\ln|\theta_e + \pi| + C$$

where

$$M_1(z) = \frac{1}{2}\ln\Big(\big(z + \frac{c-a}{2(\pi-\frac{1}{k})}\big)^{\frac{c-a}{c}}\big(z - \frac{c+a}{2(\pi-\frac{1}{k})}\big)^{\frac{c+a}{c}}\Big),$$
$$C = \text{const}.$$

Since for separatrix $y = S(\theta_e)$ inequality $(y + \frac{c-a}{2(\pi-\frac{1}{k})}(\pi+\theta_e))(y - \frac{c+a}{2(\pi-\frac{1}{k})}(\pi+\theta_e)) > 0$ is valid, we get that the separatrix in domain III satisfies $M(y,\theta_e) = C_{(-\pi,-\frac{1}{k})}$ where

$$M(y,\theta_e) = \frac{1}{2}\ln\Big(\Big(y + \frac{c-a}{2(\pi-\frac{1}{k})}(\pi+\theta_e)\Big)^{\frac{c-a}{c}}\Big(y - \frac{c+a}{2(\pi-\frac{1}{k})}(\pi+\theta_e)\Big)^{\frac{c+a}{c}}\Big),$$
$$C = C_{(-\pi,-\frac{1}{k})} = \lim_{\theta_e\to-\frac{1}{k}-0} M(d,\theta_e) = \frac{1}{2}\ln\Big((d + \frac{c-a}{2})^{\frac{c-a}{c}}(d - \frac{c+a}{2})^{\frac{c+a}{c}}\Big).$$

Thus, separatrix $y = S(\theta_e)$ in domain III is described by equation

$$\Big(y + \frac{c-a}{2(\pi-\frac{1}{k})}(\pi+\theta_e)\Big)^{\frac{c-a}{c}}\Big(y - \frac{c+a}{2(\pi-\frac{1}{k})}(\pi+\theta_e)\Big)^{\frac{c+a}{c}} = (d + \frac{c-a}{2})^{\frac{c-a}{c}}(d - \frac{c+a}{2})^{\frac{c+a}{c}}. \tag{A.22}$$

To determine the conservative lock-in frequency, we firstly need to determine $y_l^c = S(-\pi)$. Substituting $\theta_e = -\pi$ into (A.22), we get

$$y_l^c = (d + \frac{c-a}{2})^{\frac{c-a}{2c}}(d - \frac{c+a}{2})^{\frac{c+a}{2c}}. \tag{A.23}$$

Substituting (A.23) into (A.4) and taking into account formulae (A.10), (A.13), (A.18), we get (6). Theorem 1 and Theorem 2 are proved. ■

## Appendix B Octave code for Fig. A.2

Code below can be runned on https://octave-online.net/ in order to obtain phase portrait on Fig. A.2 and verify formulae (4) and (6). The code simulates trajectories of system (A.2) numerically and additionally plots two points: $(0, y_l)$ and $(-\pi, y_l^c)$ where $y_l$ and $y_l^c$ are used in lock-in range formulae (A.3) and (A.4). Since these points are lying on the separatrices, formulae (A.3) and (A.4) are validated numerically.

[9]Taking derivative of $M_1(z)$, we have

$$M_1'(z) = \frac{1}{2}\frac{1}{\big(z + \frac{c-a}{2(\pi-\frac{1}{k})}\big)^{\frac{c-a}{c}}\big(z - \frac{c+a}{2(\pi-\frac{1}{k})}\big)^{\frac{c+a}{c}}}\Big(\frac{c-a}{c}\big(z + \frac{c-a}{2(\pi-\frac{1}{k})}\big)^{\frac{-a}{c}}\big(z - \frac{c+a}{2(\pi-\frac{1}{k})}\big)^{\frac{c+a}{c}} +$$
$$+ \frac{c+a}{c}\big(z + \frac{c-a}{2(\pi-\frac{1}{k})}\big)^{\frac{c-a}{c}}\big(z - \frac{c+a}{2(\pi-\frac{1}{k})}\big)^{\frac{a}{c}}\Big) = \frac{1}{2}\Big(\frac{c-a}{c}\big(z + \frac{c-a}{2(\pi-\frac{1}{k})}\big)^{-1} + \frac{c+a}{c}\big(z - \frac{c+a}{2(\pi-\frac{1}{k})}\big)^{-1}\Big) =$$
$$= \frac{1}{2(z + \frac{c-a}{2(\pi-\frac{1}{k})})(z - \frac{c+a}{2(\pi-\frac{1}{k})})}\Big(\frac{c-a}{c}\big(z - \frac{c+a}{2(\pi-\frac{1}{k})}\big) + \frac{c+a}{c}\big(z + \frac{c-a}{2(\pi-\frac{1}{k})}\big)\Big) = \frac{z}{(z + \frac{c-a}{2(\pi-\frac{1}{k})})(z - \frac{c+a}{2(\pi-\frac{1}{k})})} =$$
$$= \frac{z}{(z^2 - \frac{a}{\pi-\frac{1}{k}}z - \frac{1}{\pi-\frac{1}{k}})}.$$

```
clear all;
close all;
clc;

% VCO input gain
K_vco = 250;

% Loop filter transfer function F(s) = (1+s tau_2)/(s tau_1), tau_1 > 0,
% tau_2 > 0
tau_2 = 0.0225;
tau_1 = 0.0633;

% The slope coefficient of piecewise-linear PD characteristic
% it becomes triangular with this coefficient
k=2/pi;

function y = draw_saddles_symmetric(ode, saddle, V, periods, options)
% draw_saddles_symmetric draws phase portrait of the system ode,
% starting from saddle with eigenvectors V for given number of periods
% options are used to tune ODE solver

    % Integration time
    TIME_POSITIVE = 0:0.005:20;
    TIME_NEGATIVE = 0:-0.005:-20;

    v1 = 0.01 .* flip(V(:,1)');
    v2 = 0.01 .* flip(V(:,2)');

    % Calculate saddle separatrices and plot them
    [T_1, X_1] = ode45(ode, TIME_NEGATIVE, saddle+v1, options);
    [T_3, X_3] = ode45(ode, TIME_NEGATIVE, saddle-v1, options);
    for j=1:length(periods)
        plot(X_1(:,2)+periods(j),X_1(:,1));
        plot(X_3(:,2)+periods(j),X_3(:,1));
    end
    [T_2, X_2] = ode45(ode, TIME_POSITIVE, saddle+v2, options);
    [T_4, X_4] = ode45(ode, TIME_POSITIVE, saddle-v2, options);
    for j=1:length(periods)
       plot(X_2(:,2)+periods(j), X_2(:,1));
       plot(X_4(:,2)+periods(j), X_4(:,1));
    end
end

function y = sawtooth_diff(t)
% sawtooth_diff - the derivative of a triangular function
% (sawtooth (T, WIDTH) from signal package)
  remain = abs(rem(t, 2*pi));
  if (pi/2 <= remain && remain <= 3*pi/2)
      y = -2/pi;
  else
      y = 2/pi;
  end
```

```
end

% PD characteristic
v_e = @(theta_e) (sawtooth(theta_e+pi/2,0.5));
% The derivative of PD characteristic
dv_e = @(theta_e) (sawtooth_diff(theta_e));
period = 2*pi;

% Parameters a, b, c from Theorem 1 and 2
a = sqrt(K_vco/tau_1)*tau_2;
b = sqrt(abs(a^2-4/k));
c = sqrt(a^2-4/k + 4*pi);
% Computing the lock-in range and the concervative lock-in range by
% Theorem 1 and 2
syms x;
if a^2*k>4
    y_l = sqrt(pi)* ((c+b)/(c-b))^(a/(2*b));
    fcn = @(x) (x - (a-b)/2)^((b-a)/b) * (x - (a+b)/2)^((b+a)/b) -...
        pi*((c+b)/(c-b))^(a/b);
    init_param = [(a+b)/2, 10000000];
    % vpasolve numerically solves implicit equations with initial guess
    % init_param (it was proven that the equation has a unique solution
    % for x > (a+b)/2)
    d = vpasolve(fcn(x), x, init_param);
else
    if a^2*k == 4
        y_l = sqrt(pi)*exp(a/2/sqrt(pi));
        d = a/2*(1 + 1/lambertw(a/2/sqrt(pi)*exp(-a/2/sqrt(pi))));
else
        y_l = sqrt(pi)*exp(a*atan(b/c)/b);
        fcn = @(x) ((x)^2 - a*x + 1/k) * exp( 2*a/b*atan((2*x-a)/b) - pi*a/b) -...
        pi*exp(2*a/b*atan(b/c));
        init_param = [a/2, 10000000];
        % vpasolve numerically solves implicit equations with initial guess
        % init_param (it was proven that the equation has a unique solution
        % for x > a/2)
        d = vpasolve(fcn(x), x, init_param);
    end
end
y_l_c = (d-0.5*(a-c))^((c-a)/c/2) * (d-0.5*(a+c))^((c+a)/c/2);


h = figure(1);
hold on;
grid on;

% Ploting two points which correspond the lock-in range and the conservative
% lock-in range
plot([0], [y_l], 'k.', 'MarkerSize', 20);
plot([-pi], [eval(y_l_c)], 'k.', 'MarkerSize', 20);

% System establishment for numerocal integration
```

```
% y = x(1), theta_e = x(2)
pll_s = @(t,x)([- a*dv_e(x(2))*x(1) - v_e(x(2));
                x(1)]);

% One of the asymptotically stable equilibria
theta_eq = 0;
x_eq = 0;

% Draw phase portrait
saddles = [x_eq, -theta_eq+period/2-2*period;...
    x_eq, -theta_eq+period/2-period;...
    x_eq, -theta_eq+period/2;...
    x_eq, -theta_eq+period/2+period;...
    x_eq, -theta_eq+period/2+2*period];
focuses = [x_eq, theta_eq-period;...
    x_eq, theta_eq-period;...
    x_eq, theta_eq;...
    x_eq, theta_eq+period;...
    x_eq, theta_eq+2*period];

plot(-focuses(:,2), -focuses(:,1), 'r.', 'MarkerSize', 20);
plot(focuses(:,2), focuses(:,1), 'k.', 'MarkerSize', 20);
plot(-saddles(:,2), -saddles(:,1), 'r.', 'MarkerSize', 20);
plot(saddles(:,2), saddles(:,1), 'k.', 'MarkerSize', 20);

% Jacobian matrix of the system
A = [0 1;
    2/pi 2*a/pi];

% Calculating saddle eigenvectors V
[V, D] = eig(A);

% Custom simulation options
options = odeset('MaxStep', 0.001, 'RelTol', 2e-7, 'AbsTol', 2e-7);
draw_saddles_symmetric(pll_s,...
    [x_eq,period/2-theta_eq],  ...
    V, ...
    [-2*period,-period,0,period,2*period],...
    options);

% Plot adjustments
axis([-2*pi 2*pi -5 5])
xticks([-4*pi -3*pi -2*pi -pi 0 pi 2*pi, 4*pi])
xticklabels({'-4\pi','-3\pi','-2\pi','-\pi','0','\pi','2\pi','4\pi'})

xlabel('\theta_e');
ylabel('y');
```

## References

Aleksandrov, K., Kuznetsov, N., Leonov, G., Neittaanmaki, N., Yuldashev, M. & Yuldashev, R. [2016] "Computation of the lock-in ranges of phase-locked loops with PI filter," *IFAC-PapersOnLine* **49**,

36–41, doi:10.1016/j.ifacol.2016.07.971.

Alexandrov, K., Kuznetsov, N., Leonov, G., Neittaanmaki, P. & Seledzhi, S. [2015] "Pull-in range of the PLL-based circuits with proportionally-integrating filter," *IFAC-PapersOnLine* **48**, 720–724, doi: 10.1016/j.ifacol.2015.09.274.

Andronov, A., Vitt, E. & Khaikin, S. [1937] *Theory of Oscillators (in Russian)* (ONTI NKTP SSSR), [English transl.: 1966, Pergamon Press].

Bakaev, Y. [1963] "Stability and dynamical properties of astatic frequency synchronization system," *Radiotekhnika i Elektronika (in Russian)* **8**, 513–516.

Belyustina, L. [1959] "The study of a nonlinear pll system," *Izv. vuzov. Radiofizika (in Russian)* **2**, 277–291.

Best, R. [2007] *Phase locked loops: design, simulation, and applications* (McGraw-Hill Professional).

Best, R. [2018] *Costas Loops: Theory, Design, and Simulation* (Springer International Publishing).

Best, R., Kuznetsov, N., Leonov, G., Yuldashev, M. & Yuldashev, R. [2016] "Tutorial on dynamic analysis of the Costas loop," *IFAC Annual Reviews in Control* **42**, 27–49, doi:10.1016/j.arcontrol.2016.08.003.

Cheb-Terrab, E. & Kolokolnikov, T. [2003] "First-order ordinary differential equations, symmetries and linear transformations," *European Journal of Applied Mathematics* **14**, 231–246.

Chen, G., Kuznetsov, N., Leonov, G. & Mokaev, T. [2017] "Hidden attractors on one path: Glukhovsky-Dolzhansky, Lorenz, and Rabinovich systems," *International Journal of Bifurcation and Chaos in Applied Sciences and Engineering* **27**, art. num. 1750115.

Chini, M. [1924] "Sull'integrazione di alcune equazioni differenziali del primo ordine," *Rendiconti Instituto Lombardo (2)* **57**, 506–511.

Du, K. & Swamy, M. [2010] *Wireless Communication Systems: from RF subsystems to 4G enabling technologies* (Cambridge University Press).

Egan, W. [1981] *Frequency synthesis by phase lock*, 1st ed. (John Wiley & Sons, New York).

Egan, W. [2007] *Phase-Lock Basics*, 2nd ed. (John Wiley & Sons, New York).

Gardner, F. [1966] *Phaselock Techniques* (John Wiley & Sons, New York).

Gardner, F. [2005] *Phaselock Techniques*, 3rd ed. (John Wiley & Sons, New York).

Gubar', N. [1961] "Investigation of a piecewise linear dynamical system with three parameters," *Journal of Applied Mathematics and Mechanics* **25**, 1011–1023.

Huque, A. [2011] *A new derivation of the pull-out frequency for second-order phase lock loops employing triangular and sinusoidal phase detectors* (The University of Alabama in Huntsville), Ph. D. thesis.

Huque, A. & Stensby, J. [2011] "An exact formula for the pull-out frequency of a 2nd-order type II phase lock loop," *IEEE Communications Letters* **15**, 1384–1387.

Huque, A. & Stensby, J. [2013] "An analytical approximation for the pull-out frequency of a PLL employing a sinusoidal phase detector," *ETRI Journal* **35**, 218–225.

Kaplan, E. & Hegarty, C. [2017] *Understanding GPS/GNSS: Principles and Applications*, 3rd ed. (Artech House).

Kapranov, M. [1956] "The lock-in band of a phase locked loop," *Radiotekhnika (in Russian)* **11**, 37–52.

Karimi-Ghartemani, M. [2014] *Enhanced phase-locked loop structures for power and energy applications* (John Wiley & Sons).

Kolumbán, G. [2005] *The Encyclopedia of RF and Microwave Engineering, Phase-locked loops*, Vol. 4 (John Wiley & Sons, New-York).

Kuznetsov, N. [2020] "Theory of hidden oscillations and stability of control systems," *Journal of Computer and Systems Sciences International* , 647–668doi:10.1134/S1064230720050093.

Kuznetsov, N., Blagov, M., Alexandrov, K., Yuldashev, M. & Yuldashev, R. [2019a] "Lock-in range of classical PLL with piecewise-linear phase detector characteristic," *Differencialnie Uravnenia i Protsesy Upravlenia (Differential Equations and Control Processes)* , 74–89.

Kuznetsov, N., Kolumbán, G., Belyaev, Y., Tulaev, A., Yuldashev, M. & Yuldashev, R. [2022] "Estimation of PLL impact on MEMS-gyroscopes parameters," *Gyroscopy and Navigation* (in print).

Kuznetsov, N., Leonov, G., Yuldashev, M. & Yuldashev, R. [2015] "Rigorous mathematical definitions of the hold-in and pull-in ranges for phase-locked loops," *IFAC-PapersOnLine* **48**, 710–713, doi: 10.1016/j.ifacol.2015.09.272.

Kuznetsov, N., Leonov, G., Yuldashev, M. & Yuldashev, R. [2017] "Hidden attractors in dynamical models

of phase-locked loop circuits: limitations of simulation in MATLAB and SPICE," *Communications in Nonlinear Science and Numerical Simulation* **51**, 39–49, doi:10.1016/j.cnsns.2017.03.010.

Kuznetsov, N., Lobachev, M., Yuldashev, M. & Yuldashev, R. [2019b] "On the Gardner problem for phase-locked loops," *Doklady Mathematics* **100**, 568–570, doi:10.1134/S1064562419060218.

Kuznetsov, N., Lobachev, M., Yuldashev, M. & Yuldashev, R. [2021a] "The Egan problem on the pull-in range of type 2 PLLs," *Transactions on Circuits and Systems II: Express Briefs* **68**, 1467–1471, doi:10.1109/TCSII.2020.3038075.

Kuznetsov, N., Lobachev, M., Yuldashev, M., Yuldashev, R. & Kolumbán, G. [2020a] "Harmonic balance analysis of pull-in range and oscillatory behavior of third-order type 2 analog PLLs," *IFAC-PapersOnLine* **53**, 6378–6383.

Kuznetsov, N., Lobachev, M., Yuldashev, M., Yuldashev, R., Kudryashova, E., Kuznetsova, O., Rosenwasser, E. & Abramovich, S. [2020b] "The birth of the global stability theory and the theory of hidden oscillations," *2020 European Control Conference Proceedings*, pp. 769–774, doi:10.23919/ECC51009.2020.9143726.

Kuznetsov, N., Lobachev, M., Yuldashev, M., Yuldashev, R., Volskiy, S. & Sorokin, D. [2021b] "On the generalized Gardner problem for phase-locked loops in electrical grids," *Doklady Mathematics* **103**, 157–161.

Kuznetsov, N., Matveev, A., Yuldashev, M. & Yuldashev, R. [2021c] "Nonlinear analysis of charge-pump phase-locked loop: The hold-in and pull-in ranges," *IEEE Transactions on Circuits and Systems I: Regular Papers* **68**, 4049–4061, doi:10.1109/TCSI.2021.3101529.

Kuznetsov, N., Volskiy, S., Sorokin, D., Yuldashev, M. & Yuldashev, R. [2020c] "Power supply system for aircraft with electric traction," *2020 21st International Scientific Conference on Electric Power Engineering (EPE)*, pp. 1–5, doi:10.1109/EPE51172.2020.9269181.

Leonov, G. & Kuznetsov, N. [2013] "Hidden attractors in dynamical systems. From hidden oscillations in Hilbert-Kolmogorov, Aizerman, and Kalman problems to hidden chaotic attractors in Chua circuits," *International Journal of Bifurcation and Chaos in Applied Sciences and Engineering* **23**, doi:10.1142/S0218127413300024, art. no. 1330002.

Leonov, G. & Kuznetsov, N. [2014] *Nonlinear mathematical models of phase-locked loops. Stability and oscillations* (Cambridge Scientific Publishers).

Leonov, G., Kuznetsov, N., Yuldashev, M. & Yuldashev, R. [2012] "Analytical method for computation of phase-detector characteristic," *IEEE Transactions on Circuits and Systems - II: Express Briefs* **59**, 633–647, doi:10.1109/TCSII.2012.2213362.

Leonov, G., Kuznetsov, N., Yuldashev, M. & Yuldashev, R. [2015a] "Hold-in, pull-in, and lock-in ranges of PLL circuits: rigorous mathematical definitions and limitations of classical theory," *IEEE Transactions on Circuits and Systems–I: Regular Papers* **62**, 2454–2464, doi:10.1109/TCSI.2015.2476295.

Leonov, G., Kuznetsov, N., Yuldashev, M. & Yuldashev, R. [2015b] "Nonlinear dynamical model of Costas loop and an approach to the analysis of its stability in the large," *Signal Processing* **108**, 124–135, doi:10.1016/j.sigpro.2014.08.033.

Rosenkranz, W. & Schaefer, S. [2016] "Receiver design for optical inter-satellite links based on digital signal processing," *18th International Conference on Transparent Optical Networks (ICTON)* (IEEE), pp. 1–4.

Shakhtarin, B. [1969] "Study of a piecewise-linear system of phase-locked frequency control," *Radiotechnica and electronika (in Russian)* , 1415–1424.

Stensby, J. [1997] *Phase-Locked Loops: Theory and Applications* (Taylor & Francis).

Tricomi, F. [1933] "Integrazione di unequazione differenziale presentatasi in elettrotechnica," *Annali della R. Shcuola Normale Superiore di Pisa* **2**, 1–20.

Viterbi, A. [1959] "Acquisition and tracking behavior of phase-locked loops," *Jet Propulsion Laboratory, California Institute of Technology, Pasadena, External Publ* **673**.

Viterbi, A. [1966] *Principles of coherent communications* (McGraw-Hill, New York).

Zelenskii, A., Gapon, N., Voronin, V., Semenishchev, E., Khamidullin, I. & Cen, Y. [2021] "Robot navigation using modified slam procedure based on depth image reconstruction," *Artificial Intelligence and Machine Learning in Defense Applications III* (SPIE), pp. 73–82.

Zelensky, A., Semenishchev, E., Alepko, A., Abdullin, T., Ilyukhin, Y. & Voronin, V. [2021] "Using neuro-accelerators on fpgas in collaborative robotics tasks," *Optical Instrument Science, Technology, and Applications II* (SPIE), pp. 98–102.

Zhu, B., Wei, Z., Escalante-González, R. & Kuznetsov, N. V. [2020] "Existence of homoclinic orbits and heteroclinic cycle in a class of three-dimensional piecewise linear systems with three switching manifolds," *Chaos: An Interdisciplinary Journal of Nonlinear Science* **30**, art. num. 123143.

# PII

# THE CONSERVATIVE LOCK-IN RANGE FOR PLL WITH LEAD-LAG FILTER AND TRIANGULAR PHASE DETECTOR CHARACTERISTIC

by

M.V. Blagov, N.V. Kuznetsov, M.Y. Lobachev, M.V. Yuldashev, R.V. Yuldashev
2021

arXiv:2112.01602

# The conservative lock-in range for PLL with lead-lag filter and triangular phase detector characteristic

Blagov M.V.[a] Kuznetsov N.V.[b], Lobachev M.Y.[c], Yuldashev M.V.[d], Yuldashev R.V.[d]

***Abstract*— In the present work, a second-order PLL with lead-lag loop filter and triangular phase detector characteristic is analysed. An exact value of the conservative lock-in range is obtained for the considered model. The solution is based on analytical integration of the considered model on the linear segments.**

## I. INTRODUCTION

The interest to study phase-locked loops (PLL) comes from their wide applications. Initially described by A. Appleton in 1923 [1] and H. Bellescize [2], these circuits became widely spread in wireless communications [3]–[9], GPS navigation [10], gyroscope systems [11], [12], computer architectures [13], [14], and others.

First ideas of mathematical analysis of such systems belong to Italian academician F. Tricomi [15] and are based on the analysis of system phase portraits. These ideas were further developed in works of A.A. Andronov [16]. Fundamental monographs devoted to the problems of numerical simulation and analysis of PLL were published in 1966 by F. Gardner [17], A. Viterbi [18], V.V. Shakhgildyan, and A.A. Lyakhovkin [19]. These books are devoted mostly to engineering approaches of two-dimensional PLL models analysis.

In this article, we consider a PLL with lead-lag loop filter and triangular phase detector characteristic. Nonlinear analysis of this model and estimates of the global stability domain were conducted in [20]–[25]. Basing on these works, we analytically obtain an exact formula for the conservative lock-in range for the first time. This characterisctic considers the ability of PLL to synchronize in a short time and related to the Gardner problem [26], [27].

## II. MATHEMATICAL MODEL AND HOLD-IN RANGE

Consider analog PLL baseband model in Fig. 1 [18], [26], [28]–[30]. Here $\theta_{\rm ref}(t) = \omega_{\rm ref} t + \theta_{\rm ref}(0)$ is a phase of the reference signal, a phase of the VCO is $\theta_{\rm vco}(t)$, $\theta_e(t) = \theta_{\rm ref}(t) - \theta_{\rm vco}(t)$ is a phase error. A phase detector (PD) generates a signal $v_e(\theta_e(t))$ where $v_e(\cdot)$ is a characteristic of the phase detector. In the present paper, a piecewise-linear PD characteristic, which is continuous and corresponds to square waveforms of the reference and the VCO signals, is considered:

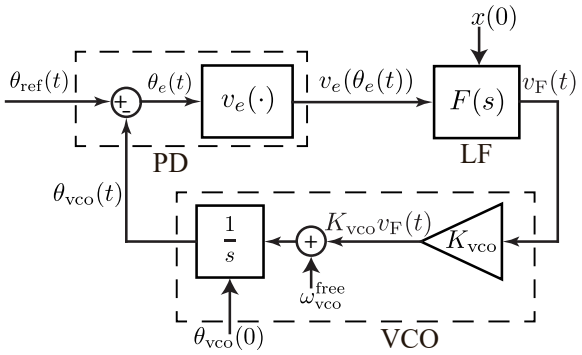


Fig. 1. Baseband model of analog PLLs.

$$v_e(\theta_e) = \begin{cases} \frac{2}{\pi}\theta_e - 4m, & -\frac{\pi}{2} + 2\pi m \le \theta_e(t) < \frac{\pi}{2} + 2\pi m, \\ -\frac{2}{\pi}\theta_e + 2 + 4m, & \frac{\pi}{2} + 2\pi m \le \theta_e(t) < -\frac{\pi}{2} + 2\pi(m+1), \end{cases} \tag{1}$$

here $m \in \mathbb{Z}$ (see Fig. 2).

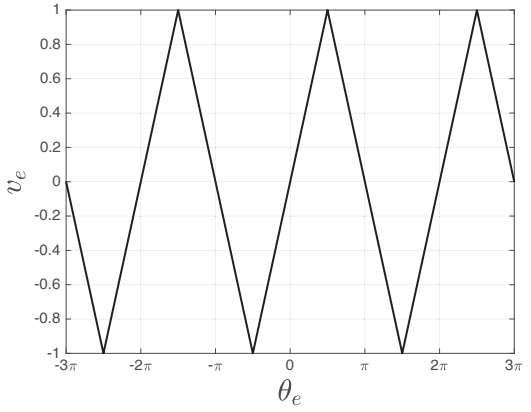


Fig. 2. Triangular PD characteristic.

The state of the loop filter is represented by $x(t) \in \mathbb{R}$ and

[a]Mikhail V. Blagov is with the Faculty of Mathematics and Mechanics, Saint Petersburg State University, Russia, with the Faculty of Mathematical Information Technology, University of Jyväskylä, Finland

[b]Nikolay V. Kuznetsov is with the Faculty of Mathematics and Mechanics, Saint Petersburg State University, Russia, with the Faculty of Mathematical Information Technology, University of Jyväskylä, Finland, with the Institute for Problems in Mechanical Engineering RAS, Russia nkuznetsov239@gmail.com

[c]Mikhail Y. Lobachev is with the Faculty of Mathematics and Mechanics, Saint Petersburg State University, Russia, with the Industrial Management Department, LUT University, Finland

[d]Marat V. Yuldashev, Renat V. Yuldashev are with the Faculty of Mathematics and Mechanics, Saint Petersburg State University, Russia

the transfer function is[1]

$$F(s) = \frac{1+\tau_2 s}{1+(\tau_1+\tau_2)s}, \quad \tau_1 > 0,\ \tau_2 \geq 0.$$

The output of the loop filter $v_{\mathrm{F}}(t) = \frac{1}{\tau_1+\tau_2}x + \frac{\tau_2}{\tau_1+\tau_2}v_e(\theta_e)$ is used to control the VCO frequency $\omega_{\mathrm{vco}}(t)$, which is proportional to the control voltage:

$$\omega_{\mathrm{vco}}(t) = \dot{\theta}_{\mathrm{vco}}(t) = \omega_{\mathrm{vco}}^{\mathrm{free}} + K_{\mathrm{vco}} v_{\mathrm{F}}(t)$$

where $K_{\mathrm{vco}} > 0$ is a gain and $\omega_{\mathrm{vco}}^{\mathrm{free}}$ is a free-running frequency of the VCO.

The behavior of PLL baseband model in the state space is described by a second-order nonlinear ODE:

$$\begin{aligned} \dot{x} &= -\frac{1}{\tau_1+\tau_2}x + \frac{\tau_1}{\tau_1+\tau_2}v_e(\theta_e), \\ \dot{\theta}_e &= \omega_e^{\mathrm{free}} - K_{\mathrm{vco}}\Big(\frac{1}{\tau_1+\tau_2}x + \frac{\tau_2}{\tau_1+\tau_2}v_e(\theta_e)\Big). \end{aligned} \tag{2}$$

where $\omega_e^{\mathrm{free}} = \omega_{\mathrm{ref}} - \omega_{\mathrm{vco}}^{\mathrm{free}}$ is a frequency error and $v_e(\theta_e)$ is defined in (1). It is usually supposed that the reference frequency (hence, $\omega_e^{\mathrm{free}}$ too) can be abruptly changed and that the synchronization occurs between those changes. Thus, existence of locked states, acquisition and transient processes after the reference frequency change are of interest.

The PLL baseband model in Fig. 1 is locked if the phase error $\theta_e(t)$ is constant. For the locked states of practically used PLLs, the loop filter state is constant too and, thus, the locked states of model in Fig. 1 correspond to the equilibria of model (2) [31].

*Definition 1:* [5], [27], [31] A *hold-in range* is the largest symmetric interval of frequency errors $|\omega_e^{\mathrm{free}}|$ such that an asymptotically stable equilibrium exists and varies continuously while $\omega_e^{\mathrm{free}}$ varies continuously within the interval.

Observe that system (2) is $2\pi$-periodic in $\theta_e$ and has an infinite number of equilibria $(x^{\mathrm{eq}},\ \theta_e^{\mathrm{eq}})$ which satisfy

$$\begin{aligned} v_e(\theta_e^{\mathrm{eq}}) &= \frac{\omega_e^{\mathrm{free}}}{K_{\mathrm{vco}}}, \\ x^{\mathrm{eq}} &= \frac{\tau_1 \omega_e^{\mathrm{free}}}{K_{\mathrm{vco}}}. \end{aligned}$$

From the boundedness of the PD characteristic it follows that there are no equilibria for sufficiently large $\omega_e^{\mathrm{free}}$. Further we suppose that $\omega_e^{\mathrm{free}} < K_{\mathrm{vco}}$ and the equilibria are

$$\left(\frac{\tau_1 \omega_e^{\mathrm{free}}}{K_{\mathrm{vco}}},\ (-1)^m \frac{\frac{\pi}{2}\omega_e^{\mathrm{free}}}{K_{\mathrm{vco}}} + \pi m\right),\ m \in \mathbb{Z}. \tag{3}$$

The characteristic polynomial of system (2) linearized at stationary states (3) is

$$\chi(\lambda) = \lambda^2 + \Big(\frac{1}{\tau_1+\tau_2} + \frac{K_{\mathrm{vco}}\tau_2}{\tau_1+\tau_2}v_e'(\theta_e^{\mathrm{eq}})\Big)\lambda + \frac{K_{\mathrm{vco}}}{\tau_1+\tau_2}v_e'(\theta_e^{\mathrm{eq}}).$$

[1]If $\tau_2 = 0$ then such filter is called a lag filter, if $\tau_2 > 0$ then it is called a lead-lag filter [26].

The nonlinearity $v_e(\theta_e)$ decreases $\left(v_e'(\pi - \frac{\frac{\pi}{2}\omega_e^{\mathrm{free}}}{K_{\mathrm{vco}}} + 2\pi m) = -\frac{2}{\pi} < 0\right)$ for $\frac{\pi}{2} + 2\pi m \leq \theta_e(t) < -\frac{\pi}{2} + 2\pi(m+1)$, and equilibria

$$\left(\frac{\tau_1 \omega_e^{\mathrm{free}}}{K_{\mathrm{vco}}},\ \pi - \frac{\frac{\pi}{2}\omega_e^{\mathrm{free}}}{K_{\mathrm{vco}}} + 2\pi m\right)$$

are saddles. The nonlinearity $v_e(\theta_e)$ increases $\left(v_e'(\frac{\frac{\pi}{2}\omega_e^{\mathrm{free}}}{K_{\mathrm{vco}}} + \pi m) = \frac{2}{\pi} > 0\right)$ for $-\frac{\pi}{2} + 2\pi m \leq \theta_e(t) < \frac{\pi}{2} + 2\pi m$, and equilibria

$$\left(\frac{\tau_1 \omega_e^{\mathrm{free}}}{K_{\mathrm{vco}}},\ \frac{\frac{\pi}{2}\omega_e^{\mathrm{free}}}{K_{\mathrm{vco}}} + 2\pi m\right)$$

are asymptotically stable ones, which can be either nodes, degenerate nodes or foci (see Appendix). Since an asymptotically stable equilibrium exists for any frequency error $\omega_e^{\mathrm{free}} < K_{\mathrm{vco}}$, the hold-in range of model (2) is $[0, \omega_h) = [0, K_{\mathrm{vco}})$ for any $\tau_1 > 0,\ \tau_2 \geq 0$.

## III. Global stability analysis

*Definition 2:* [5], [27], [31] A *pull-in range* is the largest symmetric interval of frequency errors $|\omega_e^{\mathrm{free}}|$ from the hold-in range such that an equilibrium is acquired for an arbitrary initial state.

### A. Pull-in range estimate by Lyapunov function

To obtain an estimate for the pull-in range of system (2), we apply the direct Lyapunov method and the corresponding theorem on global stability for the cylindrical phase space

*Theorem 1:* (see, e.g., [32], [33]). If there is a continuous function $V(x,\theta_e) : \mathbb{R}^2 \to \mathbb{R}$ such that

(i) $V(x,\theta_e + 2\pi) = V(x,\theta_e) \quad \forall x \in \mathbb{R}, \forall \theta_e \in \mathbb{R}$;

(ii) for any solution $(x(t),\theta_e(t))$ of system (2) the function $V(x(t),\theta_e(t))$ is nonincreasing;

(iii) if $V(x(t),\theta_e(t)) \equiv V(x(0),\theta_e(0))$, then $(x(t),\theta_e(t)) \equiv (x(0),\theta_e(0))$;

(iv) $V(x,\theta_e) + \theta_e^2 \to +\infty$ as $||x|| + |\theta_e| \to +\infty$

then any trajectory of system (2) tends to an equilibrium.

Following [32], [34], consider the following Lyapunov function:

$$\begin{aligned} V(x,\ \theta_e) &= \frac{1}{2}(x - \frac{\tau_1 \omega_e^{\mathrm{free}}}{K_{\mathrm{vco}}})^2 + \\ &+ \frac{\tau_1}{K_{\mathrm{vco}}}\int_0^{\theta_e} \Big(v_e(\sigma) - \frac{\omega_e^{\mathrm{free}}}{K_{\mathrm{vco}}} + \beta_0 |v_e(\sigma) - \frac{\omega_e^{\mathrm{free}}}{K_{\mathrm{vco}}}|\Big) d\sigma \end{aligned} \tag{4}$$

where

$$\beta_0 = -\frac{\int_0^{2\pi}(v_e(\sigma) - \frac{\omega_e^{\mathrm{free}}}{K_{\mathrm{vco}}})\ d\sigma}{\int_0^{2\pi}|v_e(\sigma) - \frac{\omega_e^{\mathrm{free}}}{K_{\mathrm{vco}}}|\ d\sigma} > 0.$$

Such form of the integrand expression makes the Lyapunov function $2\pi$-periodic. For triangular PD characteristic coefficient $\beta_0$ is

$$\beta_0 = \frac{2\omega_e^{\mathrm{free}} K_{\mathrm{vco}}}{(\omega_e^{\mathrm{free}})^2 + K_{\mathrm{vco}}^2}. \tag{5}$$

The Lyapunov function derivative along the trajectories of system (2) is

$$\dot{V}(x,\theta_e) = -\frac{1}{\tau_1+\tau_2}\Big((x-\frac{\tau_1\omega_e^{\text{free}}}{K_{\text{vco}}})^2 - \\ -\beta_0\tau_1(x-\frac{\tau_1\omega_e^{\text{free}}}{K_{\text{vco}}})(v_e(\theta_e)-\frac{\omega_e^{\text{free}}}{K_{\text{vco}}})+ \\ +\tau_1\tau_2(1-\beta_0)(v_e(\theta_e)-\frac{\omega_e^{\text{free}}}{K_{\text{vco}}})^2\Big).$$

If the loop filter parameters satisfy the inequality

$$\beta_0 < 2(-\frac{\tau_2}{\tau_1}+\frac{\sqrt{\tau_2(\tau_1+\tau_2)}}{\tau_1}) \tag{6}$$

then the Lyapunov function derivative along the trajectories of system (2) is as follows:

$$\dot{V}(x,\theta_e) < 0, \quad x \neq \frac{\tau_1\omega_e^{\text{free}}}{K_{\text{vco}}},\ v_e(\theta_e) \neq \frac{\omega_e^{\text{free}}}{K_{\text{vco}}}.$$

Since the derivative along any solution other than equilibria is not identically zero, condition (6) provides the global stability of the system. Taking into account (5) and (6), the following estimate for the pull-in range is obtained:

$$\omega_p > \Big(\frac{\tau_1}{2\sqrt{\tau_2(\tau_1+\tau_2)}-2\tau_2} - \\ -\sqrt{\frac{\tau_1^2}{(2\sqrt{\tau_2(\tau_1+\tau_2)}-2\tau_2)^2}-1}\Big)K_{\text{vco}}. \tag{7}$$

### *B. Analysis of cycles of first and second kind*

Firstly, let us analyse the dissipativity domain. Consider the following Lyapunov function:

$$V(x,\ \theta_e) = \frac{1}{2}\tau_1 x^2.$$

Its derivative along the trajectories of system (2) is:

$$\dot{V}(x,\theta_e) = -\frac{\tau_1}{\tau_1+\tau_2}x\Big(x-\tau_1 v_e(\theta_e)\Big).$$

If $|x| > \tau_1 v_e(\theta_e)$, then $\dot{V}(x,\theta_e) < 0$. Hence, $\limsup_{t\to+\infty}|x(t)| < \tau_1$ and an estimate for the dissipativity domain is $|x(t)| < \tau_1$.

Using change of variables $z = -\frac{K_{\text{vco}}}{\tau_1+\tau_2}(x-\frac{\tau_1\omega_e^{\text{free}}}{K_{\text{vco}}})$, system (2) becomes system (4.3) from [35] with $\alpha = \frac{1}{\tau_1+\tau_2}$, $\beta = \frac{1}{\tau_1+\tau_2}K_{\text{vco}}$, $a = \frac{\tau_2}{\tau_1+\tau_2}K_{\text{vco}}$. Applying Theorem 4.1 from [35] we get that any trajectory of system (2) which is bounded in $\mathbb{R}^2$ tends to an equilibrium, hence, there are no the cycles of the first kind. If there is a homoclinic orbit in the system, then it envelops an asymptotically stable equilibrium and a cycle of the second kind exists in this case due the dissipativity [21] (thus, a homoclinic orbit does not determine the global stability and the pull-in range).

Thus, depending on the system parameters $K_{\text{vco}},\ \tau_1,\ \tau_2$ there are three possibilities of the global stability loss in system (2):

- disappearance of equilibria (in this case $[0,\omega_p) = [0,\omega_h)$
- appearance of separatrix cycle
- appearance of semi-stable cycle (cycle of the second kind)

Applying Theorem 4.2 from [35] it can be shown that there are no either the separatrix cycles or the cycles of the second kind in domain $x > x^{\text{eq}}$. Since the system is piecewise-linear, its trajectories can be analytically integrated (see Appendix) and exact frequency error values for separatrix and semi-stable cycles (hence, the pull-in range) can be obtained (see, e.g., [21], [22], [36]–[38]).

## IV. Conservative lock-in range

Although a PLL model can be globally stable, the acquisition process can take long time. To decrease the synchronization time, a lock-in range concept is frequently exploited [13], [26], [28].

*Definition 3:* [5], [27], [31] A *lock-in range* is the largest interval of frequency errors $|\omega_e^{\text{free}}|$ from the pull-in range such that the PLL model being in an equilibrium, after any abrupt change of $\omega_e^{\text{free}}$ within the interval acquires an equilibrium without cycle slipping ($\sup_{t>0}|\theta_e(0)-\theta_e(t)| < 2\pi$).

From a mathematical point of view, system (2) can initially be in an unstable equilibrium (at one of the saddles) or can acquire it by a separatrix after a change of $\omega_e^{\text{free}}$ (see [38], [39]). Corresponding behavior is not observed in practice: system state is disturbed by noise and can't remain in unstable equilibrium. Thus, two cycle-slipping-related characteristics of the system can be considered: *the lock-in range* $|\omega_e^{\text{free}}| \in [0,\omega_l)$ where the equilibria are considered to be stable and *the conservative lock-in range* $|\omega_e^{\text{free}}| \in [0,\omega_l^c) \subset [0,\omega_l)$ which takes into account the unstable behavior described above. In this article, we analyse the conservative lock-in range $[0,\omega_l^c)$.

For the considered model boundary values $\omega_l$ and $\omega_l^c$ are determined as follows: The system being in an equilibrium state is exposed to an abrupt change of $\omega_e^{\text{free}}$, and the corresponding trajectory of the system after the switch tends to the nearest unstable equilibrium by the corresponding saddle separatrix. In other words, $\sup_{t>0}|\theta_e(0)-\theta_e(t)| = \pi$ for $\theta_e(0) = 2\pi$ (see Fig. 3, lower left picture) and $\sup_{t>0}|\theta_e(0)-\theta_e(t)| = 2\pi$ for $\theta_e(0) = 3\pi$ (see Fig. 3, upper right picture). For a larger $\omega_e^{\text{free}}$ supremum $\sup_{t>0}|\theta_e(0)-\theta_e(t)| > 2\pi$ and cycle slipping occurs. Since the lock-in range is defined as a half-open interval, boundary values $\omega_e^{\text{free}} = \omega_l$ and $\omega_e^{\text{free}} = \omega_l^c$ are not included in it.

Using changes of variables we represent system (2) as the first-order differential equation [38], [40], analytically integrate it on the linear segments, formulate, and prove the theorem providing an exact value for the conservative lock-in range.

*Theorem 2:* The conservative lock-in frequency of model (2) with triangular PD characteristic (1) is $\omega_l^c$ which is the

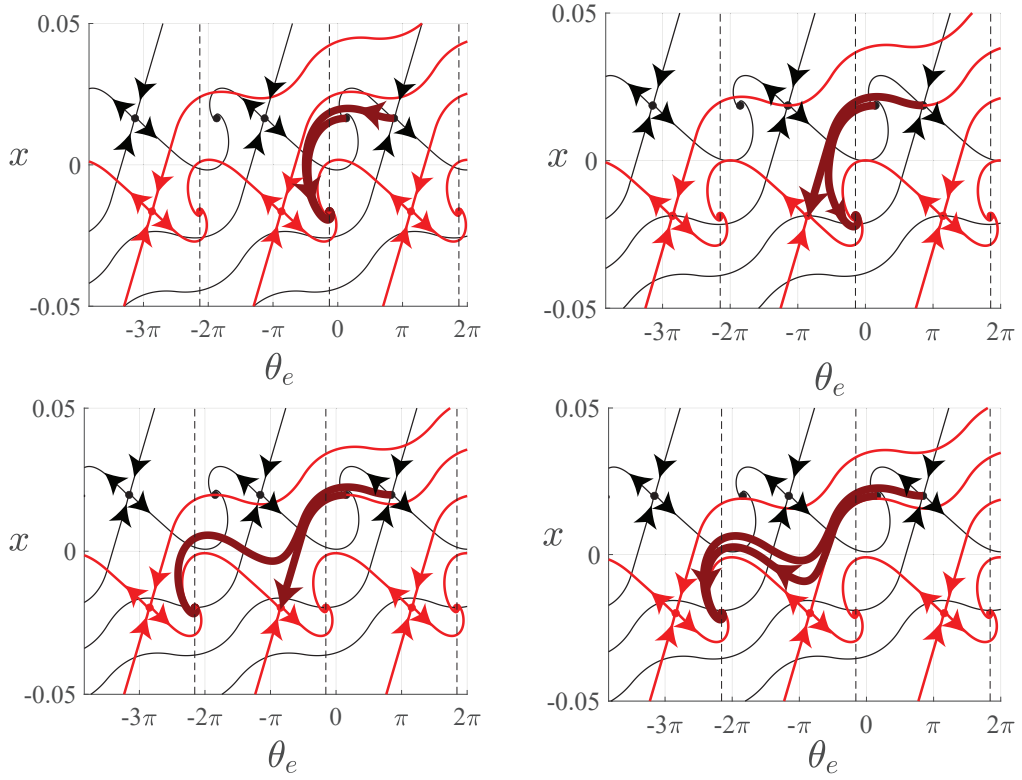


Fig. 3. Phase portraits for model (2) with the following parameters: $F(s)=\frac{1+\tau_2 s}{1+(\tau_1+\tau_2)s}$, $\tau_1=0.0633$, $\tau_2=0.0225$, $K_{\rm vco}=250$. Black dots are equilibria of the model with positive $\omega_e^{\rm free}=|\omega|$. Red color is for the model with negative $\omega_e^{\rm free}=-|\omega|$. Separatrices pass in and out of the saddles equilibria. Upper left subfigure: $\omega=65<\omega_l^c$, upper right subfigure: $\omega=\omega_l^c\approx 73.732$, lower left subfigure: $\omega=\omega_l\approx 77.7583$, lower right subfigure: $\omega=79>\omega_l$.

unique solution of system of two variables $(\omega_l^c,\ y_{\rm AB})$:

$$
\begin{cases}
(2\omega_l^c)^2\Big(\sqrt{\frac{\tau_1+\tau_2}{\frac{2}{\pi}K_{\rm vco}}}-\frac{\eta-\kappa}{\frac{2}{\pi}K_{\rm vco}}\Big)^{\frac{\kappa-\eta}{\kappa}}\Big(\sqrt{\frac{\tau_1+\tau_2}{\frac{2}{\pi}K_{\rm vco}}}-\frac{\eta+\kappa}{\frac{2}{\pi}K_{\rm vco}}\Big)^{\frac{\kappa+\eta}{\kappa}}= \\
=\Big(y_{\rm AB}-(\eta-\kappa)\frac{\omega_l^c+K_{\rm vco}}{\frac{2}{\pi}K_{\rm vco}}\Big)^{\frac{\kappa-\eta}{\kappa}}\Big(y_{\rm AB}-(\eta+\kappa)\frac{\omega_l^c+K_{\rm vco}}{\frac{2}{\pi}K_{\rm vco}}\Big)^{\frac{\kappa+\eta}{\kappa}}, \\
\Big(y_{\rm AB}-(\xi-\rho)\frac{\omega_l^c+K_{\rm vco}}{\frac{2}{\pi}K_{\rm vco}}\Big)^{\frac{\rho-\xi}{\rho}}\Big(y_{\rm AB}-(\xi+\rho)\frac{\omega_l^c+K_{\rm vco}}{\frac{2}{\pi}K_{\rm vco}}\Big)^{\frac{\rho+\xi}{\rho}}= \\
=(\kappa-\eta+\xi-\rho)^{\frac{\rho-\xi}{\rho}}\cdot \\
\cdot(\kappa-\eta+\xi+\rho)^{\frac{\rho+\xi}{\rho}}\big(\frac{K_{\rm vco}-\omega_l^c}{\frac{2}{\pi}K_{\rm vco}}\big)^2, \quad \text{if} \quad \xi>1, \\
\frac{K_{\rm vco}+\omega_l^c}{K_{\rm vco}+\omega_l^c-\frac{2}{\pi}K_{\rm vco}y_{\rm AB}}+\ln(2|y_{\rm AB}-\frac{\pi(K_{\rm vco}+\omega_l^c)}{2K_{\rm vco}}|)= \\
=\frac{1}{\kappa-\eta+1}+\ln\Big(2(\kappa-\eta+1)\frac{\pi(K_{\rm vco}-\omega_l^c)}{2K_{\rm vco}}\Big), \quad \text{if} \quad \xi=1, \\
\frac{1}{2}\ln(y_{\rm AB}^2-2\xi y_{\rm AB}\frac{\pi(K_{\rm vco}+\omega_l^c)}{2K_{\rm vco}}+(\frac{\pi(K_{\rm vco}+\omega_l^c)}{2K_{\rm vco}})^2)- \\
-\frac{\xi}{\rho}\arctan\Big(\frac{y_{\rm AB}-\xi\frac{\pi(K_{\rm vco}+\omega_l^c)}{2K_{\rm vco}}}{-(\frac{\pi(K_{\rm vco}+\omega_l^c)}{2K_{\rm vco}})\rho}\Big)+\frac{\xi}{\rho}\arctan\Big(\frac{\kappa-\eta+\xi}{\rho}\Big)= \\
=\frac{1}{2}\ln\Big(((\kappa-\eta)^2+2\xi(\kappa-\eta)+1)\Big(\frac{K_{\rm vco}-\omega_l^c}{\frac{2}{\pi}K_{\rm vco}}\Big)^2\Big)+ \\
+\frac{\pi\xi}{\rho}, \quad \text{if} \quad \xi<1
\end{cases}
\tag{8}
$$

where

$$
\xi=\frac{\frac{2}{\pi}\tau_2K_{\rm vco}+1}{2\sqrt{\frac{2}{\pi}K_{\rm vco}(\tau_1+\tau_2)}}, \quad \eta=\frac{\frac{2}{\pi}\tau_2K_{\rm vco}-1}{2\sqrt{\frac{2}{\pi}K_{\rm vco}(\tau_1+\tau_2)}},
$$

$$
\rho=\sqrt{|\xi^2-1|}, \quad \kappa=\sqrt{\eta^2+1}.
$$

*Proof:* [Proof of Theorem 2] The proof given in Appendix is based on the fact that system (2) is piecewise-linear and can be integrated analytically on the linear segments. ■

## V. Computer simulation

Based on Theorem 2 an analytical-numerical method of the conservative lock-in range calculation was implemented (see Appendix B and Fig. 4).

## VI. Conclusions

In this work, the exact value of the conservative lock-in range was obtained for a classical PLL with lead-lag filter and triangular phase detector characteristic.

## Appendix A: Proof of Theorem 2

*Proof:* Let's find the conservative lock-in range of model (2) with triangular PD characteristic (1). The conservative lock-in frequency can be determined by such an abrupt change of $\omega_e^{\rm free}$ that the corresponding trajectory tends to the

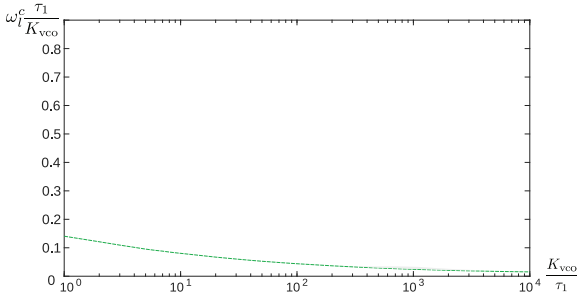


Fig. 4. The conservative lock-in frequency. Parameters: $\tau_1 = 0.5$, $\tau_2 = 0.0225$.

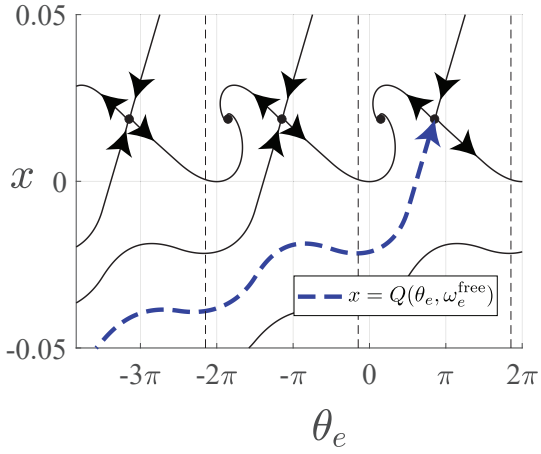


Fig. 5. Separatrix $x = Q(\theta_e, \omega_e^{\rm free})$ of the phase plane of (2). Parameters: $\tau_1 = 0.0633$, $\tau_2 = 0.0225$, $K_{\rm vco} = 250$, $\omega_e^{\rm free} = 73.732$.

nearest unstable equilibrium (by the corresponding separatrix). Suppose that initially the frequency error was equal to $\omega_e^{\rm free} = -\omega < 0$, but then changed to $\omega_e^{\rm free} = \omega > 0$. Hence, initially the system was in equilibrium $x^{\rm eq} = -\frac{\tau_1 \omega}{K_{\rm vco}}$, $\theta_e^{\rm eq} = -\pi + \frac{\frac{\pi}{2}\omega}{K_{\rm vco}}$, but after the switch the corresponding trajectory tends to $x^{\rm eq} = \frac{\tau_1 \omega}{K_{\rm vco}}$, $\theta_e^{\rm eq} = \frac{\frac{\pi}{2}\omega}{K_{\rm vco}}$ without cycle slipping if $\omega < \omega_l^c$.

Such $\omega_l^c$ is determined by such frequency error $\omega_e^{\rm free}$ that a trajectory being in unstable equilibrium (before the switch) $x^{\rm eq} = -\frac{\tau_1 \omega_l^c}{K_{\rm vco}}$, $\theta_e^{\rm eq} = -\pi + \frac{\frac{\pi}{2}\omega_l^c}{K_{\rm vco}}$ tends to the closest unstable equilibrium (after the switch) $x^{\rm eq} = \frac{\tau_1 \omega_l^c}{K_{\rm vco}}$, $\theta_e^{\rm eq} = \pi - \frac{\frac{\pi}{2}\omega_l^c}{K_{\rm vco}}$ by the corresponding separatrix. Thus, the conservative lock-in frequency $\omega_l^c$ corresponds to the case

$$-\frac{\tau_1 \omega_l^c}{K_{\rm vco}} = Q\left(\frac{\frac{\pi}{2}\omega_l^c}{K_{\rm vco}} - \pi,\ \omega_l^c\right) \tag{9}$$

where $\frac{\tau_1 \omega_e^{\rm free}}{K_{\rm vco}}$ is $x$-coordinate of equilibrium of model (2) and $x = Q(\theta_e, \omega_e^{\rm free})$ is the lower separatrix of saddle equilibrium $(\frac{\tau_1 \omega_e^{\rm free}}{K_{\rm vco}},\ \pi - \frac{\frac{\pi}{2}\omega_e^{\rm free}}{K_{\rm vco}})$ (see Fig. 5).

After the change of variables

$$\begin{aligned} y &= \sqrt{\frac{\pi(\tau_1+\tau_2)}{2K_{\rm vco}}}\omega_e^{\rm free} - \sqrt{\frac{\pi K_{\rm vco}}{2(\tau_1+\tau_2)}}\Big(x + \tau_2 v_e(\theta_e)\Big), \\ \tau &= \sqrt{\frac{2K_{\rm vco}}{\pi(\tau_1+\tau_2)}}t \end{aligned} \tag{10}$$

system (2) in intervals $\theta_e(t) \in (-\frac{\pi}{2} + 2\pi m,\ \frac{\pi}{2} + 2\pi m)$ and $\theta_e(t) \in (\frac{\pi}{2} + 2\pi m,\ -\frac{\pi}{2} + 2\pi(m+1))$, $m \in \mathbb{Z}$ is represented as follows:

$$\begin{aligned} \dot{y} &= -\frac{\pi}{2}v_e(\theta_e) - \frac{\sqrt{\pi}}{\sqrt{2K_{\rm vco}(\tau_1+\tau_2)}}(1 + K_{\rm vco}\tau_2 v_e'(\theta_e))y + \frac{\pi\omega_e^{\rm free}}{2K_{\rm vco}}, \\ \dot{\theta}_e &= y. \end{aligned} \tag{11}$$

Upper separatrix $y = S(\theta_e)$ of the phase plane of (11) corresponds to separatrix $x = Q(\theta_e, \omega_e^{\rm free})$ from (2) (see Fig. 5 and Fig. 6) and has the form

$$\begin{aligned} S(\theta_e) = &\sqrt{\frac{\pi(\tau_1+\tau_2)}{2K_{\rm vco}}}\omega_e^{\rm free} - \\ &- \sqrt{\frac{\pi K_{\rm vco}}{2(\tau_1+\tau_2)}}\Big(Q(\theta_e,\ \omega_e^{\rm free}) + \tau_2 v_e(\theta_e)\Big). \end{aligned}$$

Thus, relation (9) takes the form

$$S\left(\frac{\pi\omega_l^c}{2K_{\rm vco}} - \pi\right) = 2\omega_l^c\sqrt{\frac{\pi(\tau_1+\tau_2)}{2K_{\rm vco}}}. \tag{12}$$

The computation of $\omega_l^c$ consists of the following stages. Let's divide the phase plane to the following domains:

- $A = \{(y,\ \theta_e) \mid \frac{\pi}{2} - 2\pi \le \theta_e(t) \le -\frac{\pi}{2};\ \theta_e, y \in \mathbb{R}\}$,
- $B = \{(y,\ \theta_e) \mid -\frac{\pi}{2} \le \theta_e(t) \le \frac{\pi}{2};\ \theta_e, y \in \mathbb{R}\}$.

In the open domains, system (11) is a linear one and can be integrated analytically. Firstly, we compute $S(\frac{\pi}{2})$, which is possible due to the continuity of (2), and use it as the initial data of the Cauchy problem (see Fig. 6). Secondly, finding its solution in the domain B, we compute $S(-\frac{\pi}{2})$, which is used as the initial data of the Cauchy problem. Its solution in the domain A is used for the conservative lock-in frequency $\omega_l^c$ computation due to (12).

### A. $S(\frac{\pi}{2})$ value

The saddle separatrix is locally described by the saddle's eigenvectors

$$V_+^{\rm s} = \begin{pmatrix} 1 \\ -\kappa + \eta \end{pmatrix}, \quad V_-^{\rm s} = \begin{pmatrix} 1 \\ -\eta - \kappa \end{pmatrix}$$

where

$$\begin{aligned} \eta &= \frac{\frac{2}{\pi}\tau_2 K_{\rm vco} - 1}{2\sqrt{\frac{2}{\pi}K_{\rm vco}(\tau_1+\tau_2)}}, \\ \kappa &= \sqrt{\eta^2 + 1}. \end{aligned}$$

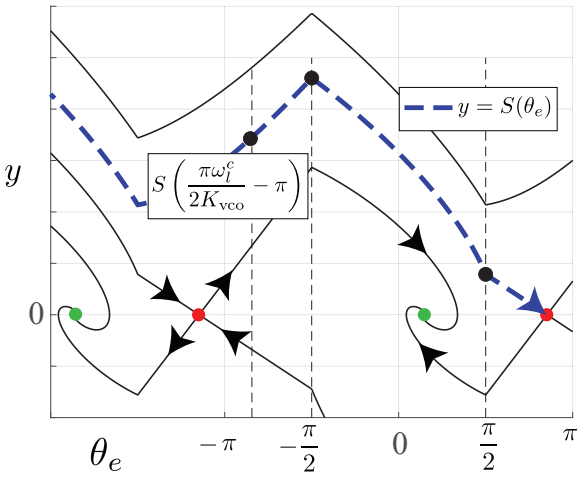


Fig. 6. Separatrix $y = S(\theta_e)$ of the phase plane of (11) integration. Firstly, we compute $S(\frac{\pi}{2})$ and use it as the initial data of the Cauchy problem. Secondly, finding its solution in the domain B, we compute $S(-\frac{\pi}{2})$, which is used as the initial data of the Cauchy problem. Its solution in the domain A is used for the conservative lock-in frequency $\omega_l^c$ computation due to (12). Parameters: $\tau_1 = 0.0633$, $\tau_2 = 0.0225$, $K_{\text{vco}} = 250$, $\omega_e^{\text{free}} = 73.732$.

Eigenvector $V_-^s$ points to a saddle and $V_+^s$ has the opposite direction. Since in the considered domain the system is a linear one, then the separatrix coincides with the line corresponding to $V_-^s$:

$$S(\theta_e) = (\kappa - \eta)(-\theta_e + \pi - \frac{\pi\omega_e^{\text{free}}}{2K_{\text{vco}}}), \quad \frac{\pi}{2} < \theta_e < \pi. \tag{13}$$

Let's obtain the limit value in $\theta_e = \frac{\pi}{2}$:

$$S(\frac{\pi}{2}) = (\kappa - \eta)(\frac{\pi}{2} - \frac{\pi\omega_e^{\text{free}}}{2K_{\text{vco}}}).$$

*B. Analytical integration in domain B*

In domain B, $v_e(\theta_e) = \frac{2}{\pi}\theta_e, v_e'(\theta_e) = \frac{2}{\pi}$ and (11) can be rewritten as

$$\begin{aligned} \dot{y} &= -\theta_e - 2\xi y + \frac{\pi\omega_e^{\text{free}}}{2K_{\text{vco}}}, \\ \dot{\theta}_e &= y \end{aligned} \tag{14}$$

where

$$\xi = \frac{\frac{2}{\pi}\tau_2 K_{\text{vco}} + 1}{2\sqrt{\frac{2}{\pi}K_{\text{vco}}(\tau_1 + \tau_2)}} > 0.$$

In the domains $\{y > 0\}$ and $\{y < 0\}$, variable $\theta_e(t)$ changes monotonically and the behaviour of system (14) can be described by the first-order differential equation:

$$\frac{dy}{d\theta_e} = -2\xi - \frac{\theta_e - \frac{\omega_e^{\text{free}}}{\frac{2}{\pi}K_{\text{vco}}}}{y}. \tag{15}$$

The obtained equation is Chini's equation [41], [42], which is a generalization of Abel and Riccati equations. The change of variables $z = \frac{y}{\theta_e - \frac{\omega_e^{\text{free}}}{\frac{2}{\pi}K_{\text{vco}}}}$ maps equation (15) into a separable one:

$$\frac{zdz}{z^2 + 2\xi z + 1} = -\frac{d\theta_e}{\theta_e - \frac{\omega_e^{\text{free}}}{\frac{2}{\pi}K_{\text{vco}}}}. \tag{16}$$

If $\theta_e \neq \frac{\omega_e^{\text{free}}}{\frac{2}{\pi}K_{\text{vco}}}$ and $z^2 + 2\xi z + 1 \neq 0$ then the solutions of system (15) and system (16) coincide in domains $0 < \theta_e < \frac{\pi}{2}$ and $-\frac{\pi}{2} < \theta_e < 0$. Depending on the type of an asymptotically stable equilibrium, the following cases appear:

- $\xi > 1$ (the equation $z^2 + 2\xi z + 1 = 0$ corresponds the eigenvectors of the stable node),
- $\xi = 1$ (the equation $z^2 + 2\xi z + 1 = (z + \xi)^2 = 0$ corresponds the eigenvector of the stable degenerate node),
- $0 < \xi < 1$ (here the case $z^2 + 2\xi z + 1 = 0$ is not possible).

It can be shown that if $\xi \geq 1$ then in domain $B$ separatrix $y = S(\theta_e)$ satisfies $N(y, \theta_e) = N(S(\frac{\pi}{2}), \frac{\pi}{2})$ where

$$\begin{aligned} &N(y, \theta_e) = \frac{1}{2}\ln\Big(\big(y + (\xi - \rho)(\theta_e - \frac{\pi\omega_e^{\text{free}}}{2K_{\text{vco}}})\big)^{\frac{\rho - \xi}{\rho}} \cdot \\ &\cdot \big(y + (\xi + \rho)(\theta_e - \frac{\pi\omega_e^{\text{free}}}{2K_{\text{vco}}})\big)^{\frac{\rho + \xi}{\rho}}\Big), \quad \xi > 1, \\ &N(y, \theta_e) = \frac{\theta_e - \frac{\pi\omega_e^{\text{free}}}{2K_{\text{vco}}}}{y + \theta_e - \frac{\pi\omega_e^{\text{free}}}{2K_{\text{vco}}}} + \ln(2|y + \theta_e - \frac{\pi\omega_e^{\text{free}}}{2K_{\text{vco}}}|), \quad \xi = 1, \\ &\rho = \sqrt{|\xi^2 - 1|}. \end{aligned} \tag{17}$$

Similarly, if $\xi < 1$ then

- in domain $-\frac{\pi}{2} < \theta_e < \frac{\pi\omega_e^{\text{free}}}{2K_{\text{vco}}}$ separatrix $y = S(\theta_e)$ satisfies $N(y, \theta_e) = N(S(\frac{\pi}{2}), \frac{\pi}{2}) + \frac{\pi\xi}{\rho}$,
- in domain $\frac{\pi\omega_e^{\text{free}}}{2K_{\text{vco}}} < \theta_e < \frac{\pi}{2}$ separatrix $y = S(\theta_e)$ satisfies $N(y, \theta_e) = N(S(\frac{\pi}{2}), \frac{\pi}{2})$

where

$$\begin{aligned} &N(y, \theta_e) = \frac{1}{2}\ln(y^2 + 2\xi y(\theta_e - \frac{\pi\omega_e^{\text{free}}}{2K_{\text{vco}}}) + (\theta_e - \frac{\pi\omega_e^{\text{free}}}{2K_{\text{vco}}})^2) - \\ &- \frac{\xi}{\rho}\arctan\Big(\frac{y + \xi(\theta_e - \frac{\pi\omega_e^{\text{free}}}{2K_{\text{vco}}})}{(\theta_e - \frac{\pi\omega_e^{\text{free}}}{2K_{\text{vco}}})\rho}\Big). \end{aligned} \tag{18}$$

Let us denote $y_{\text{AB}} = S(-\frac{\pi}{2})$ and use this value as the initial data of the Cauchy problem:

$$\begin{aligned} &N\Big(y_{\text{AB}}, -\frac{\pi}{2}\Big) = N(S(\frac{\pi}{2}), \frac{\pi}{2}) \quad \xi \geq 1, \\ &N\Big(y_{\text{AB}}, -\frac{\pi}{2}\Big) = N(S(\frac{\pi}{2}), \frac{\pi}{2}) + \frac{\pi\xi}{\rho} \quad \xi < 1. \end{aligned} \tag{19}$$

Taking into account equations (17) and (18), equations (19) provide the last three formulae in (8).

### C. Analytical integration in domain A

In domain A, $v_e(\theta_e) = -\frac{2}{\pi}\theta_e + 2, v'_e(\theta_e) = -\frac{2}{\pi}$ and (11) can be rewritten as

$$\begin{aligned} \dot{y} &= (\theta_e + \pi) + 2\eta y + \frac{\pi\omega_e^{\text{free}}}{2K_{\text{vco}}}, \\ \dot{\theta}_e &= y. \end{aligned} \tag{20}$$

In the domains $\{y > 0\}$ and $\{y < 0\}$, variable $\theta_e(t)$ changes monotonically and the behaviour of system (20) can be described by the first-order differential equation:

$$\frac{dy}{d\theta_e} = \frac{2}{\mu}\eta + \frac{\theta_e + \pi + \frac{\pi\omega_e^{\text{free}}}{2K_{\text{vco}}}}{y}. \tag{21}$$

The change of variables $z = \frac{y}{\theta_e + \pi + \frac{\pi\omega_e^{\text{free}}}{2K_{\text{vco}}}}$ maps equation (21) into a separable one:

$$\frac{zdz}{z^2 - 2\eta z - 1} = -\frac{d\theta_e}{\theta_e + \pi + \frac{\pi\omega_e^{\text{free}}}{2K_{\text{vco}}}}. \tag{22}$$

If $\theta_e \neq -(\frac{\pi\omega_e^{\text{free}}}{2K_{\text{vco}}} + \pi)$ and $z^2 - 2\eta z - \neq 0$ then the solutions of system (21) and system (22) coincide.

It can be shown that in domain $A$ separatrix $y = S(\theta_e)$ satisfies $M(y, \theta_e) = M(y_{\text{AB}}, -\frac{\pi}{2})$ where

$$\begin{aligned} M(y, \theta_e) = \frac{1}{2}\ln\Bigg(\Big(y + \frac{\theta_e + \pi + \frac{\pi\omega_e^{\text{free}}}{2K_{\text{vco}}}}{\kappa + \eta}\Big)^{\frac{\kappa-\eta}{\kappa}} \cdot \\ \cdot \Big(y + \frac{\theta_e + \pi + \frac{\pi\omega_e^{\text{free}}}{2K_{\text{vco}}}}{\eta - \kappa}\Big)^{\frac{\kappa+\eta}{\kappa}}\Bigg). \end{aligned} \tag{23}$$

Finally, the first equation in (8) is obtained by consideration (12) and (23):

$$M\left(2\omega_l^c\sqrt{\frac{\tau_1 + \tau_2}{kK_{\text{vco}}}},\ \frac{(\pi - \frac{1}{k})\omega_l^c}{K_{\text{vco}}} - \pi\right) = M(y_{\text{AB}}, -\frac{1}{k}).$$

■

## APPENDIX B: CALCULATION OF THE CONSERVATIVE LOCK-IN FREQUENCY

Calculation of the conservative lock-in frequency for PLL with lead-lag filter and triangular phase-detector characteristic.

```
function out = omega_1_conservative(
    tau_1, tau_2, k, K_vco)

    out = 0;
    mu = pi*k - 1;
    xi = (k*tau_2*K_vco + 1)/(2*sqrt(k*
        K_vco*(tau_1 + tau_2)));
    eta = (k*tau_2*K_vco - mu)/(2*sqrt(k
        *K_vco*(tau_1 + tau_2)));
    rho = sqrt(abs(xi^2 - 1));
    kappa = sqrt(eta^2 + mu);

syms y_ab zomega_lc;

curve1 = (2*zomega_lc)^2*...
    (sqrt((tau_1 + tau_2)/(k*K_vco))
        - ...
    (eta - kappa)/(k*K_vco))^((kappa
        - eta)/kappa)*...
    (sqrt((tau_1 + tau_2)/(k*K_vco))
        - ...
    (eta + kappa)/(k*K_vco))^((kappa
        + eta)/kappa) == ...
    (y_ab - (eta - kappa)*((
        zomega_lc + K_vco)/...
    (k*K_vco)))^((kappa - eta)/kappa
        )*...
    (y_ab - (eta + kappa)*((
        zomega_lc + K_vco)/...
    (k*K_vco)))^((kappa + eta)/kappa
        );

if xi > 1
    curve2 = (y_ab - (xi - rho)*((
        zomega_lc + K_vco)/...
    (k*K_vco)))^((rho - xi)/(rho))
        *...
        (y_ab - (xi + rho)*...
        ((zomega_lc + K_vco)/(k*
            K_vco)))^((rho + xi)/(rho
            )) == ...
        (kappa - eta + xi - rho)^((
            rho - xi)/...
        (rho))*(kappa - eta + xi +
            rho)^((rho + xi)/(rho))
            *...
        ((K_vco - zomega_lc)/(k*
            K_vco))^2;
else
    if (abs(xi - 1) < 0.001)
        curve2 = (-(K_vco +
            zomega_lc)/(k*K_vco))/...
        (y_ab -(K_vco + zomega_lc)/(
            k*K_vco)) + ...
             log(2*abs(y_ab -(K_vco +
                 zomega_lc)/(k*K_vco)
                 )) == ...
             1/(kappa - eta + 1) +
                 ...
             ln(2*(kappa - eta + 1)*(
                 K_vco - zomega_lc)/(k
                 *K_vco));
    else
        curve2 = 1/2*log(y_ab^2 - 2*
            xi*y_ab*(K_vco +
            zomega_lc)/...
```

```
            (k*K_vco) + ((K_vco +
                zomega_lc)/(k*K_vco))^2)
                -...
                 xi/rho*atan((y_ab - xi*(
                     K_vco + zomega_lc)/(k
                     *K_vco))/...
                 (-(K_vco + zomega_lc)/(k
                     *K_vco)*rho)) == ...
            1/2*log(...
            ((kappa - eta)^2 + 2*xi*(
                kappa-eta) + 1)*...
            ((K_vco - zomega_lc)/(k*
                K_vco))^2 ...
            ) - xi/rho*atan((kappa - eta
                + xi)/rho) + pi*xi/rho;
        end
    end

    res = vpasolve([curve1, curve2], [0
        Inf; 0 K_vco]);
    if ~isempty(eval(res.zomega_lc))
        out = eval(res.zomega_lc);
    end
end
```

## REFERENCES


[1] E V Appleton. *Automatic synchronization of triode oscillators*, volume 21. 1923.

[2] H Bellescize. *La réception synchrone*, volume 11. 1932.

[3] K.L. Du and M.N.S. Swamy. *Wireless Communication Systems: from RF subsystems to 4G enabling technologies*. Cambridge University Press, 2010.

[4] T.J. Rouphael. *Wireless Receiver Architectures and Design: Antennas, RF, Synthesizers, Mixed Signal, and Digital Signal Processing*. Elsevier Science, 2014.

[5] R E Best, N V Kuznetsov, G A Leonov, M V Yuldashev, and R V Yuldashev. Tutorial on dynamic analysis of the {C}ostas loop. *IFAC Annual Reviews in Control*, 42:27–49, 2016.

[6] P˜S. Cho. *Optical Phase-Locked Loop Performance in Homodyne Detection Using Pulsed and CW LO*. Optical Society of America, 2006.

[7] K.P. Ho. *Phase-Modulated Optical Communication Systems*. Springer, 2005.

[8] G. M. Helaluddin. An improved optical Costas loop PSK receiver: simulation analysis. *Journal of Scientific & Industrial Research*, 67:203–208, 2008.

[9] W. Rosenkranz and S. Schaefer. Receiver design for optical intersatellite links based on digital signal processing. In *18th International Conference on Transparent Optical Networks (ICTON)*, pages 1–4. IEEE, 2016.

[10] E.D. Kaplan and C.J. Hegarty. *Understanding GPS/GNSS: Principles and Applications*. Artech House, 3 edition, 2017.

[11] L. Aaltonen and K. A. I. Halonen. An analog drive loop for a capacitive MEMS gyroscope. *Analog Integrated Circuits and Signal Processing*, 63(3):465 – 476, 2010.

[12] N.V. Kuznetsov, G. Kolumbán, Y.V. Belyaev, A.T. Tulaev, M.V. Yuldashev, and R.V. Yuldashev. Estimation of PLL impact on MEMS-gyroscopes parameters. *Gyroscopy and Navigation*, 2022. (in print).

[13] G. Kolumbán. *The Encyclopedia of RF and Microwave Engineering, Phase-locked loops*, volume 4. John Wiley & Sons, New-York, 2005.

[14] R E Best. *Costas Loops: Theory, Design, and Simulation*. Springer International Publishing, 2018.

[15] F. Tricomi. Integrazione di unequazione differenziale presentatasi in elettrotechnica. *Annali della R. Shcuola Normale Superiore di Pisa*, 2(2):1–20, 1933.

[16] A A Andronov, E A Vitt, and S E Khaikin. *Theory of Oscillators (in Russian)*. ONTI NKTP SSSR, 1937.

[17] F.M. Gardner. *Phaselock Techniques*. John Wiley & Sons, New York, 1966.

[18] A. Viterbi. *Principles of coherent communications*. McGraw-Hill, New York, 1966.

[19] V.V. Shakhgil'dyan and A.A. Lyakhovkin. *Fazovaya avtopodstroika chastoty (in Russian)*. Svyaz', Moscow, 1 edition, 1966.

[20] M.V. Kapranov. The lock-in band of a phase locked loop. *Radiotekhnika (in Russian)*, 11(12):37–52, 1956.

[21] N.A. Gubar'. Investigation of a piecewise linear dynamical system with three parameters. *Journal of Applied Mathematics and Mechanics*, 25(6):1011–1023, 1961.

[22] B.I. Shakhtarin. Study of a piecewise-linear system of phase-locked frequency control. *Radiotechnica and electronika (in Russian)*, (8):1415–1424, 1969.

[23] W. Lindsey. *Synchronization systems in communication and control*. Prentice-Hall, New Jersey, 1972.

[24] Tetsuro Endo and Kenzo Tada. Analysis of the pull-in range of phase-locked loops by the Galerkin procedure. *Electronics and Communications in Japan (Part I: Communications)*, 69(5):90–98, 1986.

[25] J. Stensby. An exact formula for the half-plane pull-in range of a PLL. *Journal of the Franklin Institute*, 348(4):671–684, 2011.

[26] F.M. Gardner. *Phaselock Techniques*. John Wiley & Sons, New York, 3 edition, 2005.

[27] G.A. Leonov, N.V. Kuznetsov, M.V. Yuldashev, and R.V. Yuldashev. Hold-in, pull-in, and lock-in ranges of PLL circuits: rigorous mathematical definitions and limitations of classical theory. *IEEE Transactions on Circuits and Systems–I: Regular Papers*, 62(10):2454–2464, 2015.

[28] R E Best. *Phase-Locked Loops: Design, Simulation and Application*. McGraw-Hill, 6th edition, 2007.

[29] G.A. Leonov, N.V. Kuznetsov, M.V. Yuldashev, and R.V. Yuldashev. Analytical method for computation of phase-detector characteristic. *IEEE Transactions on Circuits and Systems - II: Express Briefs*, 59(10):633–647, 2012.

[30] G.A. Leonov, N.V. Kuznetsov, M.V. Yuldashev, and R.V. Yuldashev. Nonlinear dynamical model of Costas loop and an approach to the analysis of its stability in the large. *Signal Processing*, 108:124–135, 2015.

[31] N.V. Kuznetsov, G.A. Leonov, M.V. Yuldashev, and R.V. Yuldashev. Rigorous mathematical definitions of the hold-in and pull-in ranges for phase-locked loops. *IFAC-PapersOnLine*, 48(11):710–713, 2015.

[32] G.A. Leonov and N.V. Kuznetsov. *Nonlinear mathematical models of phase-locked loops. Stability and oscillations*. Cambridge Scientific Publishers, 2014.

[33] N.V. Kuznetsov, M.Y. Lobachev, M.V. Yuldashev, R.V. Yuldashev, E.V. Kudryashova, O.A. Kuznetsova, E.N. Rosenwasser, and S.M. Abramovich. The birth of the global stability theory and the theory of hidden oscillations. In *2020 European Control Conference Proceedings*, pages 769–774, 2020.

[34] Yu.N. Bakaev and A A Guzh. Optimal reception of {F}{M} signal in a {D}oppler effect. *Radiomekhanika i Elektronika*, 10(1):171–175, 1965.

[35] G.A. Leonov and S.M. Seledzhi. *The Phase-Locked Loop for Array Processors*. Nevskii dialect, St.Petersburg [in Russian], 2002.

[36] M.V. Blagov, N.V. Kuznetsov, G.A. Leonov, M.V. Yuldashev, and R.V. Yuldashev. Simulation of PLL with impulse signals in MATLAB: Limitations, hidden oscillations, and pull-in range. *International Congress on Ultra Modern Telecommunications and Control Systems and Workshops (ICUMT 2015)*, 2016-January:85–90, 2016.

[37] M.V. Blagov, E.V. Kudryashova, N.V. Kuznetsov, G.A. Leonov, M.V. Yuldashev, and R.V. Yuldashev. Computation of lock-in range for classic pll with lead-lag filter and impulse signals. *IFAC-PapersOnLine*, 49(14):42–44, 2016.

[38] N.V. Kuznetsov, M.V. Blagov, K.D. Alexandrov, M.V. Yuldashev, and R.V. Yuldashev. Lock-in range of classical PLL with piecewise-linear phase detector characteristic. *Differencialnie Uravnenia i Protsesy*

*Upravlenia (Differential Equations and Control Processes)*, (3):74–89, 2019.

[39] N.V. Kuznetsov, M.Y. Lobachev, M.V. Yuldashev, R.V. Yuldashev, and G. Kolumbán. Harmonic balance analysis of pull-in range and oscillatory behavior of third-order type 2 analog PLLs. *IFAC-PapersOnLine*, 53(2):6378–6383, 2020.

[40] L N Belyustina. Study of a nonlinear system of phase-locked frequency control. *Radiofizika*, 2(2):277–291, 1959.

[41] Mineo Chini. Sull'integrazione di alcune equazioni differenziali del primo ordine. *Rendiconti Instituto Lombardo (2)*, 57:506–511, 1924.

[42] E.S. Cheb-Terrab and T. Kolokolnikov. First-order ordinary differential equations, symmetries and linear transformations. *European Journal of Applied Mathematics*, 14(2):231–246, 2003.

# PIII

# HOLD-IN, PULL-IN AND LOCK-IN RANGES FOR PHASE-LOCKED LOOP WITH TANGENTIAL CHARACTERISTIC OF THE PHASE DETECTOR

by

M.V. Blagov, O.A. Kuznetsova, E.V. Kudryashova, N.V. Kuznetsov, T.N. Mokaev, R.N. Mokaev, M.V. Yuldashev, R.V. Yuldashev 2019, JuFo 1

Procedia Computer Science, Vol. 150, pp. 558–566,
https://doi.org/10.1016/j.procs.2019.02.093

Available online at www.sciencedirect.com

ScienceDirect

Procedia Computer Science 150 (2019) 558–566

Procedia Computer Science

www.elsevier.com/locate/procedia

13th International Symposium "Intelligent Systems" (INTELS'18)

# Hold-in, Pull-in and Lock-in Ranges for Phase-locked Loop with Tangential Characteristic of the Phase Detector

M.V. Blagov[a,c,*], O.A. Kuznetsova[a], E.V. Kudryashova[a], N.V. Kuznetsov[a,b,c], T.N. Mokaev[a], R.N. Mokaev[a,c], M.V. Yuldashev[a], R.V. Yuldashev[a]

[a] *Faculty of Mathematics and Mechanics, Saint-Petersburg State University, Universitetskiy pr. 28, St. Petersburg, Russia*
[b] *Institute of Problems of Mechanical Engineering RAS, V.O., Bolshoj pr., 61. St. Petersburg, Russia*
[c] *Dept. of Mathematical Information Technology, University of Jyväskylä, Mattilanniemi 2, Agora, Jyväskylä, Finland*

**Abstract**

In the present paper the phase-locked loop (PLL), an electric circuit widely used in telecommunications and computer architectures is considered. A new modification of the PLL with tangential phase detector characteristic and active proportionally-integrating (PI) filter is introduced. Hold-in, pull-in and lock-in ranges for given circuit are studied rigorously. It is shown that lock-in range of the new PLL model is infinite, compared to the finite lock-in range of the classical PLL.



*Keywords:* capture range; hold-in range; pull-in range; lock-in range; nonlinear analysis; phase-locked loop; PLL.

## 1. Introduction

Phase-locked loop (PLL) is a non-linear control circuit, which is used in many intelligent systems [1, 2, 3]: wireless communication, computer architectures, navigation, power systems and others [4, 5, 6, 7, 8, 9]. The circuit allows to tune frequency (phase) of the controlled oscillator to the frequency (phase) of the reference signal. State of circuit, when the oscillators are synchronized, is called a locked state. The main characteristics of PLL are hold-in, pull-in (capture), and lock-in ranges (rigorous definitions are given in e.g. [10]), which are widely used by engineers (see e.g., [5, 4, 11]). These concepts define frequency ranges in which PLL-based circuits can achieve lock under various additional conditions ([12, 13, 14, 15, 7]). It is well known that hold-in and pull-in ranges are infinite for the PI loop filter, but the lock-in range is finite [16]. In this article we propose and study model of PLL with tangential phase detector, which has infinite lock-in range.

* Corresponding author.
*E-mail address:* vogal.mv@gmail.com

1877-0509 
10.1016/j.procs.2019.02.093

In section 2 modified PLL model with tangent phase detector characteristic function is considered. In section 3 hold-in, pull-in and lock-in ranges proved to be infinite. In section 4 it is shown that modified PLL model locks without cycle slipping, unlike classical model.

## 2. Mathematical model of PLL

Mathematical model of PLL in signal space (circuit level) is not suitable for analytical study of PLLs, because it consists of non-linear non-autonomous differential equations. In [17, 18, 19] it was rigorously shown, that for estimation of lock-in and pull-in range it is possible to use averaged model, which is also called signal's phase space model. It was originally proposed in pioneering books on PLLs [20, 21, 22] and considers only phases of signals, discarding waveforms (see Fig. 1)[1]. This simplification allows to apply control theory methods such as Lyapunov functions and phase-portrait analysis to study PLL.

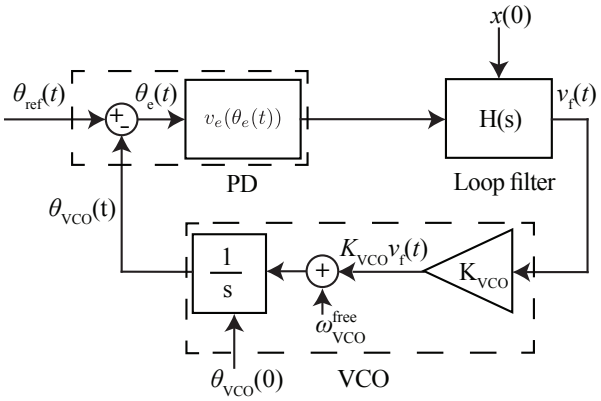


Fig. 1. Model of the classical PLL in signal's phase space.

Here $\theta_{\text{ref}}(t)$ is the phase of input signal with instantaneous frequency $\dot{\theta}_{\text{ref}}(t) = \omega_{\text{ref}}(t)$. The phase of voltage controlled oscillator (VCO) is $\theta_{\text{vco}}(t)$ with it's instantaneous frequency $\dot{\theta}_{\text{vco}}(t) = \omega_{\text{vco}}(t)$. The phase detector generates a signal

$$v_e(\theta_e(t)) = v_e(\theta_{\text{ref}}(t) - \theta_{\text{vco}}(t)), \tag{1}$$

where $v_e(\cdot)$ is periodic function called phase-detector characteristics which depends only on phase difference $\theta_e(t) = \theta_{\text{ref}}(t) - \theta_{\text{vco}}(t)$. For the classical PLL $v_e(\theta_e) = \frac{1}{2}\sin(\theta_e)$, and for proposed model $v_e(\theta_e) = \tan(\theta_e)$.

The relationship between input $v_e(\theta_e(t))$ and output $v_f(t)$ of for the proportionally-integrating Loop filter with transfer function $H(s) = \frac{\tau_2 s+1}{\tau_1 s}$, $\tau_1 > 0$, $\tau_2 > 0$ is

$$\begin{cases} \dot{x} = \frac{1}{\tau_1} v_e(\theta_e), \\ v_f = x + \frac{\tau_2}{\tau_1} v_e(\theta). \end{cases} \tag{2}$$

[1] Remark that the averaging method has some restrictions, rigorous discussion of which is often omitted, (see, e.g. classical books [20, p.7],[21, p.12,15-17]), and their violation may lead to unreliable results (see, e.g. [23, 24, 25]).

The control signal $v_f(t)$ adjusts the VCO frequency:

$$\dot{\theta}_{\text{vco}}(t) = \omega_{\text{vco}}(t) = \omega_{\text{vco}}^{\text{free}} + K_{\text{vco}} v_f(t), \tag{3}$$

where $\omega_{\text{vco}}^{\text{free}}$ is the VCO free-running frequency and $K_{\text{vco}} > 0$ is the VCO gain. Nonlinear VCO models can be similarly considered, see, e.g. [26, 27, 28, 29]. The frequency of input signal (reference frequency) is usually assumed to be constant (see, e.g. [20]):

$$\dot{\theta}_{\text{ref}}(t) = \omega_{\text{ref}}(t) \equiv \omega_{\text{ref}}. \tag{4}$$

The difference between the reference frequency and the VCO free-running frequency is denoted as $\omega_e^{\text{free}}$:

$$\omega_e^{\text{free}} \equiv \omega_{\text{ref}} - \omega_{\text{vco}}^{\text{free}}. \tag{5}$$

By combining equations (2), and (3)–(5) a *nonlinear mathematical model in the signal's phase space* is obtained (i.e. in the state space: the filter's state $x$ and the difference between signal's phases $\theta_e$):

$$\begin{cases} \dot{x} = \frac{1}{\tau_1} \tan(\theta_e), \\ \dot{\theta}_e = \omega_e^{\text{free}} - K_{\text{vco}} \left( x + \frac{\tau_2}{\tau_1} \tan(\theta_e) \right). \end{cases} \tag{6}$$

Initial state of the loop is $\theta_{\text{vco}}(0)$ (initial phase shift of the VCO signal with respect to the reference signal) and $x(0)$ (initial state of the Loop filter).

Note, that (6) with $\tan(\cdot)$ characteristic is not changed under the transformation

$$(\omega_e^{\text{free}}, x(t), \theta_e(t)) \to (-\omega_e^{\text{free}}, -x(t), -\theta_e(t)), \tag{7}$$

and it allows to study system (6) for $\omega_e^{\text{free}} > 0$ only, introducing the concept of *frequency deviation* (or *frequency offset*):

$$|\omega_e^{\text{free}}| = |\omega_{\text{ref}} - \omega_{\text{vco}}^{\text{free}}|. \tag{8}$$

Further system (6) is studied and hold-in range, pull-in range, and lock-in range are computed.

## 3. Calculation of hold-in range, pull-in range, and lock-in range

### 3.1. Hold-in range

**Definition 1** (Hold-in range of the *signal's phase space* model, see [10])**.** *The largest interval* $[0, \omega_h)$ *such that a certain stable equilibrium varies continuously when* $\omega_e^{free}$ *is changed within the range*[2] *is called hold-in range. Here* $\omega_h$ *is called a* hold-in frequency *(see [20, p.38]).*

In other words, loop re-acquires lock after small perturbations of signals' frequencies and phases, and the filter's state, if given frequency deviation is in the hold-in set. This effect is also called *steady-state* stability. To find the $\omega_h$ one should find and analyze equilibria of the system

$$\begin{cases} \dot{x} = \frac{1}{\tau_1}\tan(\theta_e), \\ \dot{\theta}_e = \omega_e^{\text{free}} - K_{\text{vco}}\left(x + \frac{\tau_2}{\tau_1}\tan(\theta_e)\right). \end{cases} \tag{9}$$

This system has an infinite sequence of equilibria

$$\left(x^{\text{eq}}, \theta_e^{\text{eq}}\right) = \left(\pi n, \frac{\omega_e^{free}}{K_{\text{vco}}}\right), \quad n \in \mathbb{Z}. \tag{10}$$

Stability of the equilibria can be studied using characteristic polynomial of the linearized system:

$$\chi(\lambda) = \lambda^2 + K_{\text{vco}}\frac{\tau_2}{\tau_1}\lambda + \frac{K_{\text{vco}}}{\tau_1}. \tag{11}$$

Since $\tau_1 > 0$, $\tau_2 > 0$ and $K_{\text{vco}} > 0$, all equilibria are asymptotically stable for arbitrary $\omega_e^{free}$ by Routh-Hurwitz criterion. Thus, $\omega_h$ is infinite.

### 3.2. Pull-in range

Another important characteristic of the PLL circuit is the set of $|\omega_e^{\text{free}}|$ such that the model acquires locked state for any initial state.

**Definition 2** (Pull-in range of the *signal's phase space* model, see [10, 30, 31])**.** *The largest interval of frequency deviations* $|\omega_e^{\text{free}}| \in [0, \omega_{\text{pull-in}})$ *such that the* signal's phase space *model* (6) *acquires a locked state for arbitrary initial state* $(x(0), \theta_e(0))$ *is called a* pull-in range*,* $\omega_{\text{pull-in}}$ *is called a* pull-in frequency.

Denote $y = x - \frac{\omega_e^{free}}{K_{\text{vco}}}$. Then system (9) becomes

$$\begin{cases} \dot{y} = \frac{1}{\tau_1}\tan(\theta_e), \\ \dot{\theta}_e = -K_{\text{vco}}y - K_{\text{vco}}\frac{\tau_2}{\tau_1}\tan(\theta_e). \end{cases} \tag{12}$$

[2] In general (when the stable equilibria coexist and some of them may appear or disappear), the stable equilibria can be considered as a multiple-valued function of variable $\omega_e^{\text{free}}$, in which case the existence of its continuous singlevalue branch for $|\omega_e^{\text{free}}| \in [0, \omega_h)$ is required.

In order to prove that pull-in range is infinite it is possible to use generalization of classic LaSalle's (also known as Barbashin–Krasovskii–LaSalle) invariance principle for periodic functions with infinite number of equilibria (see [32]). Consider Lyapunov function candidate

$$V(\theta_e, y) = y^2 + \frac{2}{\tau_1}\int_0^{\theta_e} \tan\theta_e d\theta_e \geqslant 0. \tag{13}$$

According to the principle, it is required to check the following conditions:

- $V$ is $\pi$-periodic in $\theta_e$;
- $\lim\limits_{|y|\to\infty} V(\theta_e, y) = \infty$;
- $\dot{V}(y, \theta_e) = -\beta K_{\text{vco}} \frac{\tau_2}{\tau_1^2} \tan^2\theta_e \leqslant 0$;
- $V(\theta_e, y) = 0$ only for $y = \frac{\omega_e^{free}}{K_{\text{vco}}}$, $\theta_e \in \pi n,\ n \in \mathbb{Z}$.

Indeed, all of these conditions are satisfied, consequently, every trajectory of system (9), except the lines $\theta_e = \frac{\pi}{2} + \pi n,\ n \in \mathbb{Z}$, tends to one of the asymptotically stable equilibria. Lines $\theta_e = \frac{\pi}{2} + \pi n,\ n \in \mathbb{Z}$ consist of unstable equilibria, which are physically unrealizable.

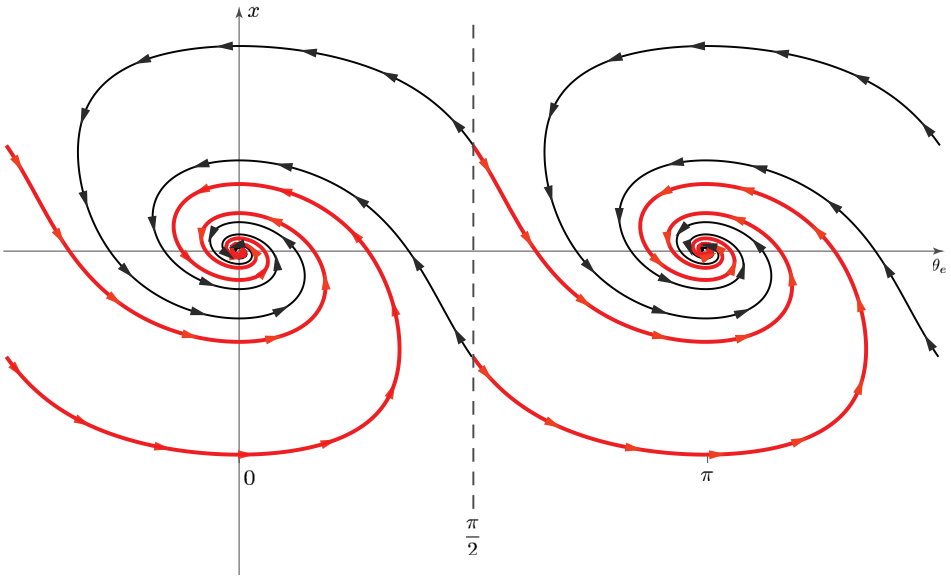


Fig. 2. Phase portrait of PLL model with tangential phase detector characteristic

### 3.3. Lock-in range

In practice it is important to guarantee that for a certain frequency range pull-in process completes in one cycle of oscillations. This frequency range is related to lock-in range.

First lets introduce the notion of cycle slipping.

**Definition 3** (Cycle slipping [10]). *Let PD characteristic $v_e(\theta_e)$ be a $\pi$-periodic function. If* $\limsup\limits_{t\to\infty} |\theta_e(0) - \theta_e(t)| \geq \pi$ *then it is said that* cycle slipping *occurs.*

Now we can introduce definition of lock-in range.

**Definition 4** (Lock-in range of the *signal's phase space* model, see [30, 10, 31])**.** *The largest interval of frequency deviations from the pull-in range:* $|\omega_e^{\text{free}}| \in [0, \omega_{\text{lock-in}}) \subset [0, \omega_{\text{pull-in}})$*, is called a* lock-in range *if the signal's phase space model* (6)*, being in a (stable) locked state, after any abrupt change of* $\omega_e^{\text{free}}$ *within the interval acquires a (stable) locked state without cycle slipping.*

Note, that all trajectories starting from $-\frac{\pi}{2} < \theta_e(0) < \frac{\pi}{2}, y(0) \in \mathbb{R}$ stay within the same domain, i.e. these trajectories never cross the band borders $\theta_e = \pm\frac{\pi}{2}$. Then consider behaviour of the system near $\theta_e = \pm\frac{\pi}{2}$. The one-sided limits $\lim_{\theta\to\frac{\pi}{2}-\varepsilon}$ and $\lim_{\theta\to\frac{\pi}{2}-\varepsilon}$ show that the vector field defined by the right-hand side of (12) is directed away from the equilibria line:

$$\begin{aligned}
&\lim_{\theta\to\frac{\pi}{2}-\varepsilon} \dot{x} = \lim_{\theta\to\frac{\pi}{2}-\varepsilon} \frac{1}{\tau_1}\tan\theta = +\infty \\
&\lim_{\theta\to\frac{\pi}{2}-\varepsilon} \dot{\theta}_e = \lim_{\theta\to\frac{\pi}{2}-\varepsilon} -K_{\text{vco}}y - K_{\text{vco}}\frac{\tau_2}{\tau_1}\tan\theta = -\infty \\
&\lim_{\theta\to-\frac{\pi}{2}+\varepsilon} \dot{x} = \lim_{\theta\to-\frac{\pi}{2}+\varepsilon} \frac{1}{\tau_1}\tan\theta = -\infty \\
&\lim_{\theta\to-\frac{\pi}{2}+\varepsilon} \dot{\theta}_e = \lim_{\theta\to-\frac{\pi}{2}+\varepsilon} -K_{\text{vco}}y - K_{\text{vco}}\frac{\tau_2}{\tau_1}\tan\theta = +\infty
\end{aligned} \tag{14}$$

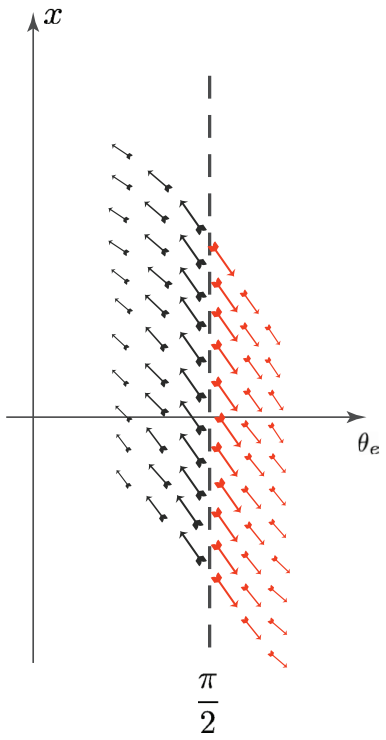


Fig. 3. Vector field of the PLL with tangential phase detector characteristic in small neighbourhood of the line $\theta_e = \frac{\pi}{2}$

Therefore cycle slipping is impossible, i.e. lock-in range is infinite.

## 4. Comparison of classic PLL and tan(·) PLL in Matlab Simulink

Consider Simulink models for both sinusoidal and tangential characteristics of the phase detector (see Fig. 4).

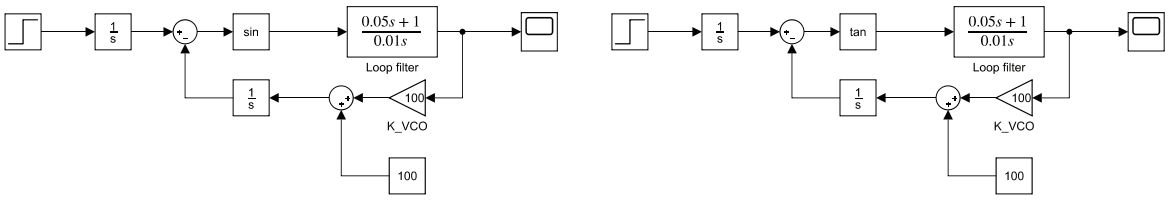


Fig. 4. Simulink models for PLL with sinusoidal (on the left hand side) and tangential (on the right hand side) phase detector characteristics. Here $\omega_{\text{vco}}^{free} = 100$, $\tau_1 = 0.01$, $\tau_2 = 0.05$, $K_{\text{vco}} = 200$. Initial input $\omega_{\text{ref}} = 100$ and then jumps to $\omega_{\text{ref}} = 350$.

Here frequency of input is modeled by Step block with initial value 100, final value 350, and switch time 5. Block $\frac{1}{s}$ integrates frequency and forms phase of input signal. After subtracting phase of VCO, resulting signal goes through PD block (sin and tan correspondingly). Loop filter is modeled by Transfer Fcn block. Output of loop filter is connected to gain $K_{\text{VCO}}$, which controls input gain of VCO. Gain block output is added to output of constant block defining free-running frequency of VCO and finally got integrated to form phase of VCO.

Results of simulation are shown in Fig. 5.

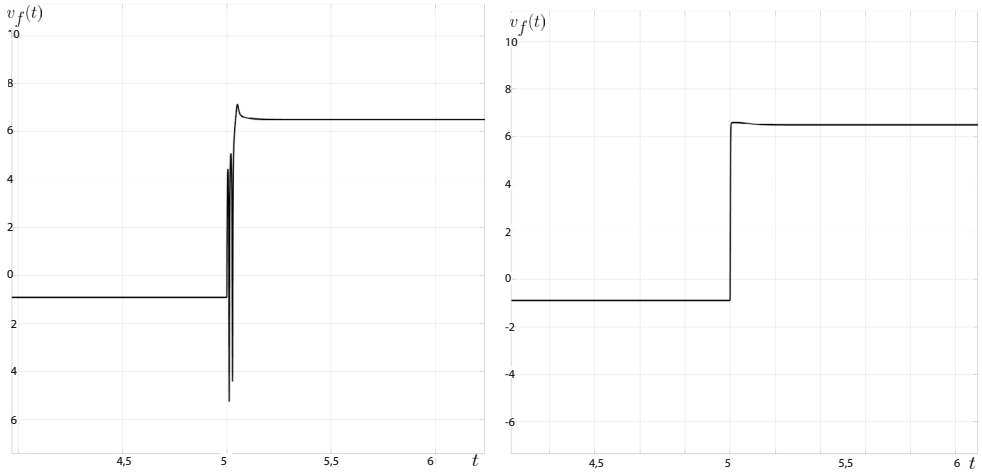


Fig. 5. Simulink modelling for PLL with sinusoidal (on the left hand side) and tangential (on the right hand side) phase detector characteristics

Here one can see, that the synchronization achieved for both models, but for model with sinusoidal phase detector characteristic cycle slipping occurs. Phase difference is shown in Fig. 6.

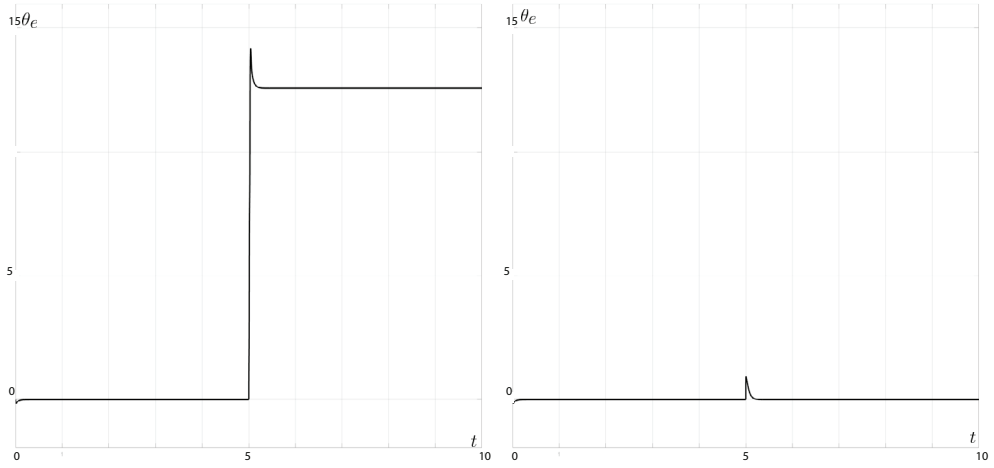


Fig. 6. Phase difference between input signal and VCO signal. Left sub-figure — cycle slipping for classic sinusoidal PD, right sub-figure — no cycle slipping for tangential PD.

This means that considered frequency difference is outside of the classic PLL lock-in range, while tan(·) PLL locks without cycle slipping. Similar results are observed for higher frequency deviations.

## 5. Conclusion

It was proven that tan(·) PD PLL the lock-in range is infinite for PI filter, which is significant improvement over classic PLL. Theoretical results were checked by simulation. To study noise characteristics one can use theory developed in [22, 33, 34]. Higher order filters can be studied by frequency criterion [35].

## Acknowledgements

The work is supported the Russian Science Foundation project 14-21-00041 (sections 1-2) and the Leading Scientific Schools of Russia project NSh-2858.2018.1 (section 3).

## References

[1] Ahamed, S., Lawrence, V.. *Design and Engineering of Intelligent Communication Systems*. Springer; 1997.
[2] Meystel, A., Meystel, A., Albus, J.. *Intelligent systems: architecture, design, and control*. Wiley; 2002.
[3] Sarma, K., Sarma, M., Sarma, M.. *Recent Trends in Intelligent and Emerging Systems*. Springer India; 2015.
[4] Best, R.. *Phase-Locked Loops: Design, Simulation and Application*. McGraw-Hill; 6th ed.; 2007.
[5] Gardner, F.. *Phaselock Techniques*. Wiley; 3rd ed.; 2005.
[6] Kroupa, V.. *Frequency Stability: Introduction and Applications*. IEEE Series on Digital & Mobile Communication. Wiley-IEEE Press; 2012.
[7] Bianchi, G.. *Phase-locked loop synthesizer simulation*. McGraw-Hill, Inc.; 2005.
[8] Ladvánszky, J.. A costas loop variant for large noise. *Journal of Asian Scientific Research* 2018;**8**(3):144–151.
[9] Ladvánszky, J., Dortschy, B.. Optical communication system and device for linearizing non-linear signal transmission characteristics. 2017. US Patent App. 15/506,645.
[10] Leonov, G., Kuznetsov, N., Yuldashev, M., Yuldashev, R.. Hold-in, pull-in, and lock-in ranges of PLL circuits: rigorous mathematical definitions and limitations of classical theory. *IEEE Transactions on Circuits and Systems–I: Regular Papers* 2015;**62**(10):2454–2464. doi:10.1109/TCSI.2015.2476295.
[11] Best, R.E.. *Costas Loops: Theory, Design, and Simulation*. Springer International Publishing; 2018.
[12] Golestan, S., Monfared, M., Freijedo, F.D., Guerrero, J.M.. Design and tuning of a modified power-based pll for single-phase grid-connected power conditioning systems. *Power Electronics, IEEE Transactions on* 2012;**27**(8):3639–3650.
[13] Tal, J.. Synchronization characteristics of controllable oscillators. *Automatica* 1977;**13**(2):153 – 159. doi:10.1016/0005-1098(77)90039-5.

[14] Wang, J., Duan, Z., Huang, L.. Control of a class of pendulum-like systems with lagrange stability. *Automatica* 2006;**42**(1):145 – 150. doi:10.1016/j.automatica.2005.08.014.
[15] Shakhtarin, B., Andrianov, M., Andrianov, I.. Application of discontinuous communications in channels with random parameters to transmit narrowband signals and signals with orthogonal frequency-division multiplexing. *Journal of communications technology and electronics* 2009; **54**(10):1175–1182.
[16] Aleksandrov, K., Kuznetsov, N., Leonov, G., Yuldashev, M., Yuldashev, R.. Lock-in range of PLL-based circuits with proportionally-integrating filter and sinusoidal phase detector characteristic. *arXiv preprint arXiv:160308401* 2016;.
[17] Leonov, G., Kuznetsov, N., Yuldashev, M., Yuldashev, R.. Analytical method for computation of phase-detector characteristic. *IEEE Transactions on Circuits and Systems - II: Express Briefs* 2012;**59**(10):633–647. doi:10.1109/TCSII.2012.2213362.
[18] Leonov, G., Kuznetsov, N., Yuldashev, M., Yuldashev, R.. Computation of the phase detector characteristic of classical PLL. *Doklady Mathematics* 2015;**91**(2):246–249.
[19] Kuznetsov, N., Leonov, G., Seledzhi, S., Yuldashev, M., Yuldashev, R.. Elegant computation of phase-detector characteristics of BPSK Costas loop with non-sinusoidal signals. 2017, doi:10.1109/ECCTD.2017.8093255; art. num. 8093255.
[20] Gardner, F.. *Phaselock techniques*. New York: John Wiley & Sons; 1966.
[21] Viterbi, A.. *Principles of coherent communications*. New York: McGraw-Hill; 1966.
[22] Shakhgil'dyan, V., Lyakhovkin, A.. *Fazovaya avtopodstroika chastoty (in Russian)*. Moscow: Svyaz'; 1966.
[23] Piqueira, J., Monteiro, L.. Considering second-harmonic terms in the operation of the phase detector for second-order phase-locked loop. *IEEE Transactions On Circuits And Systems-I* 2003;**50**(6):805–809.
[24] Kuznetsov, N., Kuznetsova, O., Leonov, G., Neittaanmaki, P., Yuldashev, M., Yuldashev, R.. Limitations of the classical phase-locked loop analysis. *Proceedings - IEEE International Symposium on Circuits and Systems* 2015;**2015-July**:533–536. doi:10.1109/ISCAS.2015.7168688.
[25] Best, R., Kuznetsov, N., Kuznetsova, O., Leonov, G., Yuldashev, M., Yuldashev, R.. A short survey on nonlinear models of the classic Costas loop: rigorous derivation and limitations of the classic analysis. In: *Proceedings of the American Control Conference*. IEEE; 2015, p. 1296–1302. doi:10.1109/ACC.2015.7170912; art. num. 7170912.
[26] Margaris, N.. *Theory of the Non-Linear Analog Phase Locked Loop*. New Jersey: Springer Verlag; 2004.
[27] Suarez, A.. *Analysis and Design of Autonomous Microwave Circuits*. Wiley Series in Microwave and Optical Engineering. Wiley-IEEE Press; 2009.
[28] Bonnin, M., Corinto, F., Gilli, M.. Phase noise, and phase models: Recent developments, new insights and open problems. *Nonlinear Theory and Its Applications, IEICE* 2014;**5**(3):365–378. doi:10.1587/nolta.5.365.
[29] Bianchi, G., Kuznetsov, N., Leonov, G., Seledzhi, S., Yuldashev, M., Yuldashev, R.. Hidden oscillations in SPICE simulation of two-phase Costas loop with non-linear VCO. *IFAC-PapersOnLine* 2016;**49**(14):45–50. doi:10.1016/j.ifacol.2016.07.973.
[30] Kuznetsov, N., Leonov, G., Yuldashev, M., Yuldashev, R.. Rigorous mathematical definitions of the hold-in and pull-in ranges for phase-locked loops. *IFAC-PapersOnLine* 2015;**48**(11):710–713. doi:10.1016/j.ifacol.2015.09.272.
[31] Best, R., Kuznetsov, N., Leonov, G., Yuldashev, M., Yuldashev, R.. Tutorial on dynamic analysis of the Costas loop. *Annual Reviews in Control* 2016;**42**:27–49. doi:10.1016/j.arcontrol.2016.08.003.
[32] Gelig, A., Leonov, G., Yakubovich, V.. *Stability of Nonlinear Systems with Nonunique Equilibrium (in Russian)*. Nauka; 1978. (English transl: Stability of Stationary Sets in Control Systems with Discontinuous Nonlinearities, 2004, World Scientific).
[33] Shakhtarin, B., Sizykh, V., Sidorkina Yu, A.. Sinkhronizatsiya v radiosvyazi i radionavigatsii [synchronization in radio communication and navigation]. *Moscow, Goryachaya Liniya-Telekom Publ* 2011;.
[34] Ladvánszky, J., Mészáros, G., Fűzy, C.. Spectral cleaning for oscillators. In: *Signal Processing (ICSP), 2012 IEEE 11th International Conference on*; vol. 1. IEEE; 2012, p. 206–209.
[35] Leonov, G., Aleksandrov, K.. Frequency-domain criteria for the global stability of phase synchronization systems. In: *Doklady. Mathematics*; vol. 92. Springer; 2015, p. 769–772.

# PIV

## COMPUTATION OF LOCK-IN RANGE FOR CLASSIC PLL WITH LEAD-LAG FILTER AND IMPULSE SIGNALS

by

M.V. Blagov, E.V. Kudryashova, N.V. Kuznetsov, G.A. Leonov, M.V. Yuldashev, R.V. Yuldashev 2016, JuFo 1

IFAC-PapersOnLine, Vol. 49, I. 14, pp. 42–44
https://doi.org/10.1016/j.ifacol.2016.07.972

Available online at www.sciencedirect.com

ScienceDirect

IFAC Papers Online CONFERENCE PAPER ARCHIVE

IFAC-PapersOnLine 49-14 (2016) 042–044

# Computation of lock-in range for classic PLL with lead-lag filter and impulse signals

**M.V. Blagov** * **E.V. Kudryashova** * **N.V. Kuznetsov** *,** **G.A. Leonov** *,*** **M.V. Yuldashev** * **R.V. Yuldashev** *

* *Faculty of Mathematics and Mechanics, Saint-Petersburg State University, Russia*
** *Dept. of Mathematical Information Technology, University of Jyväskylä, Finland (email: nkuznetsov239@gmail.com)*
*** *Institute of Problems of Mechanical Engineering RAS, Russia*

**Abstract:** For a classic PLL with square waveform signals and lead-lag filter for all possible parameters lock-in range is computed and corresponding diagrams are given.



*Keywords:* Phase-locked loop, nonlinear analysis, analog PLL, cycle slipping, hold-in range, pull-in range, lock-in range, definition, lead-lag filter.

## 1. INTRODUCTION

The phase-locked loop (PLL) is an electric circuit extensively used in various applications in computer architectures and telecommunications (see, e.g. Kroupa (2003); Bianchi (2005); Gardner (2005); Best (2007); Shakhtarin et al. (2009)). A PLL is essentially a nonlinear control system, which allows one to tune frequency (phase) of the controlled oscillator to the frequency (phase) of the reference oscillation (reference signal). One of the main characteristics of PLL is the *lock-in range* (Gardner, 1966; Best, 2007): the range of frequencies of the reference signal for which fast synchronization without cycle sipping is guaranteed.

In this work for a classic PLL with square waveform signals and lead-lag filter for all possible parameters the lock-in range is computed and corresponding diagrams are given. The computed lock-in range is compared with estimates in (Best, 2007).

## 2. MATHEMATICAL MODEL OF PLL WITH LEAD-LAG FILTER

Consider signal's phase space model of classic PLL circuit (see Fig. 1). Here the phase detector (PD) is a nonlinear block and the phases $\theta_{1,2}(t)$ of the input (reference) and VCO signals are PD block inputs and the output is a function $\varphi(\theta_e(t)) = \varphi(\theta_1(t) - \theta_2(t))$ named a phase detector characteristic, where

$$\theta_e(t) = \theta_1(t) - \theta_2(t), \tag{1}$$

named the phase error. Consider triangular PD characteristic (see Fig. 2):

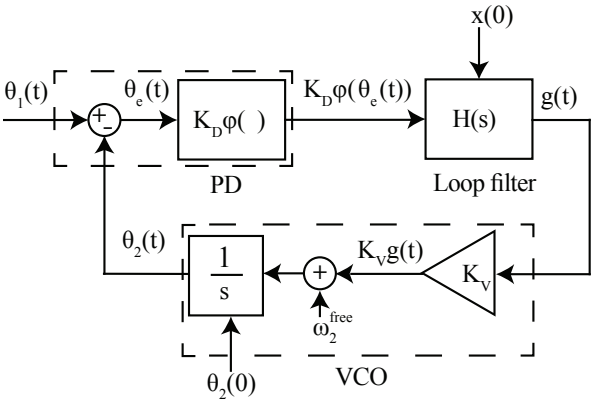


Fig. 1. PLL-based circuit in a signal's phase space.

$$\varphi(\theta_e) = \begin{cases} \frac{2}{\pi}\theta_e, & \text{for } \theta_e \in [-\frac{\pi}{2}, \frac{\pi}{2}], \\ 2 - \frac{2}{\pi}\theta_e, & \text{for } \theta_e \in [\frac{\pi}{2}, \frac{3}{2}\pi]. \end{cases} \tag{2}$$

This characteristic appears for the case of classical multiplier/mixer and impulse signal waveforms of VCO and reference. For exclusive-or (EXOR) the phase detector characteristic is also triangular. The output of the PD is connected to the input of the passive lead-lag filter with the transfer function

$$F(s) = \frac{1 + \tau_2 s}{1 + \tau_1 s}, \tag{3}$$

where $0 < \tau_2 < \tau_1$. Loop filter dynamics can be described by the following differential equations

$$\begin{aligned} \dot{x} &= -\frac{1}{\tau_1}x + \frac{1}{\tau_1}\varphi(\theta_e(t)), \\ g &= (1 - \frac{\tau_2}{\tau_1})x + \frac{\tau_2}{\tau_1}v_e(\theta_e(t)). \end{aligned} \tag{4}$$

⋆ This work was supported by Russian Science Foundation (project 14-21-00041, s. 3) Saint-Petersburg State University (project 6.38.505.2014, s. 2.)


10.1016/j.ifacol.2016.07.972

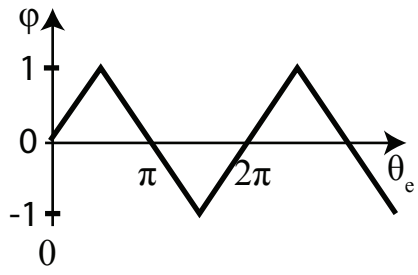


Fig. 2. Triangular PD characteristic

where $x(t)$ is a state of the loop filter, $K_D\varphi(t)$ is the PD output, and $g(t)$ is a filter output.

The output of the filter $g(t)$ adjusts the frequency of the VCO to the frequency of the input signal:

$$\dot{\theta}_2(t) = \omega_2(t) = \omega_2^{\text{free}} + K_V g(t), \tag{5}$$

where $\omega_2^{\text{free}}$ is called free-running frequency (i.e. for $g(t) \equiv 0$) and $K_V$ is the VCO gain. Nonlinear VCO models can be studied similarly (see, e.g. Margaris (2004); Suarez (2009)).

The frequency of the input signal (reference frequency) is usually assumed to be constant:

$$\dot{\theta}_1(t) = \omega_1(t) \equiv \omega_1. \tag{6}$$

The difference between the reference frequency and the VCO free-running frequency is denoted as $\omega_e^{\text{free}}$:

$$\omega_e^{\text{free}} \equiv \omega_1 - \omega_2^{\text{free}}. \tag{7}$$

Combining (4) – (6), one obtains the following equations:

$$\begin{aligned} \dot{x} &= -\frac{1}{\tau_1}x + \frac{1}{\tau_1}\varphi(\theta_e(t)), \\ \dot{\theta}_e &= \omega_e^{free} - K_{\text{V}}\left((1-\frac{\tau_2}{\tau_1})x + \frac{\tau_2}{\tau_1}v_e(\theta_e(t))\right). \end{aligned} \tag{8}$$

System (8) is periodic in $\theta_e$, therefore the analysis is restricted to the range $\theta_e \in [-\pi, \pi)$. The equilibria of (8) are denoted by $(x_{eq}, \theta_{eq})$:

$$\begin{aligned} \theta_{eq} &= \frac{\pi}{2}\frac{\omega_e^{\text{free}}}{K_{VCO}K_D}, \\ x_{eq} &= \frac{\omega_e^{\text{free}}}{K_{VCO}K_D}. \end{aligned} \tag{9}$$

Stable equilibria correspond to the locked states of the loop. Since PD characteristic (2) is an odd function ($\varphi(-\theta_e) = -\varphi(\theta_e)$), system is not changed by the transformation

$$\left(\omega_e^{\text{free}}, x(t), \theta_e(t)\right) \to \left(-\omega_e^{\text{free}}, -x(t), -\theta_e(t)\right). \tag{10}$$

This symmetric property of PD allows one the analysis of system (8) with only $\omega_e^{\text{free}} \geq 0$ and introduces the concept of *frequency deviation*

$$|\omega_e^{\text{free}}| = |\omega_1 - \omega_2^{\text{free}}|.$$

## 3. LOCK-IN RANGE DEFINITION

The concepts of *lock-in frequency* and *lock-in range* were intended to describe the set of frequency deviations for which the loop can acquire lock within one beat without cycle slipping. Next we use the definitions of the *cycle slipping* and *lock-in range* from (Kuznetsov et al., 2015; Leonov et al., 2015). If

$$\limsup_{t\to+\infty} |\theta_e(0) - \theta_e(t)| > 2\pi, \tag{11}$$

we say that cycle slipping occurs. The lock-in range may be define as follows: if the model is in an equilibrium state, then after an abrupt change of $\omega_{\text{ref}}$ within a lock-in range $|\omega_e^{\text{free}}| < \omega_{\text{lock-in}}$, the model locks without cycle slipping. Here $\omega_{\text{lock-in}}$ is called lock-in frequency.

Thus, the lock-in domain (i.e. a domain of the model states, where fast acquisition without cycle slipping is possible) contains both symmetric locked states (i.e. stable equilibrium points for the positive and negative value of the difference between the reference frequency and the VCO free-running frequency).

### *3.1 Lock-in range computation*

System (8) depends on 5 parameters: $\tau_1, \tau_2, K_V, K_D, \omega_e^{\text{free}}$. Introduce parameter $\tau = t\sqrt{K_V K_D/\tau_1}$ and reduce (8) to the following equation

$$\ddot{\theta}_e = \frac{\omega_e}{K_V K_D} - \frac{\dot{\theta}_e}{\sqrt{K_V K_D \tau_1}} - \frac{\tau_2}{\tau_1}\sqrt{K_V K_D \tau_1}\frac{d\varphi}{d\theta_e}\dot{\theta}_e - \varphi(\theta_e). \tag{12}$$

This equation contains only three parameters. The first one is the normalized frequency deviation $\frac{\omega_e}{K_V K_D}$, and two others are the normalized loop filter parameters: $\frac{\tau_2}{\tau_1}$ and $K_V K_D \tau_1$.

Consider now simple numerical algorithm for computation of the lock-in range. For each pair $(\frac{\tau_2}{\tau_1}, K_V K_D \tau_1)$ the normalized frequency deviation $\frac{\omega_e^{\text{free}}}{K_V K_D}$ is increased starting from zero. The largest possible value of frequency deviation is $\frac{\omega_e^{\text{free}}}{K_V K_D} = 1$ since there are no equilibrium points for bigger values. Taking into account that equilibria are proportional to the frequency deviation and using the symmetry $\big(x_{eq}(\omega_l), \theta_{eq}(\omega_l)\big) = -\big(x_{eq}(-\omega_l), \theta_{eq}(-\omega_l)\big)$, one can effectively determine the lock-in range. We have to increase the frequency deviation $|\omega_e^{\text{free}}|$ step by step and at each step, after the loop achieves a locked state, to change $\omega_e^{\text{free}} = \widetilde{\omega}$ abruptly to $\omega_e^{\text{free}} = -\widetilde{\omega}$ and to check if the loop can achieve a new locked state without cycle slipping. If so, then the considered value belongs to the lock-in range.

Consider example in Fig. 3. Here filter parameters $\tau_1 = 0.02$, $\tau_2 = 0.008$ correspond to a curve $\frac{\tau_2}{\tau_1} = 0.4$ (see the right-hand side axis). By substituting PD gain $K_D$ and VCO gain $K_V$ into $K_V K_D \tau_1$ one determines a point on the curve (see horizontal axis). The corresponding lock-in frequency $\omega_l$ is then computed from the corresponding value of the normalized value of the lock-in frequency $\frac{\omega_e^{\text{free}}}{K_V K_D}$ on the left-hand side of vertical axis. Note that the same diagram may be used for any filter as long as $\frac{\tau_2}{\tau_1} = 0.4$. Lock-in frequencies for other loop filter parameters are in Fig. 4. Lock-in range for considered the case is estimated in (Best (2007)) for the case of small $\frac{\tau_2}{\tau_1}$ and large loop gain $K_D K_V$:

$$\omega_l \approx K_D K_V\left(\frac{\tau_2}{\tau_1} + \frac{1}{K_D K_V \tau_1}\right). \tag{13}$$

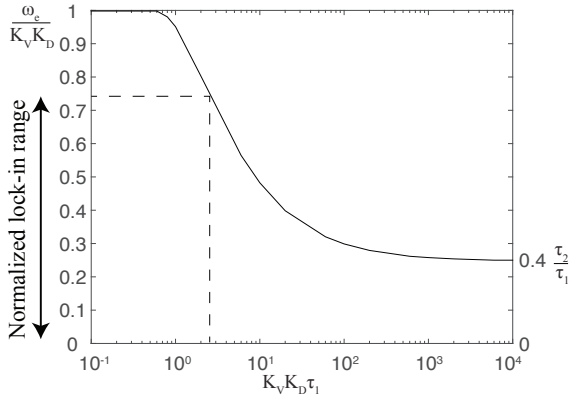


Fig. 3. Lock-in range for parameters $\tau_1 = 0.02$, $\tau_2 = 0.008$.

For $\frac{\tau_2}{\tau_1} = 0.01$ lock-in diagrams are in Fig. 5. These diagrams were constructed numerically in Matlab, by integrating system (8) with "ode15s".

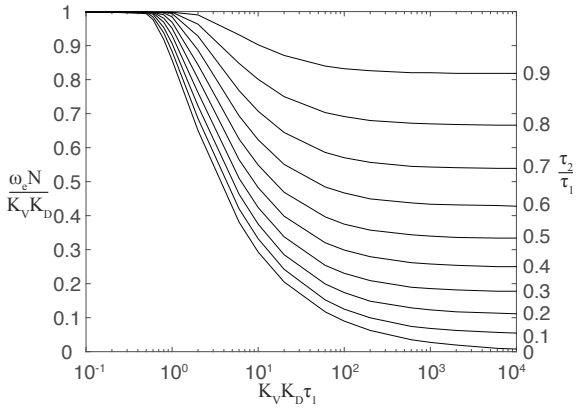


Fig. 4. Lock-in range lead-lag filter, triangular PD.

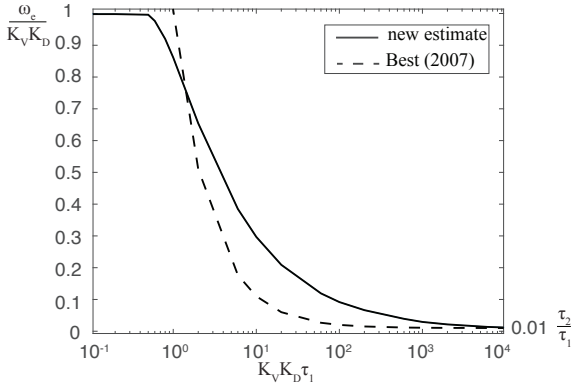


Fig. 5. Lock-in range estimates.

## REFERENCES


Best, R. (2007). *Phase-Lock Loops: Design, Simulation and Application*. McGraw-Hill, 6th edition.

Bianchi, G. (2005). *Phase-Locked Loop Synthesizer Simulation*. McGraw-Hill.

Gardner, F. (1966). *Phase-lock techniques*. John Wiley & Sons, New York.

Gardner, F. (2005). *Phaselock Techniques*. Wiley, 3rd edition.

Kroupa, V. (2003). *Phase Lock Loops and Frequency Synthesis*. John Wiley & Sons.

Kuznetsov, N., Leonov, G., Yuldashev, M., and Yuldashev, R. (2015). Rigorous mathematical definitions of the hold-in and pull-in ranges for phase-locked loops. *IFAC-PapersOnLine*, 48(11), 710–713. doi: http://dx.doi.org/10.1016/j.ifacol.2015.09.272.

Leonov, G., Kuznetsov, N., Yuldashev, M., and Yuldashev, R. (2015). Hold-in, pull-in, and lock-in ranges of PLL circuits: rigorous mathematical definitions and limitations of classical theory. *IEEE Transactions on Circuits and Systems–I: Regular Papers*, 62(10), 2454–2464. doi: http://dx.doi.org/10.1109/TCSI.2015.2476295.

Margaris, N. (2004). *Theory of the Non-Linear Analog Phase Locked Loop*. Springer Verlag, New Jersey.

Shakhtarin, B., Andrianov, M., and Andrianov, I. (2009). Application of discontinuous communications in channels with random parameters to transmit narrowband signals and signals with orthogonal frequency-division multiplexing. *Journal of communications technology and electronics*, 54(10), 1175–1182.

Suarez, A. (2009). *Analysis and Design of Autonomous Microwave Circuits*. Wiley Series in Microwave and Optical Engineering. Wiley-IEEE Press.

# PV

# SIMULATION OF PLL WITH IMPULSE SIGNALS IN MATLAB: LIMITATIONS, HIDDEN OSCILLATIONS, AND PULL-IN RANGE

by

M.V. Blagov, N.V. Kuznetsov, G.A. Leonov, M.V. Yuldashev, R.V. Yuldashev 2015, JuFo 1

2015 7th International Congress on Ultra Modern Telecommunications and Control Systems and Workshops (ICUMT), pp. 85–90.
https://doi.org/10.1109/ICUMT.2015.7382410

# Simulation of PLL with impulse signals in MATLAB: limitations, hidden oscillations, and pull-in range

Blagov M. V.*, Kuznetsov N. V.*†, Leonov G. A.*, Yuldashev M. V.*, Yuldashev R. V.*
* Faculty of Mathematics and Mechanics, Saint-Petersburg State University, Russia
† Dept. of Mathematical Information Technology, University of Jyväskylä, Finland

***Abstract*—The limitations of PLL simulation are demonstrated on an example of phase-locked loop with triangular phase detector characteristic. It is shown that simulation in MatLab may not reveal periodic oscillations (e.g. such as hidden oscillations) and thus may lead to unreliable conclusions on the width of pull-in range.**

## I. Introduction

The phase-locked loop based circuits (PLL) are widely used in various applications in computer architectures and telecommunications (see, e.g. [1]–[3]). A PLL is essentially a nonlinear control system and its nonlinear analysis is a challenging task. Important characteristics of PLL are hold-in, pull-in, and lock-in frequency deviation ranges (see [4], [5] for rigorous mathematical definitions). Hold-in range corresponds to the existence of a locally asymptotically stable locked state and can be studied by using the Routh-Hurwitz criterion (at the stage of *pre-design analysis* when all parameters of the loop can be chosen precisely) or various frequency characteristics of the loop (at the stage of *post-design analysis* when only the input and output of the loop are considered). To estimate the pull-in (capture) range, one has to check the global stability (stability in the large) of the locked states, i.e. to prove that for any initial state the loop acquires a locked state. Its rigorous study is a challenging task.

In a recent book [6, p.123] it is noted that "*the determination of the width of the capture range together with the interpretation of the capture effect in the second order type-I loops have always been an attractive theoretical problem. This problem has not yet been provided with a satisfactory solution*". Below we demonstrate that in this case the numerical analysis may lead to unreliable results and should be used carefully.

## II. PLL with triangular phase detector characteristic

The basic blocks of the PLL are voltage-controlled oscillator (VCO), linear loop filter, and phase detector (PD) [3]. Balanced mixers PDs are used in the microwave frequency range as well as in low noise frequency synthesizers [7]. This type of PD is also used in optical PLLs [8]. However, the characteristic of PD depends on the waveforms of the reference signal and VCO [9]. Next square waveform signals are considered since they are actively used in practice [1], [3]. Another popular implementation of the PD is Exclusive-OR (XOR) gate. One of the main advantages of such PD is its independence of input signals amplitudes. Although hardware implementations of PDs mentioned earlier are significantly different, they have the same characteristic. Therefore, the following analysis can be applied to both of them.

Consider now block diagram of the classic PLL with multiplier/mixer phase detector and square waveform signals on Fig. 1.

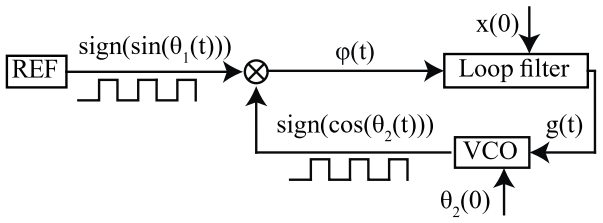


Fig. 1: Classic PLL with square waveform signals

Here a reference oscillator and VCO generate square waveform signals $\operatorname{sign}\sin(\theta_1(t))$ and $\operatorname{sign}\cos(\theta_2(t))$ with the phases $\theta_1(t)$ and $\theta_2(t)$, respectively. Analog multiplier ($\otimes$) output signal is a product $\varphi(t) = \operatorname{sign}\sin(\theta_1(t))\operatorname{sign}\sin(\theta_2(t))$. Here we consider a lead-lag loop filter with the transfer function

$$F(s) = \frac{1+\tau_2 s}{1+\tau_1 s}, \tag{1}$$

where $0 < \tau_2 < \tau_1$, $K_f > 0$, and initial filter state is $x(0)$. Loop filter dynamics can be described by the following differential equations

$$\dot{x} = -\frac{1}{\tau_1}x + (1-\frac{\tau_2}{\tau_1})\varphi(t), \quad g = \frac{1}{\tau_1}x + \frac{\tau_2}{\tau_1}\varphi(t), \tag{2}$$

where $x$ is a state of the loop filter, and $\varphi$ is the PD output.

Assume that the frequency of reference signal is a constant $\dot{\theta}_1(t) \equiv \omega_1$. The output of the loop filter adjusts the VCO frequency to the frequency of the input signal:

$$\dot{\theta}_2(t) = \omega_{free} + K_{\mathrm{VCO}}x(t), \tag{3}$$

Combining (2) and (3), one obtains the following model in

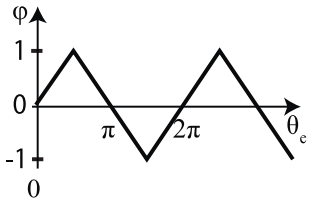


Fig. 3: Phase detector characteristic

the signal space:

$$\begin{aligned}
&\dot{x} = -\frac{1}{\tau_1}x + (1-\frac{\tau_2}{\tau_1})\varphi(t),\\
&g = \frac{1}{\tau_1}x + \frac{\tau_2}{\tau_1}\varphi(t),\\
&\dot{\theta}_2 = \omega_{free} + K_{\mathrm{VCO}}x,\\
&\varphi(t) = \operatorname{sign}\sin(\omega_1 t)\operatorname{sign}\cos(\theta_2).
\end{aligned} \tag{4}$$

Model (4) in the signal space is a nonlinear non-autonomous system with discontinuous right-hand side and its rigorous analysis is a very difficult task.

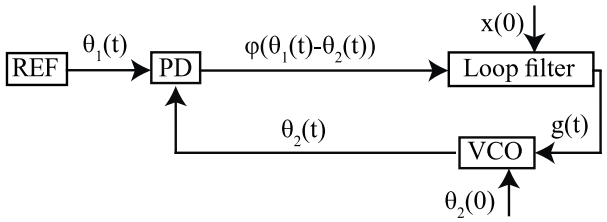


Fig. 2: The model in the signal's phase space

Consider corresponding nonlinear mathematical model of the loop in the signal's phase space (see Fig. 2):

$$\begin{aligned}
&\dot{x} = -\frac{1}{\tau_1}x + (1-\frac{\tau_2}{\tau_1})\varphi(\theta_e),\\
&\dot{\theta}_e = \omega_1 - \omega_{free} - Lg,\\
&g = \frac{1}{\tau_1}x + \frac{\tau_2}{\tau_1}\varphi(\theta_e),\\
&\varphi(\theta_e) = \begin{cases} \frac{2}{\pi}\theta_e & \text{for } \theta_e \in [-\frac{\pi}{2}, \frac{\pi}{2}]\\ 2 - \frac{2}{\pi}\theta_e & \text{for } \theta_e \in [\frac{\pi}{2}, \frac{3}{2}\pi] \end{cases}
\end{aligned} \tag{5}$$

Here PD is a nonlinear element with triangular characteristic $\varphi(\theta_e)$ (see Fig. 3), whose output depends only on the phase error $\theta_e(t) = \theta_1(t) - \theta_2(t)$. Denote $\omega_e = \omega_1 - \omega_{free}$. The model in the signal's phase space can be obtained from the model in the signal space by averaging under certain conditions [9]–[13], violation of which may lead to unreliable results (see, e.g. [14], [15]). Its rigorous analysis and simulation is much simpler since time $t$ is excluded and instead of high-frequency reference and VCO signals only difference between their phases is considered.

## III. Simulation of the loop in the signal's phase space

Consider the implementation of the signal's phase space model in MatLab Simulink (see Fig. 4).

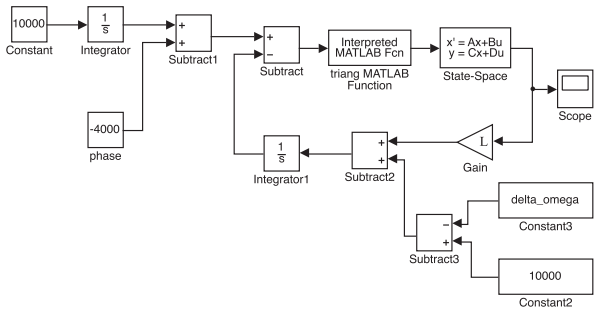


Fig. 4: Simulink model of the loop in the signal's phase space.

Here the loop filter transfer function $F(s) = \frac{1+s\tau_2}{1+s\tau_1}$, $\tau_1 = 0.02$, $\tau_2 = 0.008$, $L = 2000$, $\omega_e = 1399$, phase detector characteristic is implemented by Interpreted MatLab function "sawtooth(u+pi/2,0.5)", and filter is implemented by state-space block with the following parameters[1]:

$$A = -\frac{1}{\tau_1}, B = 1 - \frac{\tau_2}{\tau_1}, C = \frac{1}{\tau_1}, D = \frac{\tau_2}{\tau_1}. \tag{6}$$

Note that since characteristic of the phase detector is not smooth, it is better to choose a numerical method for stiff systems[2], e.g. "ode15s".

Now we demonstrate that simulation of the loop may lead to wrong results. If the simulation step is too large (e.g. default value of "Max step size" parameter is used) the model acquires lock (see Fig. 5-left) for any initial states. At the same time, for a smaller time step in the numerical procedure the loop may remain unlocked (see Fig. 5-right).

Consider the corresponding phase portrait $(\theta_e(t), x(t))$ in Fig. 6.

The green trajectory (solid green curve) in Fig. 6 corresponds to the trajectory with the loop filter initial state $x(0) = 0.004$ and the VCO phase shift $\theta_2(0) = \theta_e(0) = -3.8941$ rad. This curve tends to a periodic trajectory, therefore it will not acquire lock. All the trajectories under the green curve also tend to the same periodic trajectory.

The solid red curve corresponds to the trajectory with $x(0) = 535 \cdot 10^{-3}$ and $\theta_2(0) = \theta_e(0) = -3.8941$. This trajectory lies above the unstable periodic trajectory and tends to a stable equilibrium. In this case PLL acquires lock.

All the trajectories between the stable and unstable periodic trajectories tend to the stable one (see, e.g., a solid blue curve). Therefore, if the gap between the stable and unstable periodic trajectories is smaller than the discretization step, then the numerical procedure may

[1]Following the classical consideration [16, p.17, eq.2.20] [17, p.41, eq.4-26], where the filter's initial state is omitted, the filter is often represented in MatLab Simulink as the block *Transfer Fcn* with zero initial state. (see, e.g. [18]–[22]). It is also related to the fact that the transfer function (from $\varphi$ to $g$) of system (2) is defined by the Laplace transformation for zero initial data $x(0) \equiv 0$. Unlike "Transfer fcn" block, "State-space" block from Simulink allows one to consider nonzero initial states.

[2]Default Simulink integration method "ode45" may not work well with non-smooth systems

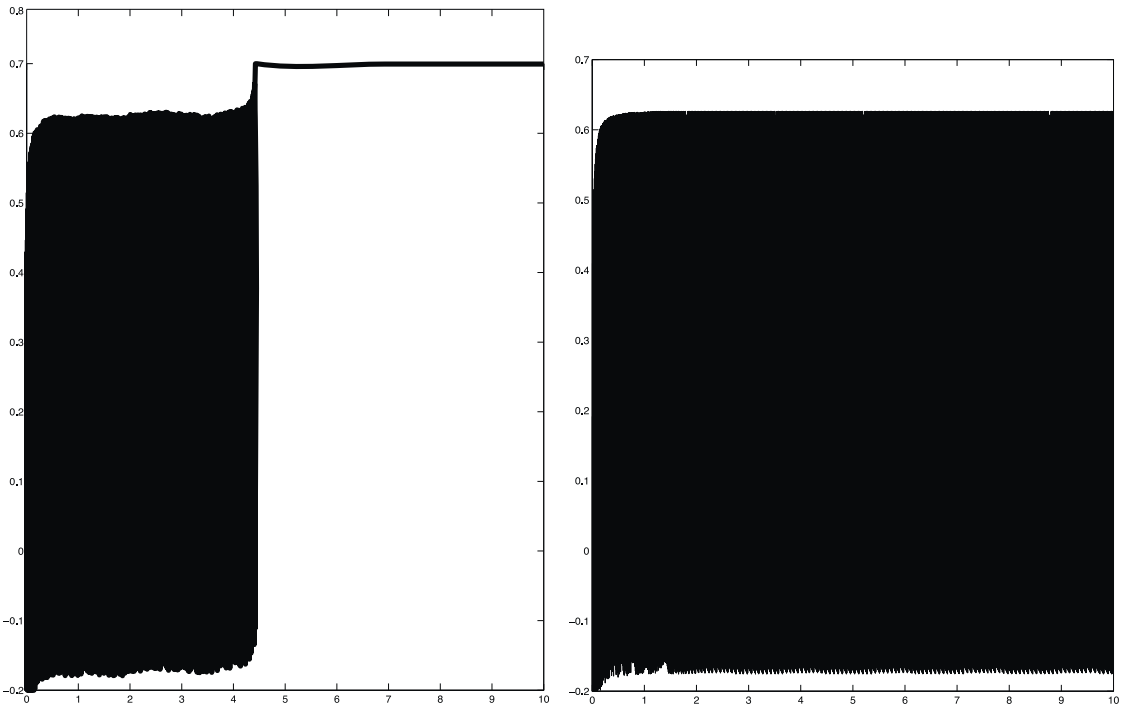

Fig. 5: (a) Max step size "auto", relative tolerance = "1e-4". (b) Max step size = "1e-4", and relative tolerance = "1e-6".

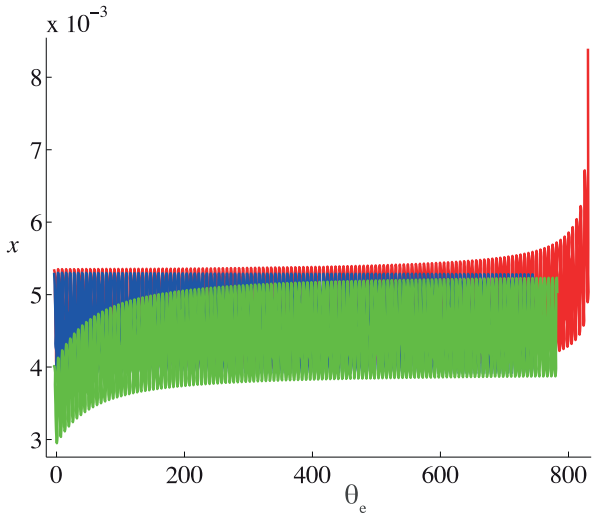


Fig. 6: Phase portrait with coexistence of stable and unstable periodic trajectories. Red trajectory tend to an equilibrium point, green trajectory tend to a periodic trajectory (blue).

slip through the stable trajectory. The case corresponds to the close coexisting attractors and the bifurcation of birth of semistable trajectory [23], [24]. In this case numerical methods are limited by the errors on account of the linear multistep integration methods (see [25], [26]). As noted in [27], low-order methods give a relatively large warping error that, in some cases, could lead to corrupted solutions (i.e., solutions that are wrong even from a qualitative point of view).

Corresponding limitations of simulation in SPICE are discussed in [28].

The above example demonstrates also the difficulties of numerical search of so-called hidden oscillations, whose basin of attraction does not overlap with the neighborhood of an equilibrium point, and thus may be difficult to find numerically. In general, an oscillation in a dynamical system can be easily localized numerically if the initial data from its open neighborhood lead to long-time behavior that approaches the oscillation. From a computational point of view, on account of the simplicity of finding the basin of attraction in the phase space, it is natural to suggest the following classification of attractors [23], [29]–[32]: *An attractor is called a* hidden attractor *if its basin of attraction does not intersect small neighborhoods of equilibria, otherwise it is called a* self-excited attractor.

For a *self-excited attractor* its basin of attraction is connected with an unstable equilibrium. Therefore, self-excited attractors can be localized numerically by the *standard computational procedure* in which after a transient process a trajectory, started from a point of unstable manifold in a neighborhood of unstable equilibrium, is attracted to the state of oscillation and traces it. Thus self-excited attractors can be easily visualized.

In contrast, for a hidden attractor its basin of attraction is not connected with unstable equilibria. For example, hidden attractors can be attractors in the systems with no equilibria or with only one stable equilibrium (a special case of multistable systems and coexistence of attractors - in this case the observation of one or another stable solution may depend on the initial data and integration step). Recent examples of hidden attractors can be found in *The*

*European Physical Journal Special Topics: Multistability: Uncovering Hidden Attractors*, 2015 (see [33]–[44]).

## IV. The pull-in range estimation

Model (5) can be effectively studied analytically by Andronov's point transformation method. One of the first considerations of the above effect is due to M. Kapranov [45] in 1956. In 1961, N. Gubar' [46] revealed a gap in the proof of Kapranov's results and specified the values of parameters for which the pull-in range was limited by a periodic or heteroclitic solution. Finally, in 1969, B. Shakhtarin fixed some misprints in the Gubar's work [47]. In 1970 [48], these results were confirmed numerically and corresponding bifurcation diagram was given (see Fig. 8) (see, also [12], [23]).

Consider, e.g., the parameters $\tau_1 = 0.02$, $\tau_2 = 0.008$ and the corresponding curve in Fig. 8 (see the right-hand side vertical axis). This curve corresponds to the bifurcation of

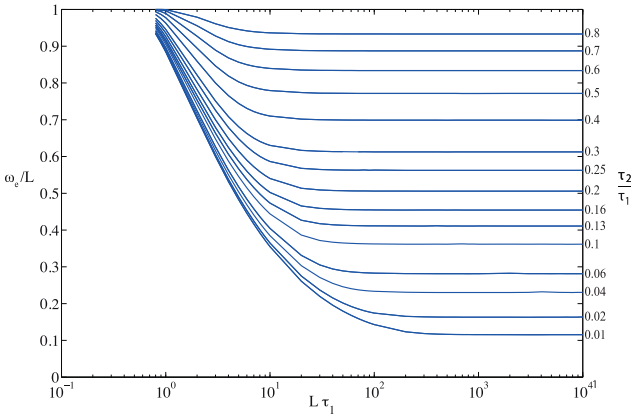


Fig. 7: PLL parameters for existence of semistable periodic trajectory.

semistable trajectory. Considering other possible bifurcations, it is possible to demonstrate that this curve restricts the area corresponding to the pull-in range. Consider this curve separately in Fig. 8. Next we choose VCO gain $L$

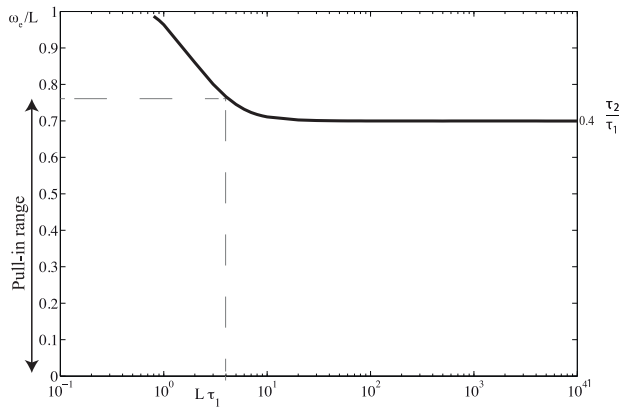


Fig. 8: Pull-in range for parameters $\tau_1 = 0.02$, $\tau_2 = 0.008$, $L = 200$.

(see horizontal axis in Fig. 8), which defines a point on the curve (e.g. $L\tau_1 = 4$, $L = \frac{4}{\tau_1}$). This point corresponds to the normalized pull-in frequency $\frac{\omega_e}{L}$ (see the left-hand side vertical axis in Fig. 8), i.e. for smaller values of $\omega_e$ the model acquires lock for any initial state. However for a larger value of $\omega_e$ this is not true.

## Conclusion

The considered example (see also the corresponding examples with sinusoidal signals [14], [15], [24]) is a motivation for the use of rigorous analytical methods for the analysis of nonlinear PLL models. Various modifications of classical stability criteria for the nonlinear analysis of control systems in cylindrical phase space were developed in the second half of the 20th century (see, e.g. [49]–[52] and recent books recent books [6], [11], [12], [53], [54]).

## ACKNOWLEDGEMENTS

Authors were supported by Saint-Petersburg State University (6.39.416.2014, sec. 1-2), Russian Foundation for Basic Research (13-01-00507, sec. 3) and the Leading Scientific Schools programm (3384.2014.1). The authors would like to thank Roland E. Best, the founder of the Best Engineering Company, Oberwil, Switzerland and the author of the bestseller on PLL-based circuits [3] for valuable discussion.

## References

[1] V. Kroupa, *Phase Lock Loops and Frequency Synthesis.* John Wiley & Sons, 2003.

[2] G. Bianchi, *Phase-Locked Loop Synthesizer Simulation.* McGraw-Hill, 2005.

[3] R. Best, *Phase-Lock Loops: Design, Simulation and Application*, 6th ed. McGraw-Hill, 2007.

[4] N. Kuznetsov, G. Leonov, M. Yuldashev, and R. Yuldashev, "Rigorous mathematical definitions of the hold-in and pull-in ranges for phase-locked loops," in *1st IFAC Conference on Modelling, Identification and Control of Nonlinear Systems.* IFAC Proceedings Volumes (IFAC-PapersOnline), 2015, pp. 720–723.

[5] G. Leonov, N. Kuznetsov, M. Yuldashev, and R. Yuldashev, "Hold-in, pull-in, and lock-in ranges of PLL circuits: rigorous mathematical definitions and limitations of classical theory," *IEEE Transactions on Circuits and Systems–I: Regular Papers*, 2015, (http://arxiv.org/pdf/1505.04262v2.pdf). 10.1109/TCSI.2015.2476295

[6] N. Margaris, *Theory of the Non-Linear Analog Phase Locked Loop.* New Jersey: Springer Verlag, 2004.

[7] D. Abramovitch, "Phase-locked loops: A control centric tutorial," in *American Control Conf. Proc.*, vol. 1. IEEE, 2002, pp. 1–15.

[8] R. J. Steed, F. Pozzi, M. J. Fice, C. C. Renaud, D. C. Rogers, I. F. Lealman, D. G. Moodie, P. J. Cannard, C. Lynch, L. Johnston, M. J. Robertson, R. Cronin, L. Pavlovic, L. Naglic, M. Vidmar, and A. J. Seeds, "Monolithically integrated heterodyne optical phase-lock loop with RF XOR phase detector," *Opt. Express*, vol. 19, no. 21, pp. 20 048–20 053, Oct 2011. 10.1364/OE.19.020048

[9] G. A. Leonov, N. V. Kuznetsov, M. V. Yuldahsev, and R. V. Yuldashev, "Analytical method for computation of phase-detector characteristic," *IEEE Transactions on Circuits and Systems - II: Express Briefs*, vol. 59, no. 10, pp. 633–647, 2012. 10.1109/TCSII.2012.2213362

[10] N. Krylov and N. Bogolyubov, *Introduction to non-linear mechanics.* Princeton: Princeton Univ. Press, 1947.

[11] J. Kudrewicz and S. Wasowicz, *Equations of phase-locked loop. Dynamics on circle, torus and cylinder*. World Scientific, 2007.

[12] G. A. Leonov and N. V. Kuznetsov, *Nonlinear Mathematical Models Of Phase-Locked Loops. Stability and Oscillations*. Cambridge Scientific Press, 2014.

[13] G. A. Leonov, N. V. Kuznetsov, M. V. Yuldashev, and R. V. Yuldashev, "Nonlinear dynamical model of Costas loop and an approach to the analysis of its stability in the large," *Signal processing*, vol. 108, pp. 124–135, 2015. 10.1016/j.sigpro.2014.08.033

[14] N. Kuznetsov, O. Kuznetsova, G. Leonov, P. Neittaanmaki, M. Yuldashev, and R. Yuldashev, "Limitations of the classical phase-locked loop analysis," in *International Symposium on Circuits and Systems (ISCAS)*. IEEE, 2015, pp. 533–536, http://arxiv.org/pdf/1507.03468v1.pdf.

[15] R. Best, N. Kuznetsov, O. Kuznetsova, G. Leonov, M. Yuldashev, and R. Yuldashev, "A short survey on nonlinear models of the classic Costas loop: rigorous derivation and limitations of the classic analysis," in *American Control Conference (ACC)*. IEEE, 2015, pp. 1296–1302, http://arxiv.org/pdf/1505.04288v1.pdf.

[16] A. Viterbi, *Principles of coherent communications*. New York: McGraw-Hill, 1966.

[17] F. Gardner, *Phase-lock techniques*. New York: John Wiley & Sons, 1966.

[18] S. Brigati, F. Francesconi, A. Malvasi, A. Pesucci, and M. Poletti, "Modeling of fractional-N division frequency synthesizers with SIMULINK and MATLAB," in *8th IEEE International Conference on Electronics, Circuits and Systems, 2001. ICECS 2001*, vol. 2, 2001, pp. 1081–1084 vol.2.

[19] B. Nicolle, W. Tatinian, J.-J. Mayol, J. Oudinot, and G. Jacquemod, "Top-down PLL design methodology combining block diagram, behavioral, and transistor-level simulators," in *IEEE Radio Frequency Integrated Circuits (RFIC) Symposium,*, 2007, pp. 475–478.

[20] G. Zucchelli, "Phase locked loop tutorial," http://www.mathworks.com/matlabcentral/fileexchange/14868-phase-locked-loop-tutorial, 2007.

[21] H. Koivo and M. Elmusrati, *Systems Engineering in Wireless Communications*. Wiley, 2009.

[22] R. Kaald, I. Lokken, B. Hernes, and T. Saether, "High-level continuous-time Sigma-Delta design in Matlab/Simulink," in *NORCHIP, 2009*. IEEE, 2009, pp. 1–6.

[23] G. A. Leonov and N. V. Kuznetsov, "Hidden attractors in dynamical systems. From hidden oscillations in Hilbert-Kolmogorov, Aizerman, and Kalman problems to hidden chaotic attractors in Chua circuits," *International Journal of Bifurcation and Chaos*, vol. 23, no. 1, 2013, art. no. 1330002. 10.1142/S0218127413300024

[24] N. Kuznetsov, G. Leonov, M. Yuldashev, and R. Yuldashev, "Nonlinear analysis of classical phase-locked loops in signal's phase space," *IFAC Proceedings Volumes (IFAC-PapersOnline)*, vol. 19, pp. 8253–8258, 2014. 10.3182/20140824-6-ZA-1003.02772

[25] M. Biggio, F. Bizzarri, A. Brambilla, G. Carlini, and M. Storace, "Reliable and efficient phase noise simulation of mixed-mode integer-n phase-locked loops," in *Circuit Theory and Design (ECCTD), 2013 European Conference on*. IEEE, 2013, pp. 1–4.

[26] M. Biggio, F. Bizzarri, A. Brambilla, and M. Storace, "Accurate and efficient psd computation in mixed-signal circuits: a time domain approach," *Circuits and Systems II: Express Briefs, IEEE Transactions on*, vol. 61, no. 11, 2014.

[27] A. Brambilla and G. Storti-Gajani, "Frequency warping in time-domain circuit simulation," *Circuits and Systems I: Fundamental Theory and Applications, IEEE Transactions on*, vol. 50, no. 7, pp. 904–913, 2003.

[28] G. Bianchi, N. Kuznetsov, G. Leonov, M. Yuldashev, and R. Yuldashev, "Limitations of PLL simulation: hidden oscillations in SPICE analysis," *arXiv:1506.02484*, 2015, http://arxiv.org/pdf/1506.02484.pdf, http://www.mathworks.com/matlabcentral/fileexchange/52419-hidden-oscillations-in-pll (accepted to IEEE 7th International Congress on Ultra Modern Telecommunications and Control Systems).

[29] N. V. Kuznetsov, G. A. Leonov, and V. I. Vagaitsev, "Analytical-numerical method for attractor localization of generalized Chua's system," *IFAC Proceedings Volumes (IFAC-PapersOnline)*, vol. 4, no. 1, pp. 29–33, 2010. 10.3182/20100826-3-TR-4016.00009

[30] G. A. Leonov, N. V. Kuznetsov, and V. I. Vagaitsev, "Localization of hidden Chua's attractors," *Physics Letters A*, vol. 375, no. 23, pp. 2230–2233, 2011. 10.1016/j.physleta.2011.04.037

[31] ——, "Hidden attractor in smooth Chua systems," *Physica D: Nonlinear Phenomena*, vol. 241, no. 18, pp. 1482–1486, 2012. 10.1016/j.physd.2012.05.016

[32] G. Leonov, N. Kuznetsov, and T. Mokaev, "Homoclinic orbits, and self-excited and hidden attractors in a Lorenz-like system describing convective fluid motion," *Eur. Phys. J. Special Topics*, vol. 224, no. 8, pp. 1421–1458, 2015. 10.1140/epjst/e2015-02470-3

[33] M. Shahzad, V.-T. Pham, M. Ahmad, S. Jafari, and F. Hadaeghi, "Synchronization and circuit design of a chaotic system with coexisting hidden attractors," *European Physical Journal: Special Topics*, vol. 224, no. 8, pp. 1637–1652, 2015.

[34] S. Brezetskyi, D. Dudkowski, and T. Kapitaniak, "Rare and hidden attractors in Van der Pol-Duffing oscillators," *European Physical Journal: Special Topics*, vol. 224, no. 8, pp. 1459–1467, 2015.

[35] S. Jafari, J. Sprott, and F. Nazarimehr, "Recent new examples of hidden attractors," *European Physical Journal: Special Topics*, vol. 224, no. 8, pp. 1469–1476, 2015.

[36] Z. Zhusubaliyev, E. Mosekilde, A. Churilov, and A. Medvedev, "Multistability and hidden attractors in an impulsive Goodwin oscillator with time delay," *European Physical Journal: Special Topics*, vol. 224, no. 8, pp. 1519–1539, 2015.

[37] P. Saha, D. Saha, A. Ray, and A. Chowdhury, "Memristive non-linear system and hidden attractor," *European Physical Journal: Special Topics*, vol. 224, no. 8, pp. 1563–1574, 2015.

[38] V. Semenov, I. Korneev, P. Arinushkin, G. Strelkova, T. Vadivasova, and V. Anishchenko, "Numerical and experimental studies of attractors in memristor-based Chua's oscillator with a line of equilibria. Noise-induced effects," *European Physical Journal: Special Topics*, vol. 224, no. 8, pp. 1553–1561, 2015.

[39] Y. Feng and Z. Wei, "Delayed feedback control and bifurcation analysis of the generalized Sprott b system with hidden attractors," *European Physical Journal: Special Topics*, vol. 224, no. 8, pp. 1619–1636, 2015.

[40] C. Li, W. Hu, J. Sprott, and X. Wang, "Multistability in symmetric chaotic systems," *European Physical Journal: Special Topics*, vol. 224, no. 8, pp. 1493–1506, 2015.

[41] Y. Feng, J. Pu, and Z. Wei, "Switched generalized function projective synchronization of two hyperchaotic systems with hidden attractors," *European Physical Journal: Special Topics*, vol. 224, no. 8, pp. 1593–1604, 2015.

[42] J. Sprott, "Strange attractors with various equilibrium types," *European Physical Journal: Special Topics*, vol. 224, no. 8, pp. 1409–1419, 2015.

[43] V. Pham, S. Vaidyanathan, C. Volos, and S. Jafari, "Hidden attractors in a chaotic system with an exponential nonlinear term," *European Physical Journal: Special Topics*, vol. 224, no. 8, pp. 1507–1517, 2015.

[44] S. Vaidyanathan, V.-T. Pham, and C. Volos, "A 5-D hyperchaotic rikitake dynamo system with hidden attractors," *European Physical Journal: Special Topics*, vol. 224, no. 8, pp. 1575–1592, 2015.

[45] M. Kapranov, "Locking band for phase-locked loop," *Radiofizika (in Russian)*, vol. 2, no. 12, pp. 37–52, 1956.

[46] N. A. Gubar', "Investigation of a piecewise linear dynamical

system with three parameters," *J. Appl. Math. Mech.*, vol. 25, no. 6, pp. 1011–1023, 1961.

[47] B. Shakhtarin, "Study of a piecewise-linear system of phase-locked frequency control," *Radiotechnica and electronika (in Russian)*, no. 8, pp. 1415–1424, 1969.

[48] L. Belyustina, V. Brykov, K. Kiveleva, and V. Shalfeev, "On the magnitude of the locking band of a phase-shift automatic frequency control system with a proportionally integrating filter," *Radiophysics and Quantum Electronics*, vol. 13, no. 4, pp. 437–440, 1970.

[49] A. Gelig, G. Leonov, and V. Yakubovich, *Stability of Nonlinear Systems with Nonunique Equilibrium (in Russian)*. Nauka, 1978, (English transl: Stability of Stationary Sets in Control Systems with Discontinuous Nonlinearities, 2004, World Scientific).

[50] G. A. Leonov, V. Reitmann, and V. B. Smirnova, *Nonlocal Methods for Pendulum-like Feedback Systems*. Stuttgart-Leipzig: Teubner Verlagsgesselschaft, 1992.

[51] G. A. Leonov, D. V. Ponomarenko, and V. B. Smirnova, *Frequency-Domain Methods for Nonlinear Analysis. Theory and Applications*. Singapore: World Scientific, 1996.

[52] G. A. Leonov, I. M. Burkin, and A. I. Shepelyavy, *Frequency Methods in Oscillation Theory*. Dordretch: Kluwer, 1996.

[53] A. Suarez and R. Quere, *Stability Analysis of Nonlinear Microwave Circuits*. Artech House, 2003.

[54] A. Suarez, *Analysis and Design of Autonomous Microwave Circuits*, ser. Wiley Series in Microwave and Optical Engineering. Wiley-IEEE Press, 2009.